UNIVERSIDADE FEDERAL DE PERNAMBUCO
CENTRO DE BIOCIÊNCIAS
PROGRAMA DE PÓS-GRADUAÇÃO EM CIÊNCIAS BIOLÓGICAS

ERIKA KETLEM GOMES TRINDADE

NANOIMUNOSSENSORES PARA DETECÇÃO DA CISTATINA C NO DIAGNÓSTICO DE DOENÇAS RENAIS

Recife
2019

ERIKA KETLEM GOMES TRINDADE

NANOIMUNOSSENSORES PARA DETECÇÃO DA CISTATINA C NO DIAGNÓSTICO DE DOENÇAS RENAIS

Tese apresentada ao Programa de Pós-graduação em Ciências Biológicas da Universidade Federal de Pernambuco, como um dos requisitos para obtenção do título de doutor em Ciências Biológicas.

Área de Concentração: Biotecnologia

Orientadora: Profª. Drª. Rosa Amália Fireman Dutra

Recife

2019

Catalogação na fonte:
Bibliotecário Bruno Márcio Gouveia - CRB-4/1788

Trindade, Erika Ketlem Gomes
Nanoimunossensores para detecção da cistatina C no diagnóstico de doenças renais / Erika Ketlem Gomes Trindade. – 2019.

126 f. : il.

Orientadora: Profª. Drª. Rosa Amália Fireman Dutra.
Tese (doutorado) – Universidade Federal de Pernambuco. Centro de Biociências. Programa de Pós-graduação em Ciências Biológicas, Recife, 2019.
Inclui referências e apêndices.

1. Rins – Doenças. 2. Insuficiência renal aguda. 3. Insuficiência renal crônica. I. Dutra, Rosa Amália Firemam (Orientadora). II. Título.

616.614 CDD (22.ed.) UFPE/CB – 2019 - 338

ERIKA KETLEM GOMES TRINDADE

NANOIMUNOSSENSORES PARA DETECÇÃO DA CISTATINA C NO DIAGNÓSTICO DE DOENÇAS RENAIS

Tese apresentada ao Programa de Pós-graduação em Ciências Biológicas da Universidade Federal de Pernambuco, como um dos requisitos para obtenção do título de doutor em Ciências Biológicas.

Área de Concentração: Biotecnologia

Aprovada em: 30/07/2019.

COMISSÃO EXAMINADORA

_____

Profa. Dra. Rosa Fireman Dutra
(Presidente/UFPE).

_____

Prof. Dr. Ranilson de Souza Bezerra
(Membro interno/UFPE)

_____

Profa. Dra. Maria Tereza dos Santos Correia
(Membro interno/UFPE)

_____

Profa. Dra. Madalena Carneiro da Cunha Areias
(Membro externo/UFPE)

_____

Profa. Dra. Erika Cristina de Lima Soares
(Membro externo/UNIBRA)

AGRADECIMENTOS

Agradeço em primeiro lugar aos meus pais, ***Elias e Lourdes***, pela base, apoio e incentivo aos meus estudos desde sempre, pela paciência, amor verdadeiro e oportunidades oferecidas para minha formação acadêmica e pessoal.

À minha orientadora ***Profª Drª Rosa Dutra*** por tudo que me ensinou, pelas oportunidades e pela compreensão durante esses anos de pesquisa e estudo.

A toda minha família, principalmente à minha irmã ***Keity***, ao meu tio ***Luiz Antônio*** e meu cunhado ***Everton***, pelo apoio durante os anos de estudo. E em especial à minha ***Vó Maria (in memoriam)*** que não se encontra mais aqui, mas que sempre me incentivou e me apoiou em toda a minha jornada.

Ao meu sobrinho ***Fernando*** por me fazer entender o que é amor incondicional.

Aos meus amigos pelo carinho, pelas risadas e distrações, pela amizade verdadeira, pela ajuda e por tudo durante tantos anos.

Aos professores do Programa de Pós-Graduação em Ciências Biológicas - UFPE, que contribuíram para minha formação científica e aprendizado durante o doutorado.

Aos companheiros do Laboratório de Engenharia Biomédica ***(LEB)*** pela ajuda e pelas sugestões, que tanto contribuíram para a minha pesquisa, e também pelos momentos de apoio e conversa em tempos difíceis.

À Fundação de Amparo à Ciência e Tecnologia do Estado de Pernambuco ***(FACEPE)*** e ao Conselho Nacional de Desenvolvimento Científico e Tecnológico ***(CNPq)*** pelo apoio financeiro.

Enfim, a todos que de alguma forma me ajudaram nesses últimos quatro anos tanto no trabalho quanto na minha vida pessoal.

“A tarefa não é tanto ver aquilo que ninguém viu, mas pensar o que ninguém pensou sobre aquilo que todo mundo vê.”

- Arthur Schopenhauer

RESUMO

A cistatina C (CysC) é um marcador precoce de disfunção renal, o qual é mais preciso na predição do risco de falha renal do que a creatinina, e tem se mostrado independente de sexo, idade, dieta e massa muscular. Assim, o desenvolvimento de testes diagnósticos rápidos, precisos e sem a necessidade de manipulação por pessoal especializado, como os imunossensores, é de grande importância para quantificação da CysC. Neste trabalho foram desenvolvidos ensaios imunossensores eletroquímicos para detectar a alteração nos perfis serológicos de CysC. Nanopartículas de silício (MCM-41) funcionalizadas foram utilizadas no desenvolvimento de plataforma sensora. Um eletrodo de ouro funcionalizado com monocamadas auto-organizadas (SAMs) de ácido mercaptopropiônico (MPA) foi utilizado para a imobilização do MCM-41 e as leituras feitas através da técnica de impedância eletroquímica. Além disso, buscando o melhoramento dos sensores eletroquímicos, foi desenvolvido um imunossensor utilizando nanocompósito de óxido de grafeno-aminoferroceno. Aqui, o ferroceno funciona como centro de atividade eletroquímica para leituras diretamente em sangue ou soro. Nos ensaios desenvolvidos, as monocamadas auto-organizadas de MPA permitiram a estável imobilização das nanopartículas de silício. Estas, por sua vez, foram funcionalizadas com sucesso através da adição de grupamentos amina, o que foi comprovado através da análise por Infravermelho por Transformada de Fourier (FT-IR). Além disso, as nanopartículas admitiram o aumento da capacitância na interface entre o eletrodo e a solução redox, a estável imobilização dos anticorpos e sensível detecção da CysC, com uma faixa de detecção linear de 0,2 a 1,0 µg/mL e limite de detecção de 0,06 µg/mL. No segundo trabalho, a funcionalização do grafeno com o aminoferroceno foi bem-sucedida, sendo comprovada através de análise de FT-IR. O imunossensor baseado em nanocompósito de grafeno-aminoferroceno permitiu um aumento da área eletroativa do eletrodo e da área para imobilização de biomoléculas, comprovada através da técnica de Microscopia de Força Atômica. A plataforma permitiu a detecção linear da CysC na faixa de 0,1 a 1000 ng/mL e limite de detecção de 0,03 ng/mL com alta sensibilidade, sendo uma excelente alternativa para detecção eletroquímica da CysC em tempo real sem o uso de sondas redox. As vantagens deste imunossensor incluem testes rápidos com menos etapas pelo simples uso de uma superfície redox. Os métodos aqui descritos se mostraram estáveis e sensíveis na detecção de CysC e, por consequência, de grande importância para a prevenção e detecção precoce de doenças renais.

Palavras-chave: Imunossensor. Nanopartículas silício. Aminoferroceno. Grafeno. Doenças renais. Cistatina C.

ABSTRACT

Cystatin C (CysC) is an early marker of renal dysfunction, which is more accurate in predicting the risk of renal failure than creatinine, and has been shown to be independent of gender, age, diet and muscle mass. Thus, the development of fast, accurate and no need for handling by skilled personnel, such as immunosensors, is of great importance for quantifying CysC. In this work, electrochemical immunosensor assays were developed to detect the change in CysC serological profiles. Functionalized silica nanoparticles (MCM-41) were used in the development of sensor platform. A functionalized gold electrode with self-assembled monolayers (SAMs) of mercaptopropionic acid (MPA) was used for immobilization of the MCM-41 and readings made using the electrochemical impedance technique. In addition, seeking the improvement of electrochemical sensors, an immunosensor using graphene-aminoferrocene oxide nanocomposite was developed. Here, ferrocene acts as the center of electrochemical activity for readings directly in blood or serum. In the assays developed, the self-assembled monolayers of MPA allowed stable immobilization of silica nanoparticles. These, in turn, were successfully functionalized through the addition of amine groups, which was confirmed by Fourier Transform Infrared (FT-IR) analysis. In addition, the nanoparticles allowed for increased capacitance at the interface between the electrode and redox solution, stable immobilization of antibodies and sensitive CysC detection, with a linear detection range of 0.2 to 1.0 µg/mL and limit detection rate of 0.06 µg/mL. In the second work, the functionalization of graphene with aminoferrocene was successful, being confirmed by FT-IR analysis. The graphene-aminoferrocene nanocomposite-based immunosensor allowed an increase in the electrode electroactive area and the area for immobilization of biomolecules, proven by the Atomic Force Microscopy technique. The platform allowed linear detection of CysC in the range 0.1 to 1000 ng/mL and detection limit of 0.03 ng/mL with high sensitivity, making it an excellent alternative for real time electrochemical detection of CysC without the use of redox probes. Advantages of this immunosensor include rapid testing with fewer steps by simple use of a redox surface. The methods described herein have been shown to be stable and sensitive in detecting CysC and therefore of great importance for the prevention and early detection of kidney disease.

Keywords: Immunosensor. Silica nanoparticles. Aminoferrocene. Graphene. Kidney diseases. Cystatin C.

LISTA DE FIGURAS

LISTA DE QUADROS E TABELAS

LISTA DE ABREVIAÇÕES E SIGLAS

AFM	Microscópio de Força Atômica, do inglês Atomic Force Microscopy
AKI	Akute Kidney Injury
Anti-CysC	Anticorpo anti-Cistatina C
APTES	(Aminopropyl)triethoxysilane
ATR-FT-IR	Módulo de reflexão atenuada do Infravermelho por transformada de Fourier, do inglês Attenuated Total Reflectance Infrared Fourier Transform
CKD	Chronic Kidney Disease
CV	Cyclic Voltammetry
CysC	Cistatina C
DNA	Ácido Desoxirribonucleico do inglês Deoxyribonucleic Acid
DRC	Doença Renal Crônica
E	Potencial
EA	Eletrodo Auxiliar
EDC	1-etil-3- (3-dimetilaminopropil) carbodiimida
EFRD	Estágio Final de Doença Renal
EIS	Espectroscopia de Impedância Eletroquímica, do inglês Electrochemical Impedance Spectroscopy
ELISA	Imunoensaio enzimático, do inglês Enzyme-Linked Immunosorbent Assay
ER	Eletrodo de Referência
ESRD	End-stage Renal Disease
Fc	Ferroceno
FT-IR	Infravermelho por transformada de Fourier, do inglês Infrared Fourier Transform

GFR	Glomerular Filtration Rate
GO	Óxido de Grafeno, do inglês Graphene Oxide
I	Corrente
ICU	Intensive Care Unit
Ipa	Corrente de pico anódico
Ipc	Corrente de pico catódico
IRA	Insuficiência Renal Aguda
IV	Infravermelho
LOD	Lower Detection Limit
MCM-41	Mobile Crystalline Material 41, também conhecido como nanopartículas de silício
MPA	Ácido Mercaptopropiônico, do inglês Mercaptopropionic Acid
MSN	Nanopartículas de sílica mesoporosa, do inglês Mesoporous Silica Nanoparticle
NHS	N-hidroxisuccinimida
OMS	Organização Mundial de Saúde
PEI	Polietilenimina
PENIA	Ensaio nefelométrico, do inglês particle-enhanced nephelometry immunoassay
PETIA	Ensaio turbidimétrico, do inglês Particle-enhanced turbidimetric immunoassay
Rct	Resistência de transferência de carga
RGO	Óxido de grafeno reduzido, do inglês Reduced Graphene Oxide
SAMs	Monocamadas auto-organizadas, do inglês Self-Assembled Monolayers
SPR	Ressonância de Plásmon de Superfície, do inglês Surface Plasmon Ressonance

SUS	Sistema Único de Saúde
SWV	Square Wave Voltammetry
TGF	Taxa de Filtração Glomerular
UTI	Unidade de Terapia Intensiva
VC	Voltametria Cíclica
VOQ	Voltametria de Onda Quadrada
VPD	Voltametria de Pulso Diferencial

SUMÁRIO

1 INTRODUÇÃO

A Cistatina C (CysC) é uma proteína de 13 kDa considerada um marcador precoce para diagnóstico de doenças renais e é relacionada à taxa de filtração glomerular (TFG) (LAU et al., 2017; TAO; ZHAO; ZENG, 2016). Evidências sugerem que o aumento dos níveis séricos de CysC pode detectar a disfunção renal mais precocemente do que a creatinina, que é atualmente o marcador diagnóstico mais utilizado (GAYGISIZ et al., 2016). Estudos recentes indicaram que a concentração sérica de CysC é mais estável e precisa na estimativa da TFG e é independente de sexo, dieta e massa muscular (FOX et al., 2014; MI et al., 2016; RAVN et al., 2017). Assim, este marcador pode indicar sinais precoces de doença renal, permitindo um diagnóstico precoce de Insuficiência Renal Aguda (IRA) e diminuição dos casos de Doença Renal Crônica (DRC), bem como o monitoramento desta condição em pacientes fazendo uso de diálise. Estudos recentes mostraram que a incidência de IRA é de até 20% nos EUA e muito similar em outros países, ao passo que a DRC tem uma alta prevalência global, estimada em 11 a 13%. Nesse sentido, a busca de métodos analíticos alternativos de menor custo que combinam a possibilidade de fornecer resultados de forma mais prática, imediata e sem a necessidade de pessoal especializado para monitoramento da CysC é imperativo.

Até o momento, várias estratégias analíticas têm sido usadas para a detecção de CysC sérica, como ensaio imunoenzimático (ELISA do inglês Enzyme-Linked Immunosorbent Assay), imunoensaios turbidimétricos e nefelométricos (DELANAYE et al., 2014; FONSECA et al., 2015; JIANG et al., 2014). No entanto, estes são métodos demorados e exigem pessoal especializado para operar. Devido a isso e ao grande interesse na detecção rápida de CysC, foram feitas tentativas para desenvolver biossensores e imunossensores para CysC. YANG et al., (2016) foi capaz de desenvolver um genossensor eletroquímico usando nanopartículas de ouro e óxido de ferro para amplificar o sinal. Embora o limite de detecção tenha sido baixo para este trabalho, não é clinicamente relevante e o sensor requer muitos passos para a conversão do sinal. Alguns sensores ópticos também foram desenvolvidos, como o trabalho de GORODKIEWICZ & LUSZCZYN, (2011) e TAO et al. (2016), que utilizaram imagens de ressonância de plásmon de superfície e pontos quânticos de

infravermelho próximo, respectivamente, para detecção de CysC. O principal problema nos sistemas ópticos é a difícil miniaturização dos métodos. Neste contexto, os imunossensores amperométricos eletroquímicos têm a vantagem de detecção específica e sensível, e fácil miniaturização.

No desenvolvimento de imunossensores, os nanomateriais vêm sendo amplamente utilizados devido à constante busca por melhores, mais estáveis e sensíveis plataformas para a imobilização de antígenos e anticorpos. Dentre os nanomateriais recentemente utilizados, deve-se destacar o Material Cristalino Móvel (MCM-41), também conhecido como sílica mesoporosa ou nanopartícula de silício. Este vem sendo utilizado em variadas aplicações como liberação de drogas, imagem e biosensoriamento (KHALILZADEH et al., 2016). Estas muitas aplicações são possíveis devido à sua grande eficácia na imobilização de proteínas, bem como a presença de numerosos grupamentos silano na sua superfície, tornando possível a fácil modificação e funcionalização destes com várias funções orgânicas (OMIDFAR et al., 2012; SZEGEDI et al., 2011). O material mais comum para funcionalização da superfície das nanopartículas de silício é o Aminopropil-trietoxisilano (APTES), o qual tem a capacidade de formar uma camada funcionalizante em materiais de sílica, com grupamentos amina livres para ligação de biomoléculas. O MCM-41 funcionalizado com o APTES permite um melhoramento na área superficial e na imobilização organizada de biomoléculas e consequentemente, na sensibilidade do imunossensor.

Outro nanomaterial que merece destaque é o Óxido de Grafeno (GO do inglês Graphene Oxide). Este atraiu grande atenção devido à sua alta área de superfície teórica, excelente condutividade elétrica, alta estabilidade química, forte resistência mecânica e o fato de que o carbono é um dos elementos mais baratos e abundantes (RODRIGUEZ et al., 2015). A excelente transferência de elétrons entre o GO e seus grupos funcionais é de grande importância para a aplicação em eletrônicos, sensores e biossensores, uma vez que facilita a deslocalização de elétrons (RABTI; RAOUAFI; MERKOÇI, 2016; RODRIGUEZ et al., 2015; SONG et al., 2016). Este, portanto, tem sido amplamente utilizado no desenvolvimento de imunossensores eletroquímicos. Entretanto, em imunossensores eletroquímicos “label-free”, as espécies redox são indispensáveis para a detecção eletroquímica e o método mais comum é adicionar as espécies redox nas soluções eletrolíticas (WANG; GAO; MA, 2017). Uma das desvantagens desse método é que ele exige lavagens e várias etapas que atrasam

uma detecção “point-of-care” real. Recentemente, grande foco tem sido dado a plataformas livres de sonda redox (ou redox probe-free) para aplicações em imunossensores (MOREIRA et al., 2011; TRINDADE; DUTRA, 2018). Nesse sentido, moléculas redox ativas, como unidades de ferroceno (Fc), podem ser conectadas à superfície do sensor como o centro da atividade eletroquímica, dispensando o uso de sonda redox externa, como usado no imunossensor convencional (YAMANAKA; VESTERGAARD; TAMIYA, 2016). Rápida taxa de transferência de elétrons e estabilidade redox de dois estados são outras características eletroquímicas atrativas exibidas por Fc e compostos derivados, tornando-os excelentes mediadores, principalmente quando usados em associação com diferentes nanomateriais (CHO et al., 2018; RABTI et al., 2016), como por exemplo o óxido de grafeno.

Nesta tese, descreve-se o desenvolvimento de um imunossensor baseado em nanopartículas de silício visando ao desenvolvimento de um sensor eletroquímico impedimétrico para detecção direta de anti-CysC, com maior sensibilidade devido ao maior número de moléculas imobilizadas em sua ampla área superficial. Também foi desenvolvido um imunossensor eletroquímico baseado em grafeno e ferroceno para aumentar a área eletroativa e a superfície de imobilização para anticorpos anti-CysC, permitindo alternativa sem sonda redox para o monitoramento de doenças renais. Essas metodologias podem ser consideradas excelentes alternativas para complementar e auxiliar a detecção precoce de falha renal. Por fim foi realizado uma extensiva pesquisa do estado da arte em biossensores para Cistatina C, o qual foi abarcado em um artigo de revisão sobre o tema.

2 FUNDAMENTAÇÃO TEÓRICA

2.1 INSUFICIÊNCIA RENAL AGUDA E DOENÇA RENAL CRÔNICA

Estudos têm demonstrado que a incidência de Insuficiência Renal Aguda (IRA) vem aumentando nas últimas décadas e pode muito provavelmente resultar em dano renal permanente (COCA; SINGANAMALA; PARIKH, 2012). A incidência de IRA tem sido relatada em até 20% nos EUA e muito similar em outros países (GHARAIBEH et al., 2018; HOSTE et al., 2015). Estima-se que a IRA ocorra em torno de 20 a 200 por milhão da população, 7 a 18% dos pacientes internados e aproximadamente 50% dos pacientes em Unidade de Terapia Intensiva (UTI), sendo considerada uma preocupação crescente para a saúde em todo o mundo (CHAWLA et al., 2017; HOSTE et al., 2015). A IRA tem sido associada à alta morbimortalidade, matando cerca de 2 milhões de pessoas todos os anos no mundo e as taxas de mortalidade hospitalar em pacientes hospitalizados com IRA são muito altas entre os pacientes que necessitam de diálise (CHAWLA et al., 2014, 2017; HOSTE et al., 2015). Uma vez que a IRA é um fator de risco independente para Doença Renal Crônica (DRC), Estágio Final de Doença Renal (EFDR), doenças cardíacas e morte, ela se configura como uma preocupação significativa de saúde pública em todo o mundo (COCA; SINGANAMALA; PARIKH, 2012).

Atualmente, a DRC tem uma alta prevalência global, estimada em 11 a 13%, com maior prevalência dos estágios finais (estágios 3 a 5), e é uma causa significativa de morbidade e mortalidade (GIFFORD et al., 2017; HILL et al., 2016). Os países de baixa e média renda sofreram um aumento alarmante no número de DRC nos últimos 20 anos, com uma significante associação com diabetes mellitus, hipertensão, doenças cardiovasculares, alto índice de massa corporal, entre outros (DE MOURA et al., 2014; GRAMS et al., 2013). Concordantemente, houve um aumento anual das despesas em programas de diálise em todo o mundo, que variou de 6% a 12% e continua a crescer (DE MOURA et al., 2014). Nos EUA, mais de 400 mil americanos apresentam doença renal terminal e mais de 300 mil desses pacientes necessitam de diálise. As taxas de mortalidade permanecem acima de 20%/ano com o uso de diálise, sendo que os custos médicos anuais diretos para doença renal terminal são quase

US $ 23 bilhões (GO et al., 2015). No Brasil, entre 2000 e 2012, a incidência aumentou 20%, ou seja, 1,8% por ano em todas as regiões do país e particularmente em grupos etários mais velhos. Com isso, a incidência e a prevalência de pacientes com DRC que receberam tratamento de diálise financiado publicamente aumentaram significantemente (DE MOURA et al., 2014). Assim, o diagnóstico precoce e o acompanhamento da evolução da doença renal são de extrema importância para a saúde pública, e diversas pesquisas têm sido desenvolvidas neste sentido.

2.1.1 Cistatina C

O conhecimento da taxa de filtração glomerular (TGF) é essencial para detecção e monitoramento de diminuição da função renal (GRUBB et al., 2014). Existe uma relação inversa entre risco de DRC e TGF que é independente da idade, sexo e outros fatores de risco. A função renal diminuída é um preditor de hospitalização, disfunção cognitiva e má qualidade de vida (HILL et al., 2016). A identificação e determinação do estágio da doença renal dependem da medida da TGF e da albuminúria (quantidade de albumina na urina). O cálculo da TGF real pela medição de marcadores de filtração externos é incômodo e impraticável (JHA et al., 2013), sendo esta, por muito tempo, estimada por equações envolvendo as concentrações séricas de creatinina (KHORGAMI et al., 2013). No entanto, a creatinina sérica é influenciada não apenas pela TGF, mas também por outros fatores, incluindo massa muscular, idade, gênero, medicamentos, estado catabólico, quantidade de carne ingerida e secreção tubular (GRUBB et al., 2014; KHORGAMI et al., 2013).

A busca por um marcador alternativo de detecção precoce de doenças renais levou à cistatina C sérica (CysC). Cistatina C e creatinina são produtos de caminhos metabólicos muito diferentes e são medidos por ensaios independentes, sendo que a CysC é menos sensível a alterações fisiológicas (GRAMS et al., 2013). Estudos recentes indicam que a concentração sérica de CysC é um melhor marcador em casos de insuficiência renal leve (FOX et al., 2014), além de ser um biomarcador de TFG mais preciso em diferentes situações (DELANAYE et al., 2014), inclusive na predição do risco de DRC em crianças e idosos (MI et al., 2016).

A CysC é uma proteína glicosilada de baixo peso molecular (13kda) da classe das inibidoras de cisteíno-proteinases (Fig. 1). Esta é produzida num ritmo constante pelas células nucleadas e encontra-se presente nos líquidos biológicos. Ela foi sugerida como um marcador alternativo para a TGF em 1979, sendo que o primeiro procedimento automatizado para análise da cistatina C foi introduzido em 1994 (GRUBB et al., 2014; LAU et al., 2017). A CysC é livremente filtrada pelos glomérulos, e a sua concentração sérica é independente de dieta, secreção tubular, massa muscular e peso corporal, não existindo diferenças significativas entre os valores de referência para o sexo feminino e o masculino. Devido a isso, esta é considerada um marcador precoce da disfunção renal relacionada à TGF (LAU et al., 2017; TAO; ZHAO; ZENG, 2016).

Figura 1. Estrutura terciária da cistatina C.

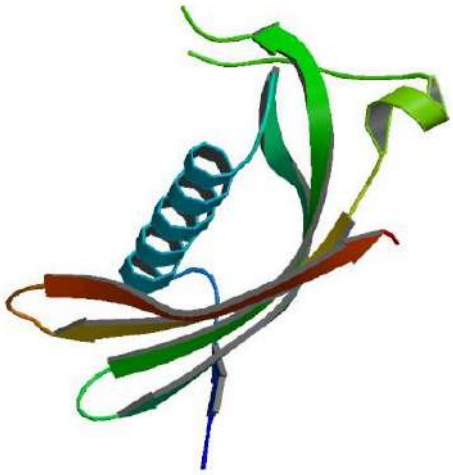

Fonte: KOLODZIEJCZYK et al., 2009.

Além disso, a CysC é um marcador que vem sendo cada vez mais utilizado no monitoramento de pacientes em diálise (hemodiálise, diálise peritoneal, etc.), por ser mais preciso do que a creatinina e a correlação entre creatinina e ureia em urina de 24 horas (HOEK et al., 2007; KHORGAMI et al., 2013). Assim, este marcador pode indicar sinais precoces de doença renal e diminuição dos casos de DRC, bem como

o monitoramento desta condição em pacientes fazendo uso de diálise. Até o momento, várias estratégias analíticas têm sido usadas para a detecção de CysC sérica, como ensaio imunoenzimático (ELISA), imunoensaios turbidimétricos (PETIA) e nefelométricos (PENIA) (DELANAYE et al., 2014; FONSECA et al., 2015; JIANG et al., 2014). No entanto, estes testes exigem unidades laboratoriais centralizadas e instrumentos manuseados por pessoal especializado. Devido a isso e ao grande interesse na detecção rápida de CysC, biossensores têm sido desenvolvidos para uma detecção precisa e direta, e uma tecnologia de fácil operação, buscando o diagnóstico precoce de falha renal.

2.2 BIOSSENSORES

Biossensores são dispositivos analíticos que utilizam componentes biológicos como elementos de reconhecimento para detecção de analitos-alvo (Fig. 2). Tais dispositivos combinam um sistema de detecção (receptor biológico que fará o reconhecimento do analito), transdução (que irá transformar essa ligação em um sinal que possa ser medido) e amplificação do sinal gerado nos processos de biorreconhecimento (que permitirão a visualização desse sinal) (CHOCARRO-RUIZ et al., 2017). Há vários tipos de biossensores, classificados de acordo com o transdutor (óptico, eletroquímico, piezelétrico, etc.), ou de acordo com a biomolécula imobilizada na superfície de detecção (biorreceptor), que podem ser enzimas, DNA, anticorpos, entre outros.

Figura 2. Esquema de funcionamento de um biossensor.

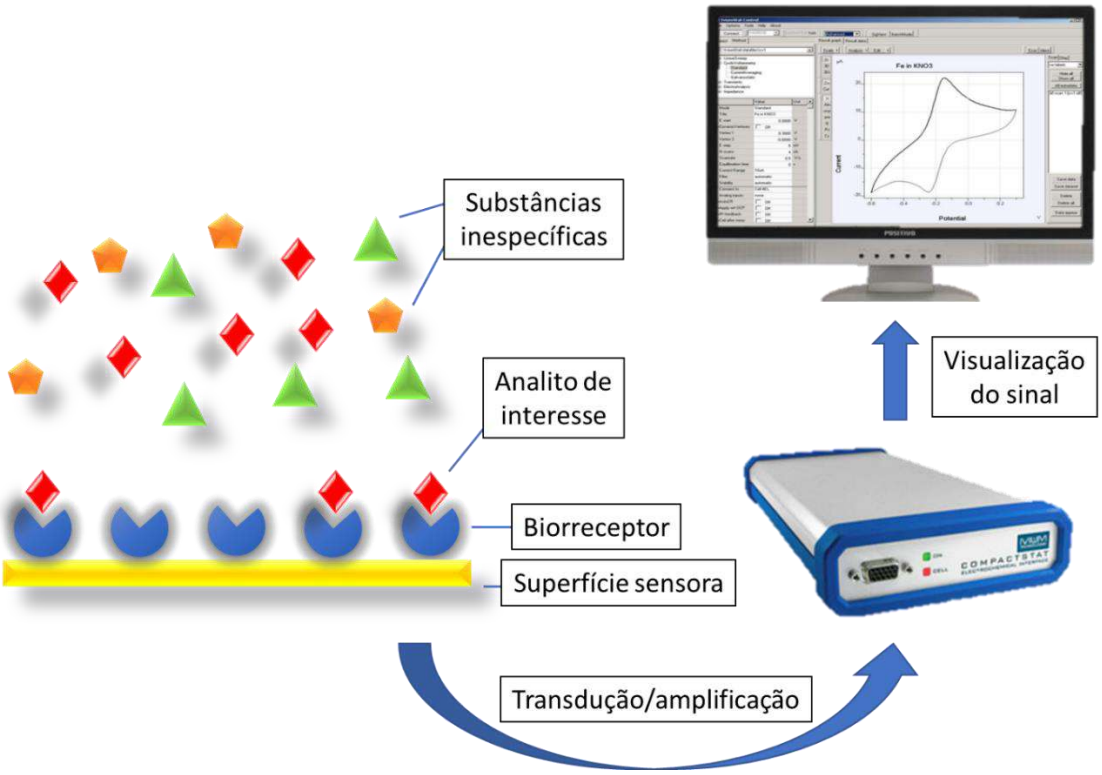

Fonte: Elaborada pela autora (2019).

Quando imunoglobulinas ou antígenos são utilizados como biorreceptor em biossensores, estes podem ser classificados como imunossensores (SHARMA; BYRNE; O'KENNEDY, 2016; WANG, 2006). Os imunossensores podem possuir inúmeras vantagens frente aos métodos tradicionais de diagnóstico, devido a serem dispositivos menores e facilmente manuseáveis, fornecendo a resposta em poucos minutos (AFKHAMI et al., 2017). Dentre os transdutores para imunossensores, os eletroquímicos são os mais comumente utilizados, visto que têm potencial para o diagnóstico rápido e preciso de doenças, com o objetivo de direcionar a um tratamento imediato e maior sobrevida dos pacientes (AFKHAMI et al., 2017; AHMED et al., 2015; ÇEVIK et al., 2016). Os imunossensores eletroquímicos são testes diagnósticos interessantes devido à sua facilidade ("user-friendly") e relativo baixo custo, podendo alcançar menores limites de detecção com pequenos volumes de analito. Além disso, a instrumentação necessária é relativamente simples e pode ser facilmente

portabilizada, instigando o desenvolvimento de eletrodos descartáveis e metodologias para quantidades insignificantes de amostras (SHARMA; BYRNE; O'KENNEDY, 2016).

Os sinais biológicos dos imunossensores podem ser reconhecidos e transduzidos utilizando várias estratégias, como a utilização de biomoléculas ligadas a marcadores (por exemplo, enzimas ou moléculas fluorescentes, entre outros). No entanto, esses métodos quase sempre requerem mais passos para que a leitura final seja realizada. Devido a isso, ensaios sem marcadores ou "label-free" são amplamente utilizados em imunossensores para diminuir etapas e tornar o processo de detecção mais estável. Ensaios "label-free" buscam interações moleculares biologicamente ativas, fornecendo informações detalhadas sobre seletividade, afinidade e, em muitos casos, também a cinética de ligação e a termodinâmica (SANG et al., 2015; TURNER, 2013). A detecção das modificações ocorridas na superfície eletródica de imunossensores eletroquímicos "label-free" são detectadas devido a flutuações na barreira de difusão de íons induzidas pelas interações entre antígenos e anticorpos, sendo as técnicas eletroquímicas extremamente sensíveis para detectar essas alterações.

2.2.1 Métodos de detecção e caracterização eletroquímica

No desenvolvimento de imunossensores eletroquímicos, as técnicas aplicadas utilizam potencial, corrente ou carga em uma célula eletroquímica, as quais são dependentes das espécies presentes na interface entre um eletrodo e a solução em que ele se encontra (HARVEY, 2019). A Voltametria Cíclica (VC) é considerada uma das técnicas mais importantes para medições eletroquímicas, na qual é registrada a resposta de corrente em diferentes voltagens aplicadas (potencial) (YANG; ROGACH, 2019). A VC oferece informações sobre a interação do eletrodo com a solução em que está em contato, realizando uma varredura de potencial em vários ciclos sucessivos e em ambas as direções (oxidação e redução), explorando o comportamento eletroquímico das espécies geradas no eletrodo (HARVEY, 2019; PACHECO et al., 2013). O voltamograma tem picos separados para a reação de oxidação (Ipc) e de

redução (Ipa) (Fig. 3), cada qual caracterizado por um potencial de pico e uma corrente de pico (HARVEY, 2019). A razão entre as correntes de pico e a diferença de pico de potencial nos segmentos catódico (oxidação) e anódico (redução) podem ser usadas para julgar se o sistema eletroquímico é reversível (YANG; ROGACH, 2019). Com isso, a VC se torna uma técnica indispensável na análise de superfícies e das reações ocorrendo através delas.

Figura 3. Voltamograma cíclico demonstrando as correntes catódica (Ipc) e anódica (Ipa).

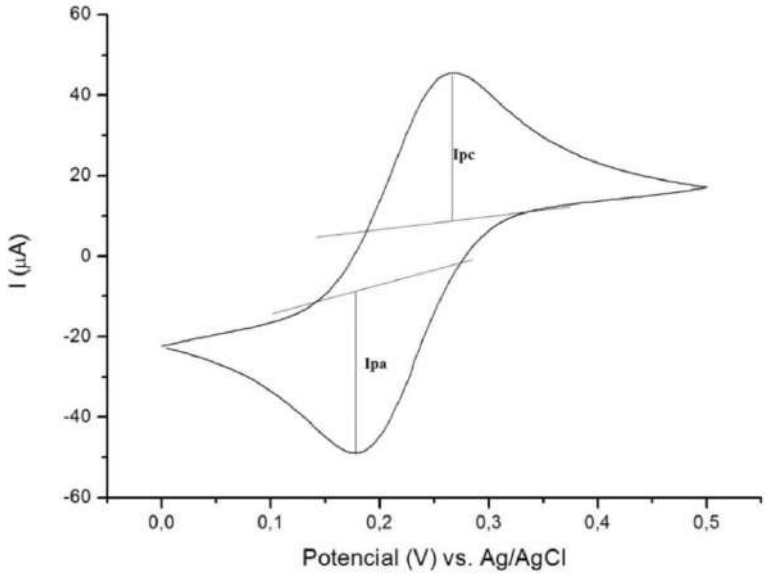

Fonte: TRINDADE, 2015.

Outra técnica de análise eletroquímica é a Voltametria de Onda Quadrada (VOQ), a qual é considerada a mais avançada e mais sofisticada técnica dentre as voltametrias (GULABOSKI; PEREIRA, 2008; MIRCESKI et al., 2013). Esta é uma técnica eletroquímica adequada para aplicação analítica, estudo mecanístico de processos de eletrodos e medições eletrocinéticas (MIRCESKI et al., 2013). A corrente de pico obtida na VOQ depende de vários parâmetros inter-relacionados, como a frequência e a amplitude, por exemplo, os quais têm uma influência combinada

na resposta da corrente de pico (AMMAR et al., 2016). A VOQ envolve a aplicação de repetidos pulsos de potencial simétricos sobrepostos em uma varredura de potencial em escada, a qual permite a discriminação efetiva de processos faradáicos de correntes (DAUPHIN-DUCHARME et al., 2017; GULABOSKI; PEREIRA, 2008). Isso é obtido impondo dois pulsos opostos de onda quadrada da mesma altura em cada degrau em potencial da escada e medindo a corrente resultante no final de cada pulso (Fig. 4) (DAUPHIN-DUCHARME et al., 2017). Desta forma, a VOQ é considerada uma das técnicas de voltametria mais sensíveis, sendo capaz de observar pequenas variações de corrente na superfície eletródica.

Figura 4. Representação do funcionamento de uma voltametria de onda quadrada.

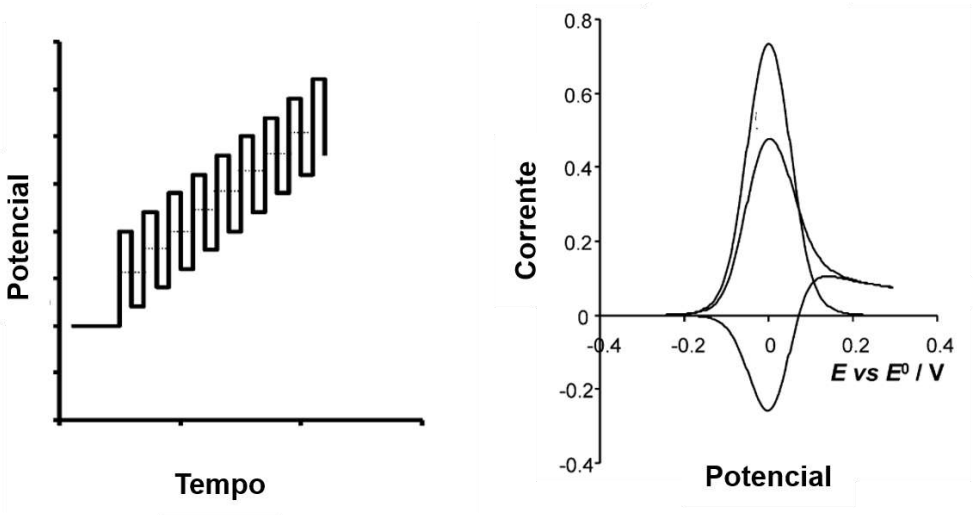

Fonte: Adaptado de MIRCESKI et al., (2013).

Também há de se falar na Espectroscopia de Impedância Eletroquímica (EIS – do inglês Electrochemical Impedance Spectroscopy), a qual é mais uma técnica de caracterização eletroquímica, considerada extremamente sensível (LASIA, 2017). Em eletroquímica, a EIS é aplicada na caracterização de eletrodos e interfaces complexas, e a resposta do sistema permite informações sobre a interface eletrodo-meio e as reações nele contidas (BARDINI, 2015). A EIS estuda a resposta do sistema em relação à aplicação de uma corrente alternada de pequena amplitude, e as medições são feitas em diferentes frequências (LASIA, 2017). Esse método é

dependente da resistência de transferência de carga (R_{ct}), que ocorre na interface eletrodo-meio, sendo que a natureza isolante de certos materiais e biomoléculas tendem a aumentar a resistência (Fig. 5) (MESSINA; FITZGERALD; MOORE, 2016; WANG et al., 2017). Do ponto de vista experimental, um potencial é aplicado e uma corrente variando de forma similar é registrada. No entanto, a resposta do sistema a uma mudança no potencial não é instantânea, isso faz com que a corrente se atrase. Isso se deve à contribuição capacitiva que ocorre na célula eletroquímica: a carga e a descarga de um capacitor relativas às mudanças de potenciais não são um processo instantâneo, ocorrendo um atraso na corrente resultante (BARDINI, 2015). Deve-se notar que a impedância de uma série de conexões de resistência e capacitância é uma soma das contribuições desses dois elementos (LASIA, 2017), tornando essa técnica mais sensível a pequenas variações nas concentrações de antígenos e anticorpos ocorridas na superfície eletródica. Imunossensores usando EIS mostraram vantagens sobre outros métodos de detecção de biomoléculas, permitindo alta sensibilidade, detecção rápida, baixo custo relativo e facilidade de miniaturização (WANG et al., 2017).

Figura 5. Gráfico de impedância mostrando menor (a) e maior (b) Rct.

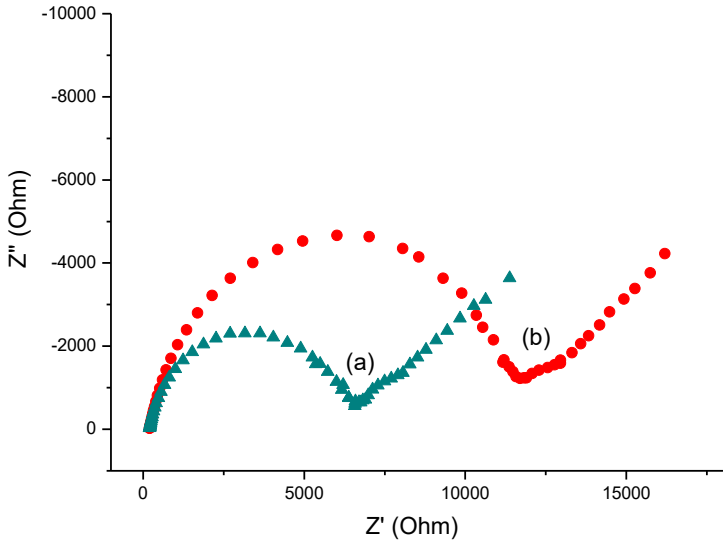

Fonte: Elaborada pela autora (2019).

2.3 CARACTERIZAÇÃO DE SUPERFÍCIES

A caracterização morfológica e estrutural das superfícies modificadas utilizadas em imunossensores são complementos necessários às técnicas de caracterização e detecção eletroquímicas. Elas servem de confirmação aos dados obtidos por outros meios, sendo possível analisar cada etapa de modificação dos eletrodos após a adição de nanomateriais, polímeros ou outras moléculas funcionalizantes. Aqui, após a modificação das superfícies, foram realizadas análises de Infravermelho por transformada de Fourier (FT-IR) e Microscopia de Força Atômica (AFM).

2.3.1 Infravermelho por Transformada de Fourier

A espectroscopia de infravermelho ou Infravermelho por Transformada de Fourier (FT-IR do inglês Fourier-Transform Infrared spectroscopy) é atualmente uma das mais importantes técnicas analíticas disponíveis. Uma das maiores vantagens da espectroscopia de infravermelho é que praticamente qualquer amostra em qualquer estado pode ser analisada, por exemplo, líquidos, soluções, pastas, pós, filmes, fibras, gases e superfícies (FAN; DAI; HUANG, 2012). Esta técnica funciona através da aplicação de radiação com diferentes frequências de infravermelho uma de cada vez, através de uma amostra, observando quais frequências são absorvidas pelo composto. Um detector localizado do lado oposto da amostra analisa os sinais de frequências, sendo que algumas passam pelo composto quase sem perda, mas outras são fortemente absorvidas. Quanto de uma frequência particular passa pelo composto é medido como porcentagem de transmissão (CLARK, 2014). Amostras diferentes apresentam espectros específicos de FT-IR que permitem a sua precisa identificação (Fig. 6).

Figura 6. Demonstração de um espectro de FT-IR de Óxido de Grafeno.

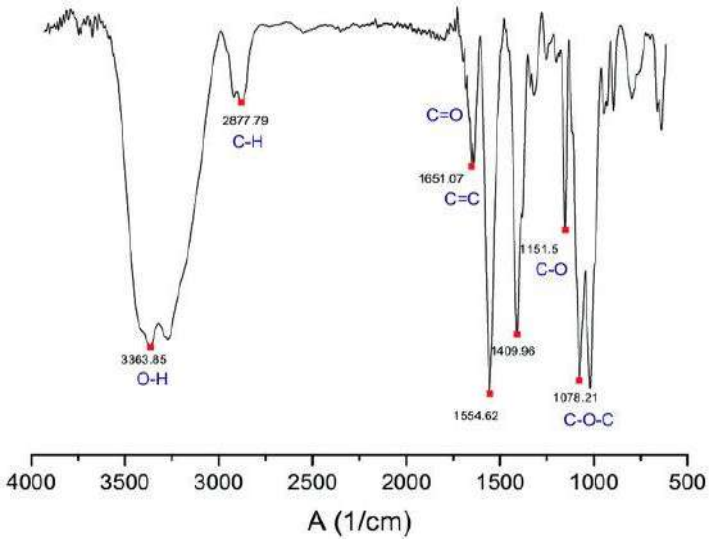

Fonte: VALENCIA et al., (2018).

O equipamento de FT-IR possui diversos acessórios para melhor se adequar aos vários tipos de amostras existentes. O módulo de Reflexão Atenuada Total (ATR) opera medindo as mudanças que ocorrem em um feixe infravermelho (IV) quando o feixe entra em contato com uma amostra. Em regiões do espectro de infravermelho onde a amostra absorve energia, a onda evanescente será atenuada e o feixe atenuado é direcionado ao detector no espectrômetro de IV (BRADLEY, 2002). O detector registra o feixe IV atenuado que pode então ser usado para gerar um espectro IV. O ATR é ideal para amostras fortemente absorventes ou espessas, que geralmente produzem picos intensos quando medidos por transmitância e funciona bem para estas amostras porque a intensidade das ondas evanescentes decai exponencialmente com a distância da superfície do cristal ATR, tornando a técnica geralmente insensível à espessura da amostra (BRADLEY, 2002).

2.3.2 Microscopia de Força Atômica

A Microscopia de Força Atômica (AFM – do inglês Atomic Force Microscopy) foi inventada em 1986 e desde então tem sido amplamente utilizada na área de nanotecnologia, criando novas oportunidades em física, química, biologia e medicina (DUFRÊNE et al., 2017). O AFM pode realizar o contorno de superfícies não-condutoras de estado sólido em resolução atômica, sem necessidade de um tratamento prévio da amostra e em condições ambientes, podendo ser usado para quantificar e mapear simultaneamente suas propriedades físicas, químicas ou biológicas (ALSTEENS et al., 2017; GIESSIBL, 2003). Na microscopia de força atômica, uma ponta afiada (“tip” sensora) é arrastada por uma superfície usando um sistema de deflexão de feixe de laser onde este laser é refletido da parte de trás da alavanca da “tip” para um detector sensível à posição (Fig. 7). Ao contrário de outras técnicas semelhantes, o AFM não precisa de uma amostra condutora, forças atômicas são usadas para mapear a interação do “tip” com a amostra (NANOSCIENCE INSTRUMENTS, 2019).

Figura 7. Mecanismo de funcionamento de um microscópio de força atômica.

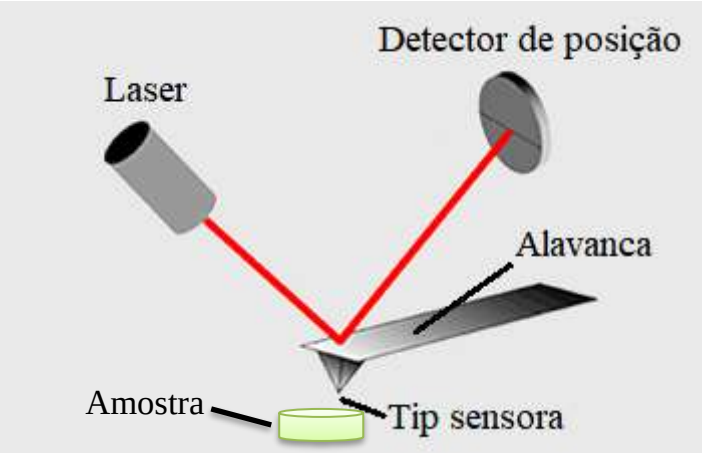

Fonte: Adaptado de NANOSCIENCE INSTRUMENTS, (2019).

2.4 BIOSSENSORES PARA CISTATINA C

Nos últimos anos, o número de pesquisas em biossensores vem crescendo de forma impressionante. Esta é uma área que vem aumentando exponencialmente nas últimas décadas, com o desenvolvimento de novos materiais e métodos de funcionalização de superfícies, ampliando as possibilidades de crescimento em diversas áreas, como saúde, meio ambiente, medicina, agricultura/veterinária e alimentação (RODRIGUEZ et al., 2015). A maioria dos biossensores desenvolvidos em pesquisa, na atualidade, é baseada em reações imunológicas ou hibridização de DNA, e os testes garantem resultados rápidos com grande sensibilidade (TURNER, 2013).

A detecção da cistatina C pode ser feita de maneira direta (através da ligação entre antígeno-anticorpo) ou de maneira indireta (via observação da atividade da enzima papaína ou através de ensaios imunológicos na conformação “sanduíche”). A papaína é uma proteína de 23 kDa, pertencente à família das cisteíno-proteinases (GORODKIEWICZ; LUSZCZYN, 2011). Sendo a CysC uma inibidora de cisteíno-proteinases, sua detecção é feita indiretamente através da observação da diminuição na atividade da papaína (DESAI et al., 2018; LIN et al., 2013). A detecção direta da cistatina C, entretanto, é feita através da ligação entre cistatina C e o anticorpo específico anti-cistatina C. Para a detecção da cistatina C sérica, biossensores, imunoensaios e imunossensores envolvendo as maneiras de detecção direta e indireta foram encontrados na literatura, como visto adiante, observando-se as vantagens e desvantagens de cada método. (Quadro 1).

Quadro 1. Comparação de métodos analíticos para detecção de CysC.

MÉTODO DE DETECÇÃO	MANEIRA DE DETECÇÃO	REFERÊNCIA
ESPECTROSCOPIA RAMAN AMPLIFICADA POR SUPERFÍCIE (ÓPTICO)/ VOLTAMETRIA DE PULSO DIFERENCIAL(ELETROQUÍMICO)	Direta	(HASSANAIN; IZAKE; AYOKO, 2018)
FOTOELETROQUÍMICA	Direta	(MI et al., 2016)
VOLTAMETRIA CÍCLICA/VOLTAMETRIA DE PULSO DIFERENCIAL (ELETROQUÍMICO)	Indireta	(DESAI et al., 2018)
VOLTAMETRIA DE VARREDURA LINEAR (ELETROQUÍMICO)	Indireta	(LOPES et al., 2019)
ELETROQUIMIOLUMINESCÊNCIA (ÓPTICO)	Indireta	(ZHAO et al., 2018)
RESSONÂNCIA DE PLÁSMON DE SUPERFÍCIE (ÓPTICO)	Indireta	(GORODKIEWICZ; LUSZCZYN, 2011)
FLUORESCÊNCIA (ÓPTICO)	Indireta	(LIN et al., 2013)
QUANTUM DOTS NO INFRAVERMELHO PRÓXIMO (ÓPTICO)	Indireta	(TAO; ZHAO; ZENG, 2016)
VOLTAMETRIA DE PULSO DIFERENCIAL (ELETROQUÍMICO)	Indireta	(YANG et al., 2016)

Fonte: Adaptada de TRINDADE; SILVA; DUTRA, 2019.

Em um dos trabalhos, YANG et al., (2016) realizaram a detecção via deslocamento da fita de DNA induzida por uma imunorreação e amplificação enzimática cíclica da proteína T7 Exonuclease. Este método, porém envolve diversos passos para leitura do analito, tornando-se um ensaio demorado. DESAI et al., (2018), por sua vez, desenvolveu um ensaio empregando o eletrodo impresso baseado em $K_3[Fe(CN)_6]$ como indicador. Embora ambos tenham atingido um alcance ótimo e um baixo limite de detecção, o uso de papaína como elemento de biorreconhecimento torna os biossensores limitados para o uso somente na urina. Assim, medidas em amostras com contaminantes proteicos como o soro são restritivas. No seu trabalho, LOPES et al., (2019) usaram eletrodos impressos para desenvolver um imunossensor eletroquímico usando um ensaio do tipo sanduíche para a cistatina C. Nanopartículas de ouro foram eletrodepositadas no eletrodo e usadas para imobilizar o anticorpo de captura, que foi então acoplado à CysC. A detecção foi realizada por anti-CysC biotinilado utilizando uma enzima marcada com estreptavidina. Esta abordagem requer diversos passos para alcançar a detecção da CysC, o que a torna muito demorada. Abordagens ópticas utilizando ressonância de plásmon de superfície (SPR) também foram aplicadas, como no trabalho de GORODKIEWICZ e LUSZCZYN (2011), entretanto, este também tem a desvantagem de utilizar a papaína. LIN et al., (2013) realizaram uma detecção óptica com nanopartículas usando também a detecção indireta. TAO; ZHAO; ZENG, (2016), por sua vez, utilizaram pontos quânticos de infravermelho próximo para detecção de CysC através da papaína. Outra abordagem de detecção óptica foi realizada por HASSANAIN et al. (2018), que usaram Espectroscopia Raman Amplificada por Superfície e Voltametria de Pulso Diferencial para a detecção de CysC. MI et al., (2016) utilizou “nanocorpos” específicos de CysC e alcançaram baixos limites de detecção em uma transdução óptica baseada na redução da fotocorrente usando uma estação de trabalho eletroquímica para medir a fotocorrente sob irradiação de luz visível com uma lâmpada de 150W Xe. Entretanto, a SPR e outros biossensores ópticos em geral têm a desvantagem de serem de mais difícil miniaturização para utilização como verdadeiro dispositivo “point-of-care” em imunossensores (HUNT; ARMANI, 2010; KIRSCH et al., 2013).

Este campo de detecção “point-of-care”, especialmente no que trata da detecção “label-free”, está passando por um grande progresso nos últimos anos. Parte

deste progresso envolve o desenvolvimento de novos métodos de detecção e nanomateriais, e o uso de novas técnicas de modificação eletródica, bem como o uso de polímeros, facilitando a modificação eletródica com moléculas e materiais (via ligações covalentes, camadas auto-organizadas, entre outros) (REVERTÉ; PRIETO-SIMÓN; CAMPÀS, 2016; SHRIVASTAVA; JADON; JAIN, 2016).

2.5 NANOMATERIAIS

Nanomateriais são materiais funcionais com características únicas relacionadas à sua forma, estrutura e tamanho (na ordem de 1 a 100 nm). Estes vêm sendo aplicados em diversas áreas, entre elas eletrônica, optoeletrônica e biologia. A contribuição dos nanomateriais permitiu o desenvolvimento de imunossensores robustos, levando a plataformas com um limite de detecção cada vez menor (RODRIGUEZ et al., 2015). Os nanomateriais também contribuíram para aumentar a sensibilidade dos biossensores, devido às suas propriedades elétricas, ópticas, acústicas e outras, que são capazes de produzir dispositivos com resultados mais reprodutíveis (CABRAL et al., 2018). Logo, vários nanomateriais têm sido utilizados no desenvolvimento de imunossensores nas últimas décadas, ocasionando diversas variações nas combinações com polímeros e outras moléculas funcionalizantes.

2.5.1 Nanopartículas de silício

As nanopartículas de sílica mesoporosa (MSNs – do inglês Mesoporous Silica Nanoparticles) foram descobertas nos anos 90 e muito estudadas devido a suas características especiais, como alta estabilidade mecânica e térmica, grande área de superfície e flexibilidade para modificações em sua superfície (KHALILZADEH et al., 2016; MEHMOOD, 2017). A primeira MSN desenvolvida, o material cristalino móvel (MCM-41) (Fig. 8), tem sido utilizado em muitas aplicações desde então, como liberação de drogas, imagem e biosensoriamento (KHALILZADEH et al., 2016). Estas muitas aplicações são possíveis devido à sua grande eficácia na imobilização de proteínas e excelente transferência de elétrons (OMIDFAR et al., 2012).

Figura 8. Representação de material cristalino móvel (MCM-41).

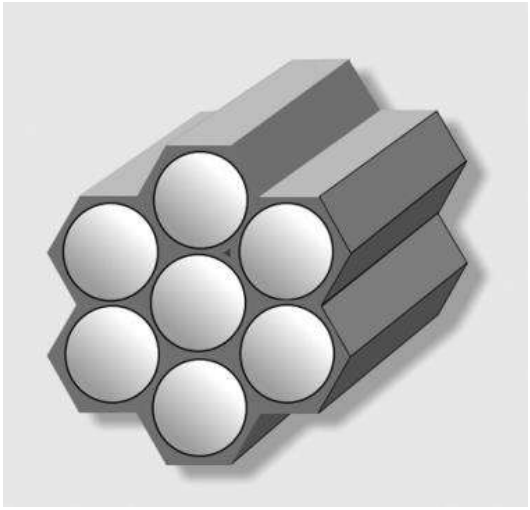

Fonte: HOFFMANN et al., 2010.

O MCM-41 possui poros cilíndricos regulares que formam um sistema de poros unidimensional bem definido, com o tamanho dos poros variando de 2 a 10 nm e com formatos 2D hexagonais e 3D cúbicos (KHALILZADEH et al., 2016; MEHMOOD, 2017). A presença de numerosos grupamentos silano na superfície do MCM-41 torna possível a fácil modificação e funcionalização destes com muitas funções orgânicas (SZEGEDI et al., 2011). As rotas mais usuais para modificação de superfície de MSNs usam a ligação entre esses grupamentos silano superficiais e agentes de acoplamento de silano, sendo o mais comum o aminopropil-trietoxisilano (APTES) (ENACHE et al., 2018), o qual possui funções amina em seus terminais. Isso permite a formação de ligações amida (ligação covalente forte) com moléculas biológicas, outros nanomateriais ou polímeros que possuam grupos carboxila em suas extremidades.

2.5.2 Óxido de grafeno

O óxido de grafeno (GO do inglês Graphene Oxide) é uma folha planar de carbono com átomos densamente empacotados em um padrão hexagonal com ligações sp2 regulares (Fig. 9), que foi produzido em laboratório pela primeira vez em 2004 (NOVOSELOV et al., 2004; YAO et al., 2012). Apesar de o óxido de grafeno

reduzido (RGO) ter uma melhor resposta eletrocatalítica, o GO em sua forma não-reduzida ainda é amplamente utilizado devido à presença de grupos funcionais e maior facilidade de produção (RODRIGUEZ et al., 2015). A síntese de GO é simples e rápida, e tem sido uma alternativa à produção em massa de grafeno. O GO é produzido a partir da oxidação do grafite e tem grupos funcionais de oxigênio polar, rico em ácidos carboxílicos nas suas bordas, e grupos epóxi e hidroxilo em seus planos basais, o que concede muitas rotas de funcionalização e boa dispersão na água (RODRIGUEZ et al., 2015; ZHU et al., 2010). Além disso, os grupos funcionais são responsáveis pela esfoliação do grafite, visto que aumentam a distância interplanar devido à formação de ligações de hidrogênio entre as folhas de grafite. As ligações de hidrogênio são fracas e podem ser facilmente quebradas por banho de ultrassom, resultando em monocamadas ou algumas folhas de carbono, que ficaram conhecidas como GO (RODRIGUEZ et al., 2015; ZHU et al., 2010).

Figura 9. Representação de uma folha de grafeno.

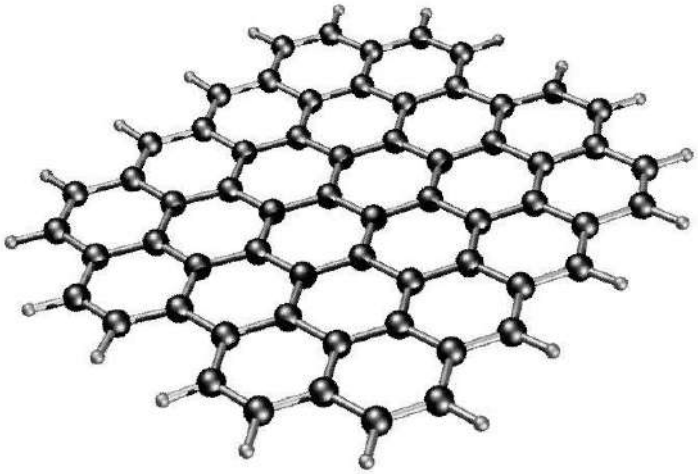

Fonte: YAN; BARRON, 2010.

O GO atraiu atenção incomum devido à sua alta área de superfície teórica, excelente condutividade elétrica, alta estabilidade química, forte resistência mecânica e o fato de que o carbono é um dos elementos mais baratos e abundantes. A excelente transferência de elétrons entre grafeno e grupos funcionais é importante para a

aplicação de materiais à base de grafeno em eletrônicos, sensores e biossensores, uma vez que facilita a deslocalização de elétrons (RABTI; RAOUAFI; MERKOÇI, 2016; RODRIGUEZ et al., 2015; SONG et al., 2016). Este é um excelente material para aplicações biológicas atribuídas aos grupos funcionais que interagem prontamente com ácidos nucleicos, proteínas, células e outras moléculas orgânicas (SHRIVASTAVA; JADON; JAIN, 2016). No entanto, o GO não é um bom condutor elétrico devido à ruptura de sua ligação de sp2 à medida que os grupos funcionais aumentam. Assim, por vezes é feita a funcionalização do óxido de grafeno com diferentes moléculas e polímeros (RODRIGUEZ et al., 2015; SHRIVASTAVA; JADON; JAIN, 2016; ZHU et al., 2010).

2.6 AGENTES FUNCIONALIZANTES E POLÍMEROS

Os passos de imobilização de biomoléculas são considerados cruciais no desenvolvimento de biossensores estáveis e reprodutíveis (TRINDADE; DUTRA, 2018). A imobilização orientada e não-aleatória de antígenos ou anticorpos é de extrema importância, visto que a porção de ligação deve permanecer exposta para que ocorra o fenômeno de biorreconhecimento. Por isso, agentes funcionalizantes de superfícies e polímeros têm sido amplamente empregados em imunossensores para garantir o ancoramento orientado e estável de biomoléculas. Por outro lado, esses polímeros e funcionalizantes podem oferecer outras vantagens, como aumento da transferência de elétrons, da área superficial ou atividade catalítica inerente.

2.6.1 Agentes de funcionalização espaçadores

Uma ligação estável entre a superfície do eletrodo e nanomateriais pode ser alcançada através da funcionalização do eletrodo via tratamentos químicos. Espaçadores químicos são moléculas flexíveis comumente imobilizadas como intermediárias entre a superfície sensora e a biomolécula ou o nanomaterial,

oferecendo mobilidade e liberdade de orientação estrutural (RÓZ et al., 2015). Um tipo de espaçador químico são as monocamadas auto-organizadas (SAMs – do inglês Self-assembled Monolayers). Estas têm sido utilizadas há bastante tempo para esse fim no desenvolvimento de imunossensores eletroquímicos (DUFFY; MOORE, 2017). As SAMs têm sido intensivamente estudadas para técnicas de nanofabricação, pois podem ser adaptadas para promover ou resistir à adesão de substâncias específicas em nível molecular (HARNETT; SATYALAKSHMI; CRAIGHEAD, 2001). Elas são formadas por interações entre moléculas que se organizam em um arranjo estável e bem definido em diferentes substratos (Fig. 10), sendo que a ordem superficial e a estabilidade das SAMs (REYES-CUELLAR, 2017) as tornam úteis para garantir a imobilização orientada de materiais e biomoléculas.

Figura 10. Representação básica de uma monocamada auto-organizada.

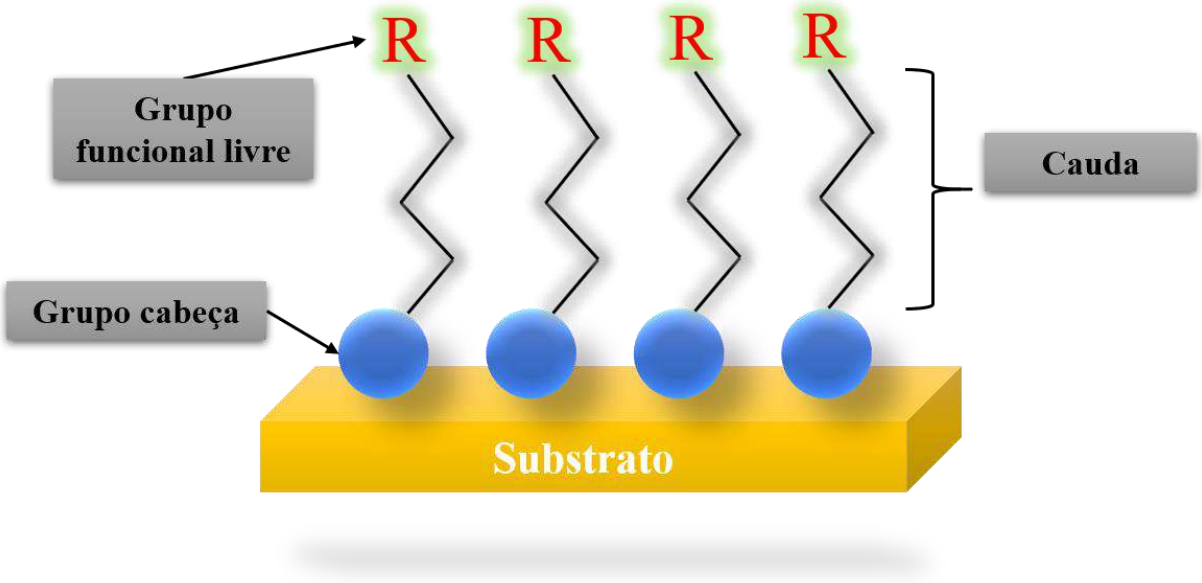

Fonte: Elaborada pela autora (2019).

Vários compostos podem ser utilizados na obtenção de SAMs, podendo-se citar os alquil-trietoxisilanos, os quais têm sido usados para formar SAMs em superfícies de sílica, metal e vidro (REYES-CUELLAR, 2017). O aminopropil-trietoxisilano (APTES) é um material composto por grupamentos silano em uma ponta, os quais reagem facilmente com outros grupamentos silano, e uma terminação amina livre na outra. Isso faz do APTES um dos compostos mais utilizados na funcionalização de

superfícies de sílica e vidro (DE MORAES; KUBOTA, 2016; ENACHE et al., 2018), podendo inclusive ser usado para funcionalizar superfícies de nanomateriais de sílica (como por exemplo nanopartículas de silício). As SAMs de APTES apresentam alta estabilidade e resistência ao aumento da temperatura, e o material funcionalizado exibe um grupo amino terminal de acoplamento direto (REYES-CUELLAR, 2017).

Outros compostos que podem ser utilizados na formação de SAMs são os tióis de cadeia curta como o ácido mercaptopropiônico (MPA – do inglês Mercaptopropionic Acid), que têm sido altamente utilizados para aplicações em imunossensores, devido à forte ligação covalente formada em superfícies de ouro (ligação S-Au), permitindo a fixação bem orientada nas superfícies dos eletrodos e deixando grupos carboxílicos funcionais livres para ligações com outros compostos, materiais ou anticorpos, oferecendo a possibilidade de uma plataforma mais estável e com espaçamento bastante regular (DUFFY; MOORE, 2017; SINGH et al., 2014). No desenvolvimento de biossensores, a presença de grupamentos funcionais livres pode permitir a ligação de nanomateriais ou anticorpos, os quais podem possuir grupamentos amina ou carboxílicos em suas extremidades. A ligação da amina com o grupamento carboxil permite uma ligação covalente amida (SILVA et al., 2013), a qual é considerada extremamente estável. Outras formas de funcionalização de superfície que permitem a obtenção de grupamentos funcionais livres envolvem a utilização de polímeros ou materiais que sejam aminados ou carboxilados.

2.6.2 Ferroceno

Uma desvantagem da detecção amperométrica para biossensores em geral é que requer um indicador redox para obter a leitura, causando dificuldades para medições em amostras reais, isto é, sangue ou soro. Para contornar essas

dificuldades, moléculas redox ativas, como unidades de ferroceno (Fc), podem ser ligadas a nanomateriais como centro de atividade eletroquímica sem sonda redox externa (YAMANAKA; VESTERGAARD; TAMIYA, 2016). O ferroceno (diciclopentadienil-ferro) foi o primeiro derivado de hidrocarboneto puro de ferro a ser preparado pela química moderna, e o crescimento rápido da química organometálica é muitas vezes atribuído ao excitamento vindo da descoberta do ferroceno e seus análogos. Desde a sua descoberta acidental em 1951, muitos derivados foram sintetizados e caracterizados. A química do ferroceno e seus derivados é agora bem conhecida, e são apreciados pela excelente estabilidade. Eles são de interesse considerável em várias áreas, como a eletroquímica, devido à oxidação quase reversível do ferro II. No ferroceno, dois anéis ciclopentadienil estão presos a lados opostos de um átomo de ferro intercalado no centro, sendo também conhecidos com compostos sanduíche (Fig. 11 (a)). O plano de cada anel é perpendicular à ligação metal-ligando com os cinco átomos de carbono aproximadamente equidistantes do metal (FERY-FORGUES; DELAVAUX-NICOT, 2000; LU et al., 2015).

Figura 11. Representação de (a) ferroceno e (b) aminoferroceno.

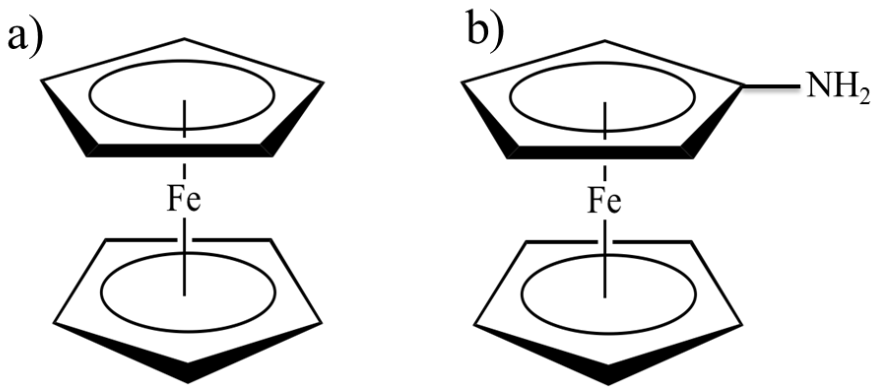

Fonte: Adaptado de SIGMA-ALDRICH, 2017.

As características eletroquímicas atrativas exibidas pelo ferroceno, isto é, taxa de transferência de elétrons rápida, baixo potencial de oxidação e estabilidade de dois estados redox faz com que o ferroceno e seus derivados sejam conhecidos como substâncias mediadoras. E assim, a fração ferro é geralmente usada como uma molécula redox para caracterizar a efetividade da modificação de nanomateriais de

carbono, pois tem estabilidade química e eletroquímica (RABTI; RAOUAFI; MERKOÇI, 2016).

Os mediadores baseados em ferroceno são amplamente utilizados para construir biossensores amperométricos, uma vez que são excelentes na transferência de elétrons. A necessidade do desenvolvimento de métodos de funcionalização de materiais e polímeros para aplicações em biossensores é porque permite a incorporação de reagentes mediadores (DERVISEVIC et al., 2015; RABTI et al., 2016). O aminoferroceno, derivado do ferroceno funcionalizado com um grupamento amina (Fig. 11 (b)), permite uma ligação covalente com nanomateriais (LU et al., 2015; RABTI; RAOUAFI; MERKOÇI, 2016), levando a uma maior estabilidade de ligação com a plataforma e desenvolvimento de nanocompósitos com atividade redox inerente, proporcionando um excelente avanço no campo de imunossensores eletroquímicos para detecção em tempo real.

2.6.3 Polietilenimina

As biomoléculas podem ser incorporadas na plataforma sensora por meio de várias estratégias, sendo que a ligação covalente é a abordagem mais utilizada para modificações na superfície do eletrodo, devido à necessidade de uma imobilização orientada da biomolécula, como mencionado anteriormente. Isto geralmente envolve a ativação da superfície ou da molécula e remoção daquelas que estão fracamente ligadas, formando superfícies muito mais estáveis (LI et al., 2017; LOJOU; BIANCO, 2006; MENDES, 2006; SINGH et al., 2014).

Os polímeros exercem um papel importante na estruturação das superfícies dos eletrodos imunossensores devido a atuar como âncoras verdadeiras para nanomateriais e/ou biomoléculas, resultando em resposta sensora mais regular devido a uma imobilização orientada (GOMES-FILHO et al., 2013; LOJOU; BIANCO, 2006). A polietilenimina (PEI) é um polímero sintético policatiônico que consiste em apenas aminas primárias no caso do PEI de cadeia linear ou aminas primárias, secundárias e terciárias para PEI ramificado (Fig. 12) (SCHULZ; LUDWIG; GORTON, 2014; TAVAHODI et al., 2016).

Figura 12. Estrutura molecular da polietilenimina de cadeia ramificada.

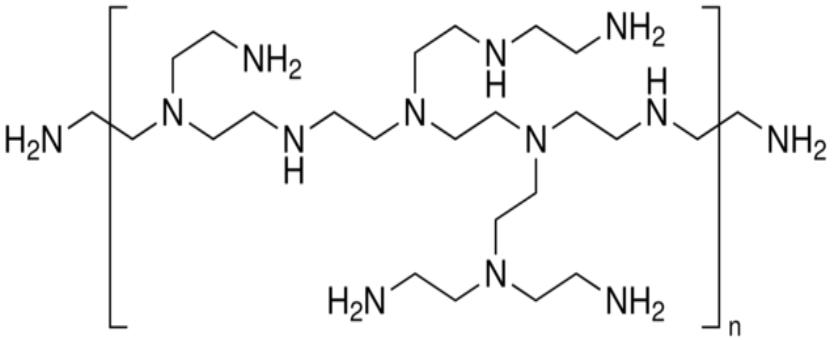

Fonte: LI et al., 2012.

O PEI de cadeia ramificada é constituído por uma alta densidade de grupamentos cátions e aminas, que tornam o PEI completamente miscível com água à temperatura ambiente. Este polímero é frequentemente usado no desenvolvimento de imunossensores devido a suas cargas positivas em pH neutro e suas propriedades adesivas (SCHULZ; LUDWIG; GORTON, 2014; TAVAHODI et al., 2016). Ademais, a presença de abundantes grupamentos amina nas extremidades do PEI facilita a imobilização de biomoléculas de forma orientada, permitindo uma maior sensibilidade do imunossensor (REVERTÉ; PRIETO-SIMÓN; CAMPÀS, 2016).

No campo de biossensores eletroquímicos, busca-se cada vez mais por alternativas com alta estabilidade, maior área para imobilização de biomoléculas e sensibilidade na detecção de variações analíticas. Têm-se buscado o desenvolvimento de estratégias de detecção utilizando inúmeros nanomateriais, polímeros e moléculas funcionalizantes, que promovam o avanço no campo de detecção eletroquímica “point-of-care”, visando o diagnóstico diversas doenças. No caso das doenças renais, alguns biossensores foram desenvolvidos, porém esta ainda é uma área que deve ser bastante explorada nos próximos anos. Devido ao envelhecimento da população, com consequente aumento de doenças metabólicas como diabetes, hipertensão, doenças cardíacas e câncer, é esperado também o aumento no número de pacientes com falha renal decorrentes diretamente destas doenças ou como consequência de infecções, especialmente em pacientes

hospitalizados e em unidades de terapia intensiva. O monitoramento da função renal, portanto, se faz imprescindível para um melhor prognóstico e qualidade de vida desses pacientes.

3 OBJETIVOS

3.1 GERAL

Desenvolver plataformas eletroquímicas nanoestruturadas para a imobilização de anticorpos anti-CysC, visando à elaboração de nanoimunossensores para o diagnóstico e acompanhamento de doenças renais.

3.2 ESPECÍFICOS

a) Realizar o estudo do estado da arte para biossensores de cistatina C, observando os avanços obtidos até presente data;
b) Realizar a funcionalização do MCM-41 com SAMs de APTES para posterior uso no desenvolvimento de plataforma sensora;
c) Desenvolver eletrodo nanoestruturado com SAMs de MPA visando a imobilização do MCM-41 funcionalizado para detecção impedimétrica de analito;
d) Estudar a funcionalização do GO com Fc para formação de nanocompósito redox-ativo;
e) Produzir superfície nanoestruturada com nanocompósito de GO-Fc no desenvolvimento de imunossensor para detecção de analito sem sonda redox;
f) Otimizar os parâmetros experimentais, tais como velocidade de varredura, concentrações e estudos de estabilidade;
g) Caracterizar as etapas de imobilização por técnicas eletroquímicas, microscópicas e estruturais;
h) Realizar a imobilização dos anticorpos anti-CysC;
i) Avaliar a resposta analítica dos imunossensores a diferentes concentrações de CysC e estabelecer as curvas analíticas de detecção.

CONCLUSÕES

No presente trabalho, foi desenvolvido um imunossensor baseado em nanopartículas de silício, na busca pelo desenvolvimento de um sensor eletroquímico impedimétrico para detecção direta de anti-CysC. O MCM-41 teve sua superfície funcionalizada com APTES-SAMs, o que permitiu a presença de grupamentos amina na sua superfície para uma imobilização regular e estável das biomoléculas. O aumento da área superficial promovido por estas nanopartículas levou a um aumento da sensibilidade devido ao maior número de anticorpos imobilizados. A detecção eletroquímica impedimétrica se mostrou sensível para pequenas variações na concentração da Cistatina C, com uma faixa de detecção linear variando de 0,2 a 1,0 µg/mL, com limite de detecção (LOD) de 0,06 µg/mL. No segundo trabalho, o óxido de grafeno foi funcionalizado com êxito utilizando aminoferroceno, o que permitiu o desenvolvimento de uma plataforma de imobilização nanoestruturada para detecção CysC. Esta plataforma foi capaz de leituras sem sondas redox, devido à atividade redox inerente do Fc ligado covalentemente com os grupos carboxílicos presentes no GO. O filme de PEI depositado sobre o nanocompósito deixou suficientes grupos amina livres para ligar aos grupos carboxílicos presentes no final da cadeia pesada dos anticorpos, possibilitando uma imobilização orientada. Este imunossensor mostrou uma resposta linear de 0,1 a 1000 ng/mL e LOD de 0,03 ng/mL de CysC. Suas vantagens incluem teste rápido com etapas mínimas pelo simples uso de uma superfície redox com espécies eletroativas liberadas em potencial de redução, evitando potenciais interferentes na leitura em soro. Ambas as plataformas se encontram de acordo com os níveis clínicos de referência (0.51 a 1.02 µg/mL), sendo que estas metodologias podem ser consideradas excelentes alternativas para complementar e auxiliar a detecção precoce de falha renal. Por fim, foi realizada uma ampla revisão bibliográfica focada no estado da arte dos biossensores para Cistatina C, o qual foi abarcado em um artigo de revisão sobre o tema.

REFERÊNCIAS

AFKHAMI, A. et al. Impedimetric immunosensor for the label-free and direct detection of botulinum neurotoxin serotype A using Au nanoparticles/graphene-chitosan composite. **Biosensors and Bioelectronics**, v. 93, n. June 2016, p. 124–131, 2017.

AHMED, M. U. et al. Toward the development of smart and low cost point-of-care biosensors based on screen printed electrodes. **Critical Reviews in Biotechnology**, v. 00, n. 00, p. 1–11, 2015.

ALSTEENS, D. et al. Atomic force microscopy-based characterization and design of biointerfaces. **Nature Reviews Materials**, v. 2, n. 5, p. 1–16, 2017.

AMMAR, H. B. et al. Boron doped diamond sensor for sensitive determination of metronidazole: Mechanistic and analytical study by cyclic voltammetry and square wave voltammetry. **Materials Science and Engineering C**, v. 59, p. 604–610, 2016.

BARDINI, L. **EIS 101 , an introduction to electrochemical spectroscopy .ResearchGate**, 2015.

BRADLEY, M. **FTIR Sample Techniques: Attenuated Total Reflection (ATR)**. Disponível em: <https://www.thermofisher.com/uk/en/home/industrial/spectroscopy-elemental-isotope-analysis/spectroscopy-elemental-isotope-analysis-learning-center/molecular-spectroscopy-information/ftir-information/ftir-sample-handling-techniques/ftir-sample-handling-tec>. Acesso em: 20 jun. 2019.

CABRAL, D. G. A. et al. Point-of-Care Electrochemical Immunosensors Applied to Diagnostic in Health. In: YURISH, S. Y. (Ed.). . **Advances in Biosensors: Reviews. Volume 2**. [s.l.] IFSA Publishing, S. L., 2018. p. 43–63.

ÇEVIK, E. et al. Construction of novel electrochemical immunosensor for detection of prostate specific antigen using ferrocene-PAMAM dendrimers. **Biosensors and Bioelectronics**, v. 86, p. 1074–1079, 2016.

CHAWLA, L. S. et al. Acute Kidney Injury and Chronic Kidney Disease as Interconnected Syndromes. **New England Journal of Medicine**, v. 371, n. 1, p. 58–66, 2014.

CHAWLA, L. S. et al. Acute kidney disease and renal recovery: Consensus report of the Acute Disease Quality Initiative (ADQI) 16 Workgroup. **Nature Reviews Nephrology**, v. 13, n. 4, p. 241–257, 2017.

CHO, I. et al. Current Technologies of Electrochemical Immunosensors : Perspective on Signal Amplification. **Sensors (Basel, Switzerland)**, v. 18, n. 207, p. 1–18, 2018.

CHOCARRO-RUIZ, B. et al. Nanophotonic label-free biosensors for environmental monitoring. **Current Opinion in Biotechnology**, v. 45, p. 175–183, 2017.

CLARK, J. **What is an infra-red spectrum?** Disponível em:

<https://www.chemguide.co.uk/analysis/ir/background.html>. Acesso em: 13 abr. 2018.

COCA, S. G.; SINGANAMALA, S.; PARIKH, C. R. Chronic kidney disease after acute kidney injury: A systematic review and meta-analysis. **Kidney International**, v. 81, n. 5, p. 442–448, 2012.

DAUPHIN-DUCHARME, P. et al. Simulation-Based Approach to Determining Electron Transfer Rates Using Square-Wave Voltammetry. **Langmuir**, v. 33, n. 18, p. 4407–4413, 9 maio 2017.

DE MORAES, A.; KUBOTA, L. Recent Trends in Field-Effect Transistors-Based Immunosensors. **Chemosensors**, v. 4, n. 4, p. 20, 2016.

DE MOURA, L. et al. Dialysis for end stage renal disease financed through the Brazilian National Health System, 2000 to 2012. **BMC nephrology**, v. 15, p. 111, 2014.

DELANAYE, P. et al. Detection of decreased glomerular filtration rate in intensive care units: serum cystatin C versus serum creatinine. **BMC Nephrology**, v. 15, n. 1, p. 9, 2014.

DERVISEVIC, M. et al. Construction of novel xanthine biosensor by using polymeric mediator/MWCNT nanocomposite layer for fish freshness detection. **Food Chemistry**, v. 181, p. 277–283, 2015.

DESAI, D. et al. Ultrasensitive sensor for detection of early stage chronic kidney disease in human. **Biosensors and Bioelectronics**, v. 105, n. January, p. 90–94, 2018.

DUFFY, G. F.; MOORE, E. J. Electrochemical Immunosensors for Food Analysis: A Review of Recent Developments. **Analytical Letters**, v. 50, n. 1, p. 1–32, 2017.

DUFRÊNE, Y. F. et al. Imaging modes of atomic force microscopy for application in molecular and cell biology. **Nature Nanotechnology**, v. 12, n. 4, p. 295–307, 2017.

ENACHE, D. F. et al. Schiff base-functionalized mesoporous silicas (MCM-41, HMS) as Pb(ii) adsorbents. **RSC Advances**, v. 8, n. 1, p. 176–189, 2018.

FAN, M.; DAI, D.; HUANG, B. Fourier Transform Infrared Spectroscopy for Natural Fibres. In: **Fourier Transform - Materials Analysis**. [s.l: s.n.]. p. 46–68.

FERY-FORGUES, S.; DELAVAUX-NICOT, B. Ferrocene and ferrocenyl derivatives in luminescent systems. **Journal of Photochemistry and Photobiology A: Chemistry**, v. 132, p. 137–159, 2000.

FONSECA, I. et al. A triple-biomarker approach for the detection of delayed graft function after kidney transplantation using serum creatinine, cystatin C, and malondialdehyde. **Clinical Biochemistry**, v. 48, n. 16–17, p. 1033–1038, 2015.

FOX, J. A. et al. Cystatin C as a marker of early renal insufficiency in children with congenital neuropathic bladder. **The Journal of urology**, v. 191, n. 5 Suppl, p.

1602–1607, 2014.

GAYGISIZ, Ü. et al. Can admission serum cystatin C level be an early marker subclinical acute kidney injury in critical care patients? **Scandinavian Journal of Clinical and Laboratory Investigation**, v. 76, n. 2, p. 143–150, 2016.

GHARAIBEH, K. A. et al. Cystatin C Predicts Renal Recovery Earlier Than Creatinine Among Patients With Acute Kidney Injury. **Kidney International Reports**, v. 3, n. 2, p. 337–342, 2018.

GIESSIBL, F. J. Advances in atomic force microscopy. **REVIEWS OF MODERN PHYSICS**, v. 75, n. July, 2003.

GIFFORD, F. J. et al. Endemic Nephropathy Around the World. **Kidney International Reports**, v. 2, n. 2, p. 282–292, 2017.

GO, A. S. et al. Chronic kidney disease and the risks of death, cardiovascular events, and hospitalization. **The New England journal of medicine**, v. 351, n. 13, p. 1296–1305, 2015.

GOMES-FILHO, S. L. R. et al. A carbon nanotube-based electrochemical immunosensor for cardiac troponin T. **Microchemical Journal**, v. 109, n. 0, p. 10–15, 2013.

GORODKIEWICZ, E.; LUSZCZYN, J. Surface Plasmon Resonance Imaging (SPRI) Sensor for Cystatin Determination Based on Immobilized Papain. **Protein and Peptide Letters**, v. 18, n. 1, p. 23–29, 2011.

GRAMS, M. E. et al. Trends in the prevalence of reduced GFR in the United States: A comparison of creatinine- and cystatin c-based estimates. **American Journal of Kidney Diseases**, v. 62, n. 2, p. 253–260, 2013.

GRUBB, A. et al. Generation of a new cystatin C-based estimating equation for glomerular filtration rate by use of 7 assays standardized to the international calibrator. **Clinical Chemistry**, v. 60, n. 7, p. 974–986, 2014.

GULABOSKI, R.; PEREIRA, C. M. Electroanalytical Techniques and Instrumentation in Food Analysis. In: OTLES, S. (Ed.). . **Handbook of Food Analysis Instruments**. [s.l.] CRC Press, 2008. p. 379–402.

HARNETT, C. K.; SATYALAKSHMI, K. M.; CRAIGHEAD, H. G. Bioactive Templates Fabricated by Low-Energy Electron Beam Lithography of Self-Assembled Monolayers. **Langmuir**, v. 17, n. 12, p. 178–182, 2001.

HARVEY, D. **ANALYTICAL CHEMISTRY 2.0**. [s.l.] LibreTexts, 2019. v. 1

HASSANAIN, W. A.; IZAKE, E. L.; AYOKO, G. A. Spectroelectrochemical Nanosensor for the Determination of Cystatin C in Human Blood. **Analytical Chemistry**, 2018.

HILL, N. R. et al. Global Prevalence of Chronic Kidney Disease – A Systematic Review and Meta-Analysis. **PLoS ONE**, p. 1–18, 2016.

HOEK, F. J. et al. Estimation of residual glomerular filtration rate in dialysis patients from the plasma cystatin C level. **Nephrology Dialysis Transplantation**, v. 22, n. 6, p. 1633–1638, 2007.

HOFFMANN, F. et al. Silica-Based Mesoporous Organic–Inorganic Hybrid Materials. In: **The Supramolecular Chemistry of Organic-Inorganic Hybrid Materials**. [s.l: s.n.]. p. 39–111.

HOSTE, E. A. J. et al. Epidemiology of acute kidney injury in critically ill patients: the multinational AKI-EPI study. **Intensive Care Medicine**, v. 41, n. 8, p. 1411–1423, ago. 2015.

HUNT, H. K.; ARMANI, A. M. Label-free biological and chemical sensors. **Nanoscale**, v. 2, p. 1544–1559, 2010.

JHA, V. et al. Chronic kidney disease: Global dimension and perspectives. **The Lancet**, v. 382, n. 9888, p. 260–272, 2013.

JIANG, R. et al. Detection of Cystatin C biomarker for clinical measurement of renal disease by developed ELISA diagnostic kits. **Journal of Translational Medicine**, v. 12, n. 1, p. 1–8, 2014.

KHALILZADEH, B. et al. Ultrasensitive caspase-3 activity detection using an electrochemical biosensor engineered by gold nanoparticle functionalized MCM-41: Its application during stem cell differentiation. **Sensors and Actuators, B: Chemical**, v. 231, p. 561–575, 2016.

KHORGAMI, Z. et al. Relationship between serum cystatin C and creatinine or dialysis adequacy in patients on chronic maintenance hemodialysis. **Nephro-urology monthly**, v. 5, n. 2, p. 733–5, 2013.

KIRSCH, J. et al. Biosensor technology: recent advances in threat agent detection and medicine. **Chemical Society reviews**, v. 42, n. 22, p. 8733–68, 2013.

KOLODZIEJCZYK, R. et al. Crystal structure of monomeric human cystatin C stabilized against aggregation. **Protein Data Bank**, 2009.

LASIA, A. **Electrochemical Impedance Spectroscopy and Its Applications**. [s.l: s.n.].

LAU, L. et al. Serum cystatin C for acute kidney injury evaluation in children treated with aminoglycosides. **Pediatric Nephrology**, p. 1–9, 2017.

LI, J. et al. Lithium Ion Cell Performance Enhancement Using Aqueous LiFePO4 Cathode Dispersions and Polyethyleneimine Dispersant. **Journal of the Electrochemical Society**, v. 160, n. 2, p. A201–A206, 2012.

LI, X. et al. A sensitive electrochemiluminescence immunosensor based on Ru(bpy)32+ in 3D CuNi oxalate as luminophores and graphene oxide–polyethylenimine as released Ru(bpy)32+ initiator. **Biosensors and Bioelectronics**, v. 89, p. 1020–1025, 2017.

LIN, H. et al. Immune-independent and label-free fluorescent assay for Cystatin C detection based on protein-stabilized Au nanoclusters. **Biosensors and Bioelectronics**, v. 41, n. 1, p. 256–261, 15 mar. 2013.

LOJOU, E.´; BIANCO, P. Application of the electrochemical concepts and techniques to amperometric biosensor devices. **Journal of Electroceramics**, v. 16, n. 1, p. 79–91, 2006.

LOPES, P. et al. Disposable electrochemical immunosensor for analysis of cystatin C, a CKD biomarker. **Talanta**, 2019.

LU, Y. et al. Ferrocene-functionalized graphene oxide nanosheets: Efficient electronic communication between ferrocene centers across graphene nanosheets. **Electrochimica Acta**, v. 156, p. 267–273, 2015.

MEHMOOD, A. Mesoporous Silica Nanoparticles: A Review. 2017.

MENDES, R. K. Investigação dos efeitos dos procedimentos de imobilização em monocamadas auto-organizadas da enzima peroxidase no desenvolvimento de um biossensor. p. 105, 2006.

MESSINA, W.; FITZGERALD, M.; MOORE, E. SEM and ECIS Investigation of Cells Cultured on Nanopillar Modified Interdigitated Impedance Electrodes for Analysis of Cell Growth and Cytotoxicity of Potential Anticancer Drugs. **Electroanalysis**, v. 28, n. 9, p. 2188–2195, 2016.

MI, L. et al. A novel photoelectrochemical immunosensor by integration of nanobody and TiO2 nanotubes for sensitive detection of serum cystatin C. **Analytica Chimica Acta**, v. 902, p. 107–114, 2016.

MIRCESKI, V. et al. Square-Wave Voltammetry : A Review on the Recent Progress. **Electroanalysis**, v. 25, n. 11, p. 2411–2422, 2013.

MOREIRA, F. T. et al. Myoglobin-biomimetic electroactive materials made by surface molecular imprinting on silica beads and their use as ionophores in polymeric membranes for potentiometric transduction. **Biosens Bioelectron**, v. 26, n. 12, p. 4760–4766, 2011.

NANOSCIENCE INSTRUMENTS. **Atomic Force Microscopy - Nanoscience Instruments**. Disponível em: <https://www.nanoscience.com/techniques/atomic-force-microscopy/>. Acesso em: 20 jun. 2019.

NOVOSELOV, K. S. et al. Electric Field Effect in Atomically Thin Carbon Films. **Science**, v. 306, n. 5696, p. 666–669, 2004.

OMIDFAR, K. et al. A high-sensitivity electrochemical immunosensor based on mobile crystalline material-41-polyvinyl alcohol nanocomposite and colloidal gold nanoparticles. **Analytical Biochemistry**, v. 421, n. 2, p. 649–656, 2012.

PACHECO, W. F. et al. Voltametrias: Uma breve revisão sobre os conceitos. **Revista Virtual de Quimica**, v. 5, n. 4, p. 516–537, 2013.

RABTI, A. et al. Ferrocene-functionalized graphene electrode for biosensing applications. **Analytica Chimica Acta**, v. 926, p. 28–35, 2016.

RABTI, A.; RAOUAFI, N.; MERKOÇI, A. Bio(Sensing) devices based on ferrocene–functionalized graphene and carbon nanotubes. **Carbon**, v. 108, p. 481–514, 2016.

RAVN, B. et al. Superiority of Serum Cystatin C Over Creatinine in Prediction of Long-Term Prognosis at Discharge From ICU. **Critical Care Medicine**, v. 1, n. 7, p. 1, 2017.

REVERTÉ, L.; PRIETO-SIMÓN, B.; CAMPÀS, M. New advances in electrochemical biosensors for the detection of toxins: Nanomaterials, magnetic beads and microfluidics systems. A review. **Analytica Chimica Acta**, v. 908, p. 8–21, 2016.

REYES-CUELLAR, J. C. Immobilization of recognition elements on a self-assembled monolayers bio-platform. **Revista DYNA**, v. 84, n. 202, p. 263–269, 2017.

RODRIGUEZ, B. A. G. et al. Nanomaterials for Advancing the Health Immunosensor. In: **Biosensors - Micro and Nanoscale Applications**. [s.l: s.n.]. p. 347–374.

RÓZ, A. L. DA et al. **Grandes áreas da nanociência. Volume 2**. [s.l.] Editora Campus, 2015.

SANG, S. et al. Progress of new label-free techniques for biosensors: a review. **Critical Reviews in Biotechnology**, v. 00, n. 00, p. 1–17, 2015.

SCHULZ, C.; LUDWIG, R.; GORTON, L. Polyethyleneimine as a promoter layer for the immobilization of cellobiose dehydrogenase from myriococcum thermophilum on graphite electrodes. **Analytical Chemistry**, v. 86, n. 9, p. 4256–4263, 2014.

SHARMA, S.; BYRNE, H.; O'KENNEDY, R. J. Antibodies and antibody-derived analytical biosensors. **Essays In Biochemistry**, v. 60, n. 1, p. 9–18, 2016.

SHRIVASTAVA, S.; JADON, N.; JAIN, R. Next-generation polymer nanocomposite-based electrochemical sensors and biosensors: A review. **TrAC - Trends in Analytical Chemistry**, v. 82, p. 55–67, 2016.

SIGMA-ALDRICH. **Ferrocene**. Disponível em: <http://www.sigmaaldrich.com/catalog/product/aldrich/f408?lang=pt&region=BR>. Acesso em: 16 out. 2017.

SILVA, B. V. M. et al. A carbon nanotube screen-printed electrode for label-free detection of the human cardiac troponin T. **Talanta**, v. 117, p. 431–437, 2013.

SINGH, S. et al. Gold–mercaptopropionic acid–polyethylenimine composite based DNA sensor for early detection of rheumatic heart disease. **Applied Biochemistry and Biotechnology**, v. 173, n. 1, p. 228–238, 2014.

SONG, Y. et al. Recent advances in electrochemical biosensors based on graphene two-dimensional nanomaterials. **Biosensors and Bioelectronics**, v. 76, p. 195–212, 2016.

SZEGEDI, A. et al. Effect of amine functionalization of spherical MCM-41 and SBA-15 on controlled drug release. **Journal of Solid State Chemistry**, v. 184, n. 5, p. 1201–1207, 2011.

TAO, J.; ZHAO, P.; ZENG, Q. The determination of cystatin C in serum based on label-free and near-infrared light emitted PbS@BSA QDs. **Journal of Materials Chemistry B**, v. 4, n. 24, p. 4258–4262, 2016.

TAVAHODI, M. et al. Direct Electron Transfer of Cellobiose Dehydrogenase on Positively Charged Polyethyleneimine Gold Nanoparticles. **ChemPlusChem**, p. 1–8, 2016.

TRINDADE, E. K. G. Desenvolvimento de nanoimunossensor para identificação de anticorpos contra o vírus da Hepatite B. **Universidade Federal de Pernambuco**, v. 1, p. 1–74, 2015.

TRINDADE, E. K. G.; DUTRA, R. F. A label-free and reagentless immunoelectrode for antibodies against hepatitis B core antigen (anti-HBc) detection. **Colloids and Surfaces B: Biointerfaces**, v. 172, n. March, p. 272–279, 2018.

TRINDADE, E. K. G.; SILVA, B. V. M.; DUTRA, R. F. A probeless and label-free electrochemical immunosensor for cystatin C detection based on ferrocene functionalized-graphene platform. **Biosensors and Bioelectronics**, v. 138, p. 111311, 1 ago. 2019.

TURNER, A. P. F. Biosensors: sense and sensibility. **Chemical Society reviews**, v. 42, n. 8, p. 3184–96, 2013.

VALENCIA, C. et al. Synthesis and Application of Scaffolds of Chitosan-Graphene Oxide by the Freeze-Drying Method for Tissue Regeneration. **molecules**, v. 25, 2018.

WANG, D. et al. Efficient separation and quantitative detection of Listeria monocytogenes based on screen-printed interdigitated electrode, urease and magnetic nanoparticles. **Food Control**, v. 73, p. 555–561, 2017.

WANG, H.; GAO, X.; MA, Z. Multifunctional substrate of label-free electrochemical immunosensor for ultrasensitive detection of cytokeratins antigen 21-1. **Scientific Reports**, v. 7, n. 1, p. 1–7, 2017.

WANG, J. Electrochemical biosensors: Towards point-of-care cancer diagnostics. **Biosensors and Bioelectronics**, v. 21, n. 10, p. 1887–1892, 2006.

YAMANAKA, K.; VESTERGAARD, M. C.; TAMIYA, E. Printable electrochemical biosensors: A focus on screen-printed electrodes and their application. **Sensors (Switzerland)**, v. 16, n. 10, p. 1–16, 2016.

YAN, Z.; BARRON, A. R. **Characterization of Graphene by Raman Spectroscopy**. Disponível em: <https://cnx.org/contents/8GImxcKk@2/Characterization-of-Graphene-b>. Acesso em: 16 out. 2017.

YANG, X.; ROGACH, A. L. Electrochemical Techniques in Battery Research: A

Tutorial for Nonelectrochemists. **Advanced Energy Materials**, v. 1900747, p. 1–10, 2019.

YANG, Z. H. et al. Highly Effective Protein Converting Strategy for Ultrasensitive Electrochemical Assay of Cystatin C. **Analytical Chemistry**, v. 88, n. 10, p. 5189–5196, 17 maio 2016.

YAO, J. et al. Chemistry, physics and biology of graphene-based nanomaterials: new horizons for sensing, imaging and medicine. **Journal of Materials Chemistry**, v. 22, n. 29, p. 14313–14329, 2012.

ZHAO, M. et al. Monolayer rubrene functionalized graphene-based eletrochemiluminscence biosensor for serum cystatin C detection with immunorecognition- induced 3D DNA machine. **Biosensors and Bioelectronic**, 2018.

ZHU, Y. W. et al. Graphene and Graphene Oxide: Synthesis, Properties, and Applications. **Advanced Materials**, v. 22, n. 46, p. 5226, 2010.

APÊNDICE A – ARTIGO PUBLICADO EM PERIÓDICO

A PROBELESS AND LABEL-FREE ELECTROCHEMICAL IMMUNOSENSOR FOR CYSTATIN C DETECTION BASED ON FERROCENE FUNCTIONALIZED-GRAPHENE PLATFORM

Erika K.G. Trindade, Bárbara V. M. Silva, Rosa F. Dutra

Biosensors & Bioelectronics, 2019

Biosensors and Bioelectronics 138 (2019) 111311

Contents lists available at ScienceDirect

Biosensors and Bioelectronics

journal homepage: www.elsevier.com/locate/bios

A probeless and label-free electrochemical immunosensor for cystatin C detection based on ferrocene functionalized-graphene platform

Erika K.G. Trindade, Bárbara V.M. Silva, Rosa F. Dutra*

Biomedical Engineering Laboratory, Department of Biomedical Engineering, Federal University of Pernambuco, Av. Prof. Moraes Rego, 1235, CEP 50610-970, Recife, Brazil

ARTICLE INFO

Keywords:
Redox probe-free
Cystatin C
Renal failure
Immunosensor
Ferrocene
Graphene

ABSTRACT

A novel electrochemical sensor with inherent redox activity mediated by ferrocene for Cystatin C (CysC), an early kidney failure biomarker, is described. The current response was mediated by graphene oxide-ferrocene nanofilm with redox-activity coming from electroactive species surface-confined. Anti-CysC antibodies were immobilized by their Fc portions on the drop-casting polyethyleneimine (PEI) film for improving the sensitivity and reproducibility. Stepwise modifications of the nanostructured surface were characterized by electrochemical techniques, FT-IR and AFM. FT-IR confirmed the formation of the Fc-GO nanocomposite and PEI deposition on the electrode surface. The AFM micrographs confirmed a nanometric film of Fc-GO and PEI. The sensor platform showed a response from 0.1 to 1000 ng/mL and lower limit of detection (LOD) of 0.03 ng/mL of CysC, with good accuracy, specificity and it was successfully applied for CysC detection. Advantages of this immunosensor include rapid testing with minimal steps by the simple use of an intrinsic redox probe, working in a reduction potential, which avoids potential interferences. This proposal attempts to circumvent amperometric detection limitations and provides a promising candidate for future point-of-care diagnostics without redox probe additional solutions for measurements.

1. Introduction

Studies have shown that the incidence of Acute Kidney Injury (AKI) has been increasing over the last decades and can very likely result in permanent kidney damage (Coca et al., 2012). AKI incidence has been reported to be as high as 20% in the USA and very similar in other countries (Gharaibeh et al., 2018; Hoste et al., 2015). Since AKI is an independent risk factor for Chronic Kidney Disease (CKD), End-Stage Renal Disease (ESRD), cardiac diseases and death, it bears a significant public health concern worldwide (Chawla et al., 2014; Coca et al., 2012; Hoste et al., 2015; Webster et al., 2017). More than half Intensive Care Unit (ICU) patients develop AKI and in-hospital death rates in hospitalized patients with AKI is very high among patients in need of dialysis (Chawla et al., 2014; Hoste et al., 2015). In attempting to increase the chances of patient survival, early detection of renal failure is important and could result in a lower burden for ICU and earlier hospital discharge. Cystatin C (CysC) is a nonglycated 13 kDa protein considered an early marker for AKI related with the glomerular filtration rate (GFR) (Lau et al., 2016; Tao et al., 2016). Evidence has suggested that the increase of serum CysC levels as a marker of renal function may detect kidney dysfunction earlier than creatinine, which is currently the most used diagnostic marker (Gaygisiz et al., 2016). Contrary to creatinine levels, recent studies indicated that serum CysC concentration is more stable and accurate in GFR estimation and is independent of sex, diet and muscle mass (Fox et al., 2014; Mi et al., 2016; Ravn et al., 2017; Shlipak et al., 2013). In this context, the development of a fast and low-cost method for CysC detection is of great importance, aiming to identify early signs of AKI and monitoring of hospitalized patients.

Thus far, a variety of analytic strategies have been used for detection of serum CysC, such as enzyme-linked immunosorbent assay (ELISA), turbidimetric and nephelometric immunoassays (Delanaye et al., 2014; Fonseca et al., 2015; Jiang et al., 2014). However, these are timeconsuming methods and require specialized personnel to operate. Due to this and the great interest in CysC rapid detection, attempts have been made to develop biosensors and immunosensors for CysC. Yang et al. (2016) were able to develop an electrochemical genosensor using gold nanoparticles and iron oxide to amplify the signal. Although the detection limit was low for this work, it is not clinically relevant and the sensor requires many steps for conversion of the signal. Some optical sensors were also developed, such as the work of Gorodkiewicz and Luszczyn (2011) and Tao et al. (2016), which used Surface Plasmon

* Corresponding author.
E-mail address: rosa.dutra@ufpe.br (R.F. Dutra).

https://doi.org/10.1016/j.bios.2019.05.016
Received 1 February 2019; Received in revised form 23 April 2019; Accepted 6 May 2019
Available online 10 May 2019
0956-5663/

Resonance Imaging and Near-Infrared Quantum Dots, respectively, for detection of CysC. The major problem in optical systems is the difficult miniaturization of the methods. In this context, electrochemical amperometric immunosensors have the advantage of specific and sensible detection, easy miniaturization and quick results.

In label-free electrochemical immunosensors, the sensing platform requires transport of the redox species to generate the amperometric signal that is proportional to the diffusion of species on electrode surface hindered by antigen/antibody adsorbed. The redox species are indispensable for label-free electrochemical detection and the most common method is to add the redox species into electrolyte solutions (Wang et al., 2017). One of the drawbacks of this method is that it requires washes and several steps that delay real point-of-care detection. Recently, the focus has been on redox probe-free platform for immunosensing applications (Moreira et al., 2018; Trindade and Dutra, 2018). In this sense, redox active molecules such as ferrocene (Fc) units can be attached to sensor surface as the center for electrochemical activity, dispensing the use of external redox probe as used in conventional immunosensor (Yamanaka et al., 2016). Electrochemistry of ferrocene and its derivatives are well known, and they are appreciated for excellent stability, being of considerable interest in electrochemistry due to the almost reversible oxidation of iron II. This site provides the redox catalytic pair released in electrochemical readings (Fery-Forgues and Delavaux-Nicot, 2000; Lu et al., 2015). The fast electron transfer rate and two-state redox stability are other attractive electrochemical characteristics exhibited by Fc and similar compounds that make them excellent mediators, mainly as used in association with different nanomaterials (Cho et al., 2018; Rabti et al., 2016).

Many strategies based on nanomaterials have been applied in electrochemical immunosensors owing to the improvement of its performances (Amani et al., 2018). Thus far, many nanomaterials have been employed in the development of sensing platforms such as metal oxide nanoparticles (Moreira et al., 2018), noble metal nanoparticles (Vilian et al., 2015) and carbon-based nanomaterials (Roushani and Abdi, 2014). Graphene is a one-atom-thick two-dimensional planar carbon nanosheet. It has attracted attention due to its high surface area and chemical stability. Since the bulk production of graphene is difficult, its derivative Graphene Oxide (GO) is more frequently used due to easy production and presence of functional groups protein-reactive (Rodriguez et al., 2015). Thus, this proof-of-concept study aimed at the functionalization of GO with aminoferrocene (Fc), which appears as an innovative approach to produce a catalytic nanocomposite in order to develop a stable sensor platform. Herein, an electrochemical immunosensor was developed, allowing for Cystatin C detection without the use of redox probes ("redox probe-free").

2. Material and methods

2.1. Reagents

Aminoferrocene (Fc), graphene oxide (GO), polyethyleneimine (PEI), 1-ethyl-3-(3 dimethylaminopropyl) carbodiimide (EDC), N-hydroxysuccinimide (NHS), potassium ferricyanide ($K_3[Fe(CN)_6]$) and potassium ferrocyanide ($K_4[Fe(CN)_6]$) were obtained from Sigma-Aldrich (United States). Cystatin C peptide was obtained from Abcam (United Kingdom). Cystatin C antibody (Anti-CysC) was obtained from Sigma (United States). All other chemicals used were of analytical grade and all the solutions were prepared in ultra-pure water acquired from a Milli-Q station (United States) with a conductivity below 18 MΩ cm^{-1}.

Spiked human serum was used to perform analytical response tests. Serum pool samples were obtained after approval by the Research Ethics Committee of the University of Pernambuco, Brazil. The blood collected from healthy individuals was centrifuged and the serum separated from the blood cells. Positive samples were spiked with CysC diluted in PBS with the same volume to obtain the wished concentrations. Likewise, negative samples were obtained, using the same volume, however without CysC adding. Serum samples were processed and freshly prepared, and all incubations with electrodes were performed at room temperature (approximately 24 °C) at 7.4 pH (Silva et al., 2015).

2.2. Apparatus

Electrochemical measurements were performed in a three-electrode system: helical platinum wire as counter electrode, Ag/AgCl (3 M KCl Sat.) as reference and working gold electrode (GE) (Ø = 1 mm). The electrochemical measurements were performed with a potentiostat/galvanostat Ivium Compact Stat (Eindhoven, Netherlands) coupled to a microcomputer and controlled by the IviumSoft software. Cyclic voltammetry (CV) and square wave voltammetry (SWV) techniques were employed to electrochemically characterize the modifications of the GE. The CV (0.05 V/s scan rate) and SWV (10 Hz frequency and 10 mV pulse amplitude) measurements were carried out at 10 mV step potential with a potential window between −0.3 and 0.2 V in 0.1 M KCl electrolyte.

Morphological analyses of modifications on the GE surface were carried out by means of Atomic Force Microscopy (AFM) in the non-contact mode, using the Nanosurf Flex AFM (Liestal, Switzerland) equipped with a C3000 controller and the TAP190AI-G tip. The images obtained were treated and analyzed by Gwyddion (free version 2.49).

Chemical surface characterization of the platform was accomplished by attenuated total reflectance with Fourier transform infrared spectroscopy (ATR-FTIR) using the Bruker IFS 66 model FT-IR spectrometer (Billerica, USA), set up for spectra from 4000 to 500 cm^{-1}. All AFM images were obtained using a circular gold electrode, with 4 mm diameter made of evaporated gold film onto an acetate sheet.

2.3. Synthesis of PEI/Fc-GO nanostructured surface

Prior to modification, the GE was cleaned by mechanical polishing with 0.5 μm alumina slurry, followed by sonication in distilled water to remove any residual alumina powder. Modifications were performed only after cleaning evaluation with CVs. To confirm GO functionalization, then electrochemical analysis was carried out with three different solutions: GO control, Fc control, and Fc-GO nanocomposite. The Fc-GO nanocomposite was obtained by mixing GO (1 mg/mL, dispersed in water) with Fc in a mixture 1:1 of 20 mM EDC and 50 mM NHS (prepared in acetate buffer 0.037 M, pH 5.0) for 1 h in an ultrasonic bath. Fc concentration was optimized by incubating the GO modified with various concentrations of Fc (0.01; 0.025; 0.05; 0.075; 0.1; 0.2; 0.3 and 0.4 M). The GE surface was modified with 5 μL of the Fc-GO solution by drop casting and dried on the incubator at 50 °C. After the solvent evaporation, the Fc-GO surface was coated with 5 μL of 2% PEI prepared in ethanol and dried at room temperature (approximately 24 °C).

2.4. Immobilization of anti-CysC and analytical measurements

For antibody immobilization, an aliquot (5 μL) of 10 mg/mL anti-CysC solution was pipetted on the nanostructured surface and incubated for 1 h at room temperature (24 °C). In order to block the remaining adsorption-reactive sites, the anti-CysC-immobilized electrode was incubated with a solution of 0.05 M glycine, also prepared in PBS (10 mM, pH 7.4) for 1 h. The electrode was carefully rinsed with distilled water between each step of immunosensor assembly.

The electrochemical detection of CysC was performed by using SWV technique using 0.1 M KCl solution as supporting electrolyte. The as-prepared immunosensor was incubated with 5 μL of CysC peptide PBS diluted at various concentrations (0.1, 1, 10, 50, 100, 500 and 1000 ng/mL) in a moist chamber at 4 °C during 15 min. The analytical response was obtained by the difference of current (ΔI) in the square wave voltammograms (SWV) before (blank) and after the addition of CysC. All graphs and statistical analyses were carried out with Origin Pro 8.0

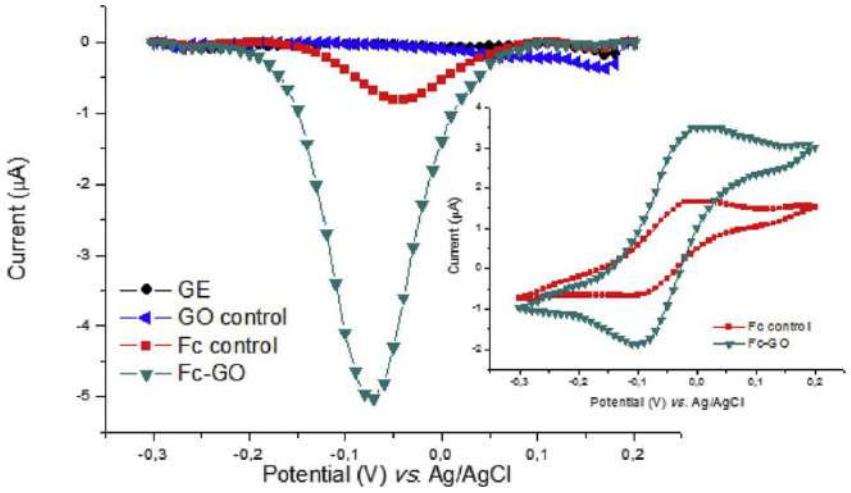

Fig. 1. SWV of the: bare electrode (GE), GO control, Fc control, and Fc-GO nanocomposite; *inset*: CVs of Fc control and Fc-GO nanocomposite showing an increase of electroactive area with Fc-GO nanocomposite.

software.

3. Results and discussion

3.1. Catalytic activity of Fc-GO electrode surface

Fc redox sites generate very distinctive redox pairs with cathodic and anodic peaks at −0.1 V and close to −0.0 V, respectively due to the almost reversible oxidation of iron II, as can be seen in Fig. 1, in which shows SWVs of the bare electrode, GO control, Fc control and Fc-GO nanocomposite, and CVs of Fc control and Fc-GO nanocomposite. All the characterizations were carried out in KCl 0.1 M as supporting electrolyte as means to not interfere with electrochemical activity inherent of Fc. SWV of the bare electrode and GO control show no cathodic peak at the potential attributed to Fc catalytic activity. Furthermore, the functionalization of graphene using Fc allowed for higher electroactive activity than the Fc control, as seen in Fig. 1 and Fig. 1 - *inset*. SWV and CV both showed a current increase after functionalization. This can be attributed to a higher electroactive area provided by GO after stable Fc attachment. The optimal concentration of Fc used for GO functionalization was found at 0.1 M of Fc and used in subsequent experiments based on highest electroactive area.

Fig. 2 (a) shows a schematic representation of nanostructured platform development steps and CV characterization of all the steps is shown in Fig. 2 (b). It can be observed that the deposition of PEI film onto the Fc-GO surface resulted in an increase of 17.8% in the electroactive area compared to Fc-GO (Fig. 2: *inset*). PEI contains a large number of amine groups that act as a crosslinker, attaching the GO by amide bonds while leaving enough amine sites free to bond with the carboxylic groups present at the Fc portion of antibodies. The functionalization of the sensing surface by introducing reactive groups for oriented immobilization of the antibodies is a crucial step to obtain an immunosensor with a high performance (Gomes-Filho et al., 2013). Addition of the antibody, glycine, and readings with CysC resulted in a decrease of the current. This was attributed to electron transfer hindering in the diffusion barrier caused by these molecules, as expected (Valipour and Roushani, 2017).

In presence of 0.1 M KCl, the immobilization of Fc on the graphene was evaluated by scan rate studies varying from 10 to 110 mV/s, at the potential window from −0.3 to 0.2 V (Fig. S1 (a)). Since the plot of the square root of the scan rate vs. current peak exhibited a linear dependence, with square R of 0.987 and 0.915 for anodic and cathodic peaks, respectively, it was concluded that the process was diffusion-controlled (Fig. S1 (b)). Additionally, by obtaining the plot of scan rate vs. log current as seen in Fig. S1 (c); the slope of cathodic and anodic peaks were 0.48 and 0.57, respectively, confirming that current was controlled by diffusion (Tavares et al., 2013), as also observed by studies with ferrocene moieties adsorbed on polyallylamine film (Jingyuan et al., 2006). This remarkable presence of the faradaic current without redox probe in bulk, with current redox peaks kept at a low potential between −0.1 and 0.0 V, and also the potentials of current peaks that practically did not change seemed to indicate a synergic effect between GO and Fc. Cathodic and anodic peaks (Ipc and Ipa, respectively) increased quasi proportional and symmetrically with scan rate (Fig. S1 (b)), The difference between redox peak potential was less 0.10 V, meaning a voltammetric behavior close to the reversible process (Bard and Faulkner, 2001). Reversibility of the Fc on the nanostructured platform was also evaluated by applying 20 consecutive cycles of CVs in a 0.1 M KCl solution (Fig. S2). The coefficient of variation showed good reproducibility for anodic and cathodic current peaks of 2 and 3%, respectively; arguing the chemical stability of Fc. This good stability was attributed to the covalent bond of the Fc-GO, as confirmed by ATR-FTIR.

AFM was used to characterize the morphology of the electrode. As seen in Fig. 3 (b), (c) and (d), the gold surface was fully covered by layers of the GO control, GO-Fc, and PEI/GO-Fc, respectively, all showing increased average roughness (Ra) when compared with the clean electrode (Ra = 1.00 nm ± 0.02) (Fig. 3 (a)), which exhibited a very smooth and regular morphology. Fig. 3 (c) showed a rougher surface (Ra = 1.80 nm ± 0.03) than that showed in (b) (Ra = 1.63 nm ± 0.03), suggesting that Fc allowed for an increase in surface area, when compared with the GO control (Shearer et al., 2016). The PEI film drop-casted on the GO-Fc nanocomposite surface (Fig. 3 (d)) produced a slight increase in roughness (Ra = 1.89 nm ± 0.04) compared to GO-Fc surface (Lau et al., 2018).

ATR-FTIR has been a valuable technique for biosensors due to allowing the characterization of chemical bonds and functional groups on the surface material. Herein, the spectra obtained at the electrode surface in each step of immunosensor are shown in Fig. 4 as follows: Fc control (spectrum I), Fc-GO nanocomposite (spectrum II) and Fc-GO with PEI (spectrum III). In spectra, I and II, the N–H stretching (ammonium ion) that is usually observed between 3400 and 3300 cm^{-1} (Fan et al., 2012; Hishikawa et al., 2017; Stuart, 2005) can indicate the presence of the amine groups attributed to Fc. In spectra I, II and III, the bands between 1650 and 1550 cm^{-1} are due to secondary amine (amide II) bending and in spectrum II the asymmetric band at

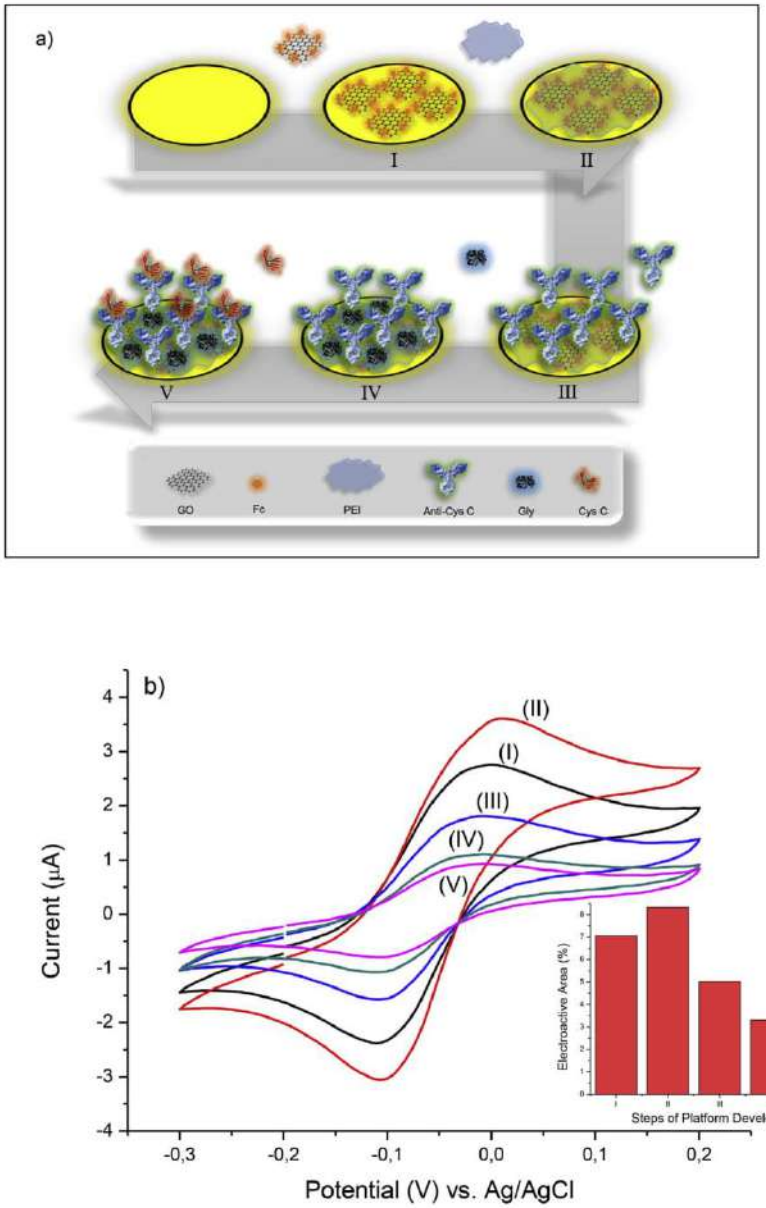

Fig. 2. **(a)** Schematic representation of nanostructured platform development, **(b)** CVs of each modification step as follows: **(I)** Fc-GO, **(II)** PEI, **(III)** Anti-CysC, **(IV)** Glycine and **(V)** Cys C; *inset:* Plot of steps for platform development *versus* electroactive area of CVs; experiments in presence of 100 mM KCl.

1637 cm^{-1} results from amide I mode (Coates, 2006; Service et al., 2010), that could be attributed to the amide bonds present in the Fc-GO nanocomposite. In spectrum II, the bands between 1242 and 1245 cm^{-1} are due to C–C, C–O and C=O stretch (Fan et al., 2012), then suggesting the presence of GO. In spectrum III, the band found at 1301 cm^{-1} is indicative of amine polymer film on the electrode surface, according to the database from the National Institute of Standards and Technology (U.S. Department of Commerce).

3.2. Analytical responses to the CysC

The analytical performance of the sensor surface was evaluated by submitting the electrode to different concentrations of CysC diluted in PBS (0.1, 1, 10, 50, 100, 500 and 1000 ng/mL). Since the incubation time exerts an important role on the analytical performance, different time incubations were tested, varying from 10 to 45 min, with 15 min adopted as optimal due to steady-state reached, similarly to previous studies (Montes et al., 2016; Singh et al., 2014). The analytical response was obtained by the difference of current (ΔI) in the SWV before and after the addition of CysC samples (Fig. 5 (a)). The analytical curve showed a decrease in the cathodic peaks proportional to CysC concentrations increase (Fig. 5 (b)). This decrease of the current peak is attributed to the hindering in electron transfer by the insulating nature of CysC increasing the diffusion barrier (Dias et al., 2013). The curve of ΔI as function of CysC concentrations exhibited in a monolog plot resulted in a broad range analytical curve linear from 0.1 to 1000 ng/mL (inset Fig. 5 (b)), with linear equation of I (μA) = 0.0045 log [CysC] + 2.63 and LOD of 0.03 ng/mL CysC (3.3 σ). These concentrations in lower values met in clinical reference that is up to 950 ng/mL (Gaygisiz et al., 2016). Therefore, for use samples needs to

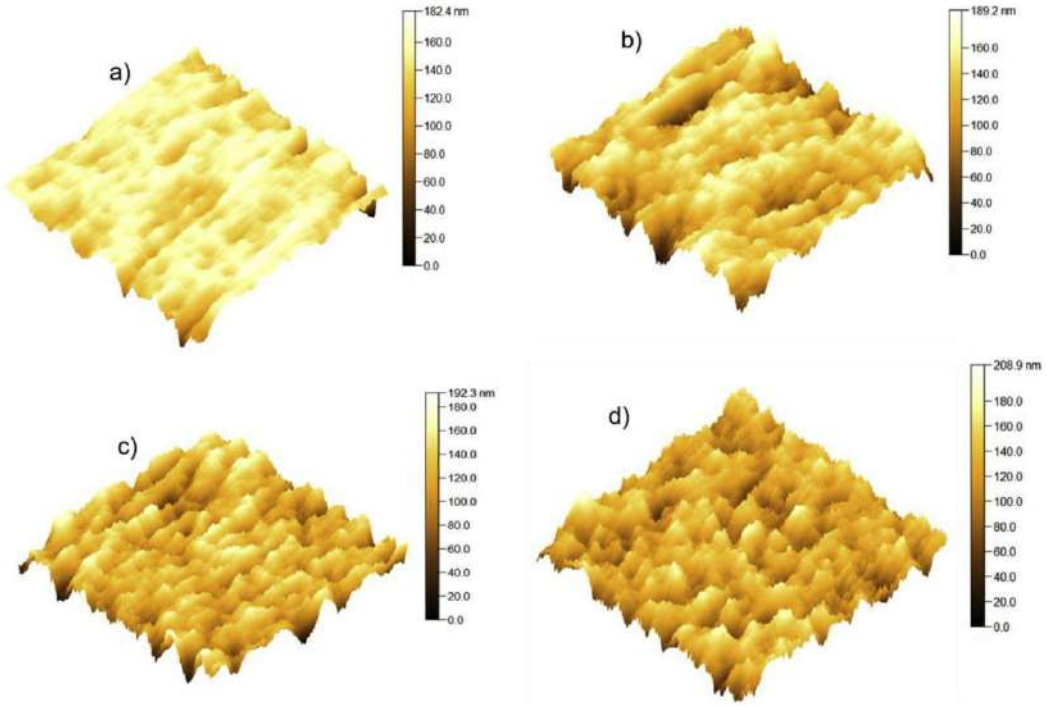

Fig. 3. 3D AFM images of the: **(a)** bare gold electrode (GE), **(b)** GO control, **(c)** Fc-GO nanocomposite and **(d)** addition of PEI.

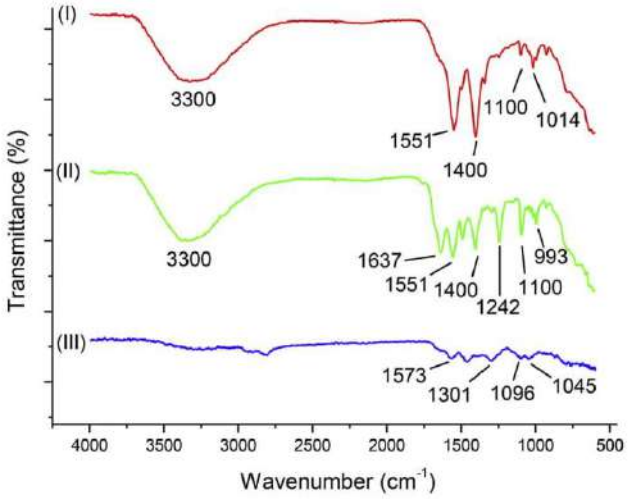

Fig. 4. FT-IR spectra of sensor platform in each step of modifications: Fc control (*spectrum I*), Fc-GO nanocomposite (*spectrum II*) and after PEI drop-casting (*spectrum III*).

be 10 to 100 times diluted in PBS before measurements, with the advantage of minimizing the non-specific bindings.

Different analytical methods for detection of CysC are shown in Table S1 (Sup information). Comparing this immunosensor with all already described for the detection of CysC, it is observed that it presents several advantages. Regarding to the amperometric sensors, this approach is more practical and faster, since it does not require further reading stages, such as the introduction of redox probe solutions and washes (Yang et al., 2016; Desai et al., 2018). While here, the samples can be diluted in PBS or even KCl being ready for reading. Additionally, detection of CysC is directly performed by the antigen-antibody reaction with more advantages, which does not occur with the cited works. In the first, Yang et al. performed the detection via immunoreaction-induced DNA strand displacement and T7 Exonuclease (T7 Exo)-assisted protein cyclic enzymatic amplification. Desai et al.(2018), the second work, developed an assay employing the screen-printed electrode based on K_3 [Fe (CN) $_6$] as an indicator. Although they have achieved an optimal range and a low limit of detection, the use of papain as sensor element, a serine protease that detects enzymatic activity, render the sensor limited for using only in urine. Thus, measurements in samples with protein contaminants like the serum are restrictive, in contrast to this proposed sensor that used antibody Anti-CysC making serological samples feasible, and detections in this fluid are easier and more commonly employed. Optical approaches by using surface plasmon resonance (SPR) was also applied by Gorodkiewicz and Luszczyn (2011) being quite sensitive, however, SPR has the disadvantage of using papain and presents itself as a technology of difficult portability, limiting as point-of-care. Lin et al. (2013) performed an optical detection with nanoparticles using also the papain. Mi et al. (2016) using CysC-specific nanobodies achieved low detection limits in optical transduction based on the photocurrent decrease using an electrochemical workstation to measure photocurrent under visible light irradiation with a 150 W Xe lamp; this application was extended to real sample by monitoring the CysC in human serum samples. Thus, the technology here developed is simpler, and quite liable for a point-of-care diagnostic. To our best knowledge, there are no electrochemical immunosensors for CysC similar to the one here developed.

The matrix effect and selectivity was also tested with this immunosensor by using a real human serum samples, since these complex samples contain a great amount of interferers. Here, it was used a pool of serum, by mixing samples of different volunteers, further increasing the possibility of interferents. As exclusion criteria in samples selections, hemolyzed or hypercholesteremic samples were not included. The assays were carried out by successive incubations with the spiked CysC (10 ng/mL) and non-spiked human serum samples at the same electrode in each experiment (Fig. 6). Analytical responses indicated a gradual decrease in the SWV peaks proportional to the increase of the

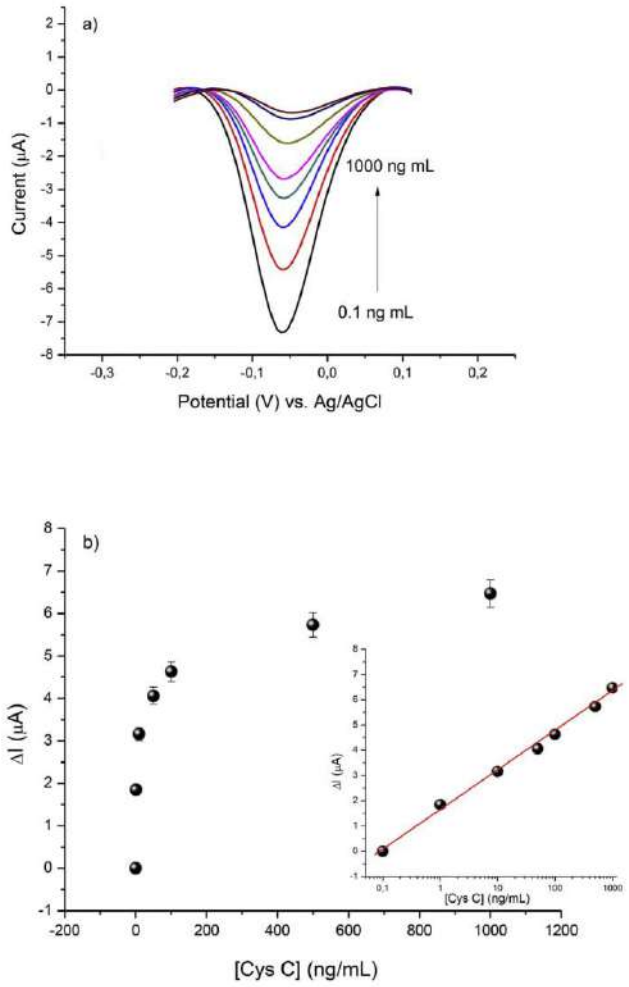

Fig. 5. **(a)** SWVs responses of immunosensor to the Cys C incubations with analytical detections measured in 100 mM KCl; **(b)** Analytical curve of Cys C antigen in PBS buffer (10 mM, pH 7.4), *inset:* Monolog plot of the Cys C concentration *vs* current variations subtracted from the blank with linear fitting. Bar error represents the standard deviations of three replicate measurements.

CysC concentrations of positive samples, contrary to the non-spiked serum response. Cutoff value was established at mean of negative sample responses plus two deviations, which was found at 20 ng/mL, thus up to this value the immunosensor was able to selectively identify CysC in positive samples, *e.g.* below of this cutoff, the presence of interferences in the samples are significant and can generate positive false.

The nanoimmunonsensor was assessed regarding repeatability (intra-assay) and reproducibility (inter-assay) (Rezaei et al., 2018; Shen et al., 2015). Good repeatability (Figure S3) with a coefficient of variation of 2% was found, using an incubation with concentration of 100 ng/mL CysC and submitting the same electrode to 20 successive SWV readings, with attention to remove the electrode from the electrochemical cell in each reading. Reproducibility tests (Figure S4) were performed showing a good performance, according to the coefficient of variation of relative peak currents of SWV that was found at less than 5% (CV = 4%) obtained by five electrodes prepared in the same conditions applying 100 ng/mL CysC in serum samples. Here, the analytical responses from different electrodes were normalized to compare themselves, *e.g.* SWV fluctuations on the blank from different electrodes due to the charge effect on the electrode by producing different DC current levels were minimized dividing by blank SWV in each electrode.

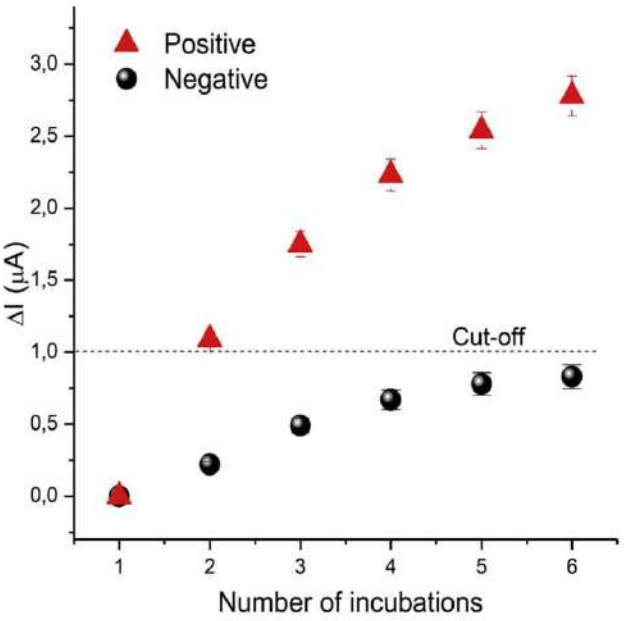

Fig. 6. Matrix effect and selectivity studied in successive incubations in real samples of human spiked serum (with 100 ng/mL Cys C in PBS) and human negative serum (diluted in PBS 10 mM, pH 7.4). Plots represent cathodic peak currents of SWVs subtracted from the blank; SWV measurements performed in presence of 100 mM KCl.

4. Conclusions

A novel electrochemical immunosensor with inherent redox activity mediated by ferrocene was developed. Amperometric responses obtained by SWV were mediated by graphene oxide-ferrocene nanofilm with redox-activity coming from electroactive species surface-confined. As a proof-of-concept, this immunosensor was applied to Cystatin C detection, a biomarker for renal failure. The detection was based on antigen-antibody interaction, differing from most CysC sensors, that have used papain to produce the current responses that allow its application to blood samples and other biological fluids. This platform is simple than optical biosensor to miniaturization and does not need redox probe solutions for measurements, simplifying the steps and being an important advancement towards real point-of-care testings.

Acknowledgments

This research was supported by CNPq Brazilian agencies under grants number 440605/2016-4 , 471065/2014-5 and 407905/2013-8. E. K. G.Trindade thank to the FACEPE and CAPES by her scholarship. The Coordenação de Aperfeiçoamento de Pessoal de Nível Superior – Brazil Code 001, financed this study in part.

Appendix A. Supplementary data

Supplementary data to this article can be found online at https://doi.org/10.1016/j.bios.2019.05.016.

References

Amani, J., Khoshroo, A., Rahimi-nasrabadi, M., 2018. Electrochemical immunosensor for the breast cancer marker CA 15 – 3 based on the catalytic activity of a CuS/reduced graphene oxide nanocomposite towards the electrooxidation of catechol. Microchim. Acta.

Bard, A.J., Faulkner, L.R., 2001. Electrochemical Methods: fundamentals and Applications. Wiley.

Chawla, L.S., Eggers, P.W., Star, R.A., Kimmel, P.L., 2014. Acute kidney injury and

chronic kidney disease as interconnected syndromes. N. Engl. J. Med. 371, 58–66. https://doi.org/10.1056/NEJMra1214243.
Cho, I., Lee, J., Kim, J., Kang, M., Paik, J.K., Ku, S., Cho, H., Irudayaraj, J., Kim, D., 2018. Current technologies of electrochemical Immunosensors : perspective on signal amplification. Sensors (Basel). 18, 1–18. https://doi.org/10.3390/s18010207.
Coates, J., 2006. Interpretation of infrared spectra, a practical approach. Encycl. Anal. Chem. 1–23. https://doi.org/10.1002/9780470027318.a5606.
Coca, S.G., Singanamala, S., Parikh, C.R., 2012. Chronic kidney disease after acute kidney injury: a systematic review and meta-analysis. Kidney Int. 81, 442–448. https://doi.org/10.1038/ki.2011.379.
Delanaye, P., Cavalier, E., Morel, J., Mehdi, M., Maillard, N., Claisse, G., Lambermont, B., Dubois, B.E., Damas, P., Krzesinski, J.-M., Lautrette, A., Mariat, C., 2014. Detection of decreased glomerular filtration rate in intensive care units: serum cystatin C versus serum creatinine. BMC Nephrol. 15, 9. https://doi.org/10.1186/1471-2369-15-9.
Desai, D., Kumar, A., Bose, D., Datta, M., 2018. Ultrasensitive sensor for detection of early stage chronic kidney disease in human. Biosens. Bioelectron. 105, 90–94. https://doi.org/10.1016/j.bios.2018.01.031.
Dias, A.C.M.S., Gomes-Filho, S.L.R., Silva, M.M.S., Dutra, R.F., 2013. A sensor tip based on carbon nanotube-ink printed electrode for the dengue virus NS1 protein. Biosens. Bioelectron. 44. https://doi.org/10.1016/j.bios.2012.12.033.
Fan, M., Dai, D., Huang, B., 2012. Fourier transform infrared spectroscopy for natural fibres. In: Fourier Transform - Materials Analysis, pp. 46–68.
Fery-Forgues, S., Delavaux-Nicot, B., 2000. Ferrocene and ferrocenyl derivatives in luminescent systems. J. Photochem. Photobiol. A Chem. 132, 137–159. https://doi.org/10.1016/S1010-6030(00)00213-6.
Fonseca, I., Reguengo, H., Oliveira, J.C., Martins, L.S., Malheiro, J., Almeida, M., Santos, J., Dias, L., Pedroso, S., Lobato, L., Henriques, A.C., Mendonça, D., 2015. A triple-biomarker approach for the detection of delayed graft function after kidney transplantation using serum creatinine, cystatin C, and malondialdehyde. Clin. Biochem. 48, 1033–1038. https://doi.org/10.1016/j.clinbiochem.2015.07.007.
Fox, J.A., Dudley, A.G., Bates, C., Cannon Jr., G.M., 2014. Cystatin C as a marker of early renal insufficiency in children with congenital neuropathic bladder. J. Urol. 191, 1602–1607. https://doi.org/10.1016/j.juro.2013.09.093.
Gaygisiz, Ü., Aydoıdu, M., Badoılu, M., Boyaci, N., Güllü, Z., Gürsel, G., 2016. Can admission serum cystatin C level be an early marker subclinical acute kidney injury in critical care patients? Scand. J. Clin. Lab. Invest. 76, 143–150. https://doi.org/10.3109/00365513.2015.1126854.
Gharaibeh, K.A., Hamadah, A.M., El-Zoghby, Z.M., Lieske, J.C., Larson, T.S., Leung, N., 2018. Cystatin C predicts renal recovery earlier than creatinine among patients with acute kidney injury. Kidney Int. Reports 3, 337–342. https://doi.org/10.1016/j.ekir.2017.10.012.
Gomes-Filho, S.L.R., Dias, A.C.M.S., Silva, M.M.S., Silva, B.V.M., Dutra, R.F., 2013. A carbon nanotube-based electrochemical immunosensor for cardiac troponin T. Microchem. J. 109. https://doi.org/10.1016/j.microc.2012.05.033.
Gorodkiewicz, E., Luszczyn, J., 2011. Surface plasmon resonance imaging (SPRI) sensor for cystatin determination based on immobilized papain. Protein Pept. Lett. 18, 23–29. https://doi.org/10.2174/092986611794328663.
Hishikawa, Y., Togawa, E., Kondo, T., 2017. Characterization of Individual Hydrogen Bonds in Crystalline Regenerated Cellulose Using Resolved Polarized FTIR Spectra. https://doi.org/10.1021/acsomega.6b00364.
Hoste, E.A.J., Bagshaw, S.M., Bellomo, R., Cely, C.M., Colman, R., Cruz, D.N., Edipidis, K., Forni, L.G., Gomersall, C.D., Govil, D., Honoré, P.M., Joannes-Boyau, O., Joannidis, M., Korhonen, A.-M., Lavrentieva, A., Mehta, R.L., Palevsky, P., Roessler, E., Ronco, C., Uchino, S., Vazquez, J.A., Vidal Andrade, E., Webb, S., Kellum, J.A., 2015. Epidemiology of acute kidney injury in critically ill patients: the multinational AKI-EPI study. Intensive Care Med. 41, 1411–1423. https://doi.org/10.1007/s00134-015-3934-7.
Jiang, R., Xu, C., Zhou, X., Wang, T., Yao, G., 2014. Detection of Cystatin C biomarker for clinical measurement of renal disease by developed ELISA diagnostic kits. J. Transl. Med. 12, 1–8. https://doi.org/10.1186/1479-5876-12-205.
Jingyuan, Chen, Koichi, Aoki, Toyohiko, Nishiumi, Li, T., 2006. Voltammetry of Suspensions of Hollow Particles with Ferrocene-Immobilized Polyallylamine Shells†. https://doi.org/10.1021/LA0610304.
Lau, L., Al-Ismaili, Z., Harel-Sterling, M., Pizzi, M., Caldwell, J.S., Piccioni, M., Lands, L.C., Mottes, T., Devarajan, P., Goldstein, S.L., Bennett, M.R., Zappitelli, M., 2016. Serum cystatin C for acute kidney injury evaluation in children treated with aminoglycosides. Pediatr. Nephrol. 1–9. https://doi.org/10.1007/s00467-016-3450-1.
Lau, S.P., Wong, K.K., Chen, S., Fan, Z., Po, K.H.L., 2018. Polyethylenimine-modified graphene oxide as a novel antibacterial agent and its synergistic effect with daptomycin for methicillin-resistant Staphylococcus aureus. ACS Appl. Nano Mater. 1, 1811–1818. https://doi.org/10.1021/acsanm.8b00219.
Lin, H., Sun, W., Zhao, C., Na, H., 2013. Self-assembly of multiwall carbon nanotubes on sulfonated poly (arylene ether ketone) as a proton exchange membrane. J. Polym. Res. 20, 306. https://doi.org/10.1007/s10965-013-0306-2.
Lu, Y., Jiang, Y., Wu, H., Chen, W., 2015. Ferrocene-functionalized graphene oxide nanosheets: efficient electronic communication between ferrocene centers across graphene nanosheets. Electrochim. Acta 156, 267–273. https://doi.org/10.1016/j.electacta.2015.01.049.
Mi, L., Wang, P., Yan, J., Qian, J., Lu, J., Yu, J., Wang, Y., Liu, H., Zhu, M., Wan, Y., Liu, S., 2016. A novel photoelectrochemical immunosensor by integration of nanobody and TiO2 nanotubes for sensitive detection of serum cystatin C. Anal. Chim. Acta 902, 107–114. https://doi.org/10.1016/j.aca.2015.11.007.
Montes, R., Céspedes, F., Baeza, M., 2016. Highly sensitive electrochemical immunosensor for IgG detection based on optimized rigid biocomposites. Biosens. Bioelectron. 78, 505–512. https://doi.org/10.1016/j.bios.2015.11.081.
Moreira, F.T.C., Rodriguez, B.A.G., Dutra, R.A.F., Sales, M.G.F., 2018. Redox probe-free readings of a B-amyloid-42 plastic antibody sensory material assembled on copper@carbon nanotubes. Sensor. Actuator. B Chem. 264, 1–9. https://doi.org/10.1016/j.snb.2018.02.166.
Rabti, A., Raouafi, N., Merkoçi, A., 2016. Bio(Sensing) devices based on ferrocene—functionalized graphene and carbon nanotubes. Carbon N. Y. 108, 481–514. https://doi.org/10.1016/j.carbon.2016.07.043.
Ravn, B., Prowle, J.R., Mårtensson, J., Martling, C.-R., Bell, M., 2017. Superiority of serum cystatin C over creatinine in prediction of long-term prognosis at discharge from ICU. Crit. Care Med. 1, 1. https://doi.org/10.1097/CCM.0000000000002537.
Rezaei, B., Shoushtari, A.M., Rabiee, M., Uzun, L., Mak, W.C., Turner, A.P.F., 2018. An electrochemical immunosensor for cardiac Troponin I using electrospun carboxylated multi-walled carbon nanotube-whiskered nanofibres. Talanta 182, 178–186. https://doi.org/10.1016/j.talanta.2018.01.046.
Rodriguez, B.A.G., Trindade, E.K.G., Cabral, D.G.A., Soares, E.C.L., Menezes, C.E.L., Ferreira, D.C.M., Mendes, R.K., Dutra, R.F., 2015. Nanomaterials for advancing the health immunosensor. In: Biosensors - Micro and Nanoscale Applications, pp. 347–374.
Roushani, M., Abdi, Z., 2014. Novel electrochemical sensor based on graphene quantum dots/riboflavin nanocomposite for the detection of persulfate. Sensor. Actuator. B Chem. 201, 503–510. https://doi.org/10.1016/j.snb.2014.05.054.
Service, R.J., Hillier, W., Debus, R.J., 2010. Evidence from FTIR difference spectroscopy for an extensive network of hydrogen bonds near the oxygen-evolving Mn4Ca cluster of photosystem II involving D1-glu65, D2-glu312, and D1-glu329. Biochemistry 49, 6655–6669. https://doi.org/10.1021/bi100730d.Evidence.
Shearer, C.J., Slattery, A.D., Stapleton, A.J., Shapter, J.G., Gibson, C.T., 2016. Accurate thickness measurement of graphene. Nanotechnology 27, 125704. https://doi.org/10.1088/0957-4484/27/12/125704.
Shen, Y., Zhang, Y., Liu, M., Liu, X., Guo, H., Zhang, X., Zhang, C., Li, H., Yao, S., 2015. A simple and sensitive electrochemical immunosensor based on thiol aromatic aldehyde as a substrate for the antibody immobilization. Talanta 141, 288–292. https://doi.org/10.1016/j.talanta.2015.04.004.
Shlipak, M.G., Matsushita, K., Ärnlöv, J., Inker, L.A., Katz, R., Polkinghorne, K.R., Rothenbacher, D., Sarnak, M.J., Astor, B.C., Coresh, J., Levey, A.S., Gansevoort, R.T., 2013. Cystatin C versus creatinine in determining risk based on kidney function. N. Engl. J. Med. 369, 932–943. https://doi.org/10.1056/NEJMoa1214234.
Silva, M.M.S., Dias, A.C.M.S., Silva, B.V.M., Gomes-Filho, S.L.R., Kubota, L.T., Goulart, M.O.F., Dutra, R.F., 2015. Electrochemical detection of dengue virus NS1 protein with a poly(allylamine)/carbon nanotube layered immunoelectrode. J. Chem. Technol. Biotechnol. 90. https://doi.org/10.1002/jctb.4305.
Singh, R., Sharma, A., Hong, S., Jang, J., 2014. Electrical immunosensor based on dielectrophoretically-deposited carbon nanotubes for detection of influenza virus H1N1. Analyst 139, 5415–5421. https://doi.org/10.1039/c4an01335b.
Stuart, B., 2005. Infrared spectroscopy. In: Kirk-Othmer Encyclopedia of Chemical Technology. American Cancer Society. https://doi.org/10.1002/0471238961.0914061810151405.A01.PUB2.
Tao, J., Zhao, P., Zeng, Q., 2016. The determination of cystatin C in serum based on label-free and near-infrared light emitted PbS@BSA QDs. J. Mater. Chem. B 4, 4258–4262. https://doi.org/10.1039/c6tb00080k.
Tavares, E.M., Carvalho, A.M., Gonçalves, L.M., Valente, I.M., Moreira, M.M., Guido, L.F., Rodrigues, J.A., Doneux, T., Barros, A.A., 2013. Chemical sensing of chalcones by voltammetry: trans-Chalcone, cardamonin and xanthohumol. Electrochim. Acta 90, 440–444. https://doi.org/10.1016/J.ELECTACTA.2012.12.040.
Trindade, E.K.G., Dutra, R.F., 2018. A label-free and reagentless immunoelectrode for antibodies against hepatitis B core antigen (anti-HBc) detection. Colloids Surfaces B Biointerfaces 172, 272–279. https://doi.org/10.1016/j.colsurfb.2018.08.050.
Valipour, A., Roushani, M., 2017. Using silver nanoparticle and thiol graphene quantum dots nanocomposite as a substratum to load antibody for detection of hepatitis C virus core antigen: electrochemical oxidation of riboflavin was used as redox probe. Biosens. Bioelectron. 89, 946–951. https://doi.org/10.1016/j.bios.2016.09.086.
Vilian, a. T.E., Veeramani, V., Chen, S.-M., Madhu, R., Kwak, C.H., Huh, Y.S., Han, Y.-K., 2015. Immobilization of myoglobin on Au nanoparticle-decorated carbon nanotube/polytyramine composite as a mediator-free H2O2 and nitrite biosensor. Sci. Rep. 5, 18390. https://doi.org/10.1038/srep18390.
Wang, H., Gao, X., Ma, Z., 2017. Multifunctional substrate of label-free electrochemical immunosensor for ultrasensitive detection of cytokeratins antigen 21-1. Sci. Rep. 7, 1–7. https://doi.org/10.1038/s41598-017-01250-0.
Webster, A.C., Nagler, E.V., Morton, R.L., Masson, P., 2017. Chronic kidney disease. Lancet 389, 1238–1252. https://doi.org/10.1016/S0140-6736(16)32064-5.
Yamanaka, K., Vestergaard, M.C., Tamiya, E., 2016. Printable electrochemical biosensors: a focus on screen-printed electrodes and their application. Sensors (Switzerland) 16, 1–16. https://doi.org/10.3390/s16101761.
Yang, Z.H., Zhuo, Y., Yuan, R., Chai, Y.Q., 2016. Highly effective protein converting strategy for ultrasensitive electrochemical assay of cystatin C. Anal. Chem. 88, 5189–5196. https://doi.org/10.1021/acs.analchem.6b00210.

APÊNDICE B – ARTIGO PUBLICADO EM PERIÓDICO

A LABEL-FREE AND REAGENTLESS IMMUNOELECTRODE FOR ANTIBODIES AGAINST HEPATITIS B CORE ANTIGEN (ANTI-HBC) DETECTION

Erika K.G. Trindade, Rosa F. Dutra

Colloids and Surfaces B: Biointerfaces, 2018

Colloids and Surfaces B: Biointerfaces 172 (2018) 272–279

Contents lists available at ScienceDirect

Colloids and Surfaces B: Biointerfaces

journal homepage: www.elsevier.com/locate/colsurfb

A label-free and reagentless immunoelectrode for antibodies against hepatitis B core antigen (anti-HBc) detection

Erika K.G. Trindade, Rosa F. Dutra*

Biomedical Engineering Laboratory, Federal University of Pernambuco, Av. Prof. Moraes Rego, 1235, 50670-000, Recife, Brazil

ARTICLE INFO

Keywords:
Immunosensor
Nanosensor
Polytyramine
Anti-HBc
Reagentless
Hepatitis B

ABSTRACT

An electrochemical immunosensor devoted the core hepatitis B antibody detection, based on polytyramine (PTy) and carbon nanotubes (CNT) composite was developed. The antibody interactions with immobilized antigens were detected by reduction on the electron transfer from ionic species coming from reactive amine groups of PTy. The synthesis in acid medium of PTy-CNT composite favorite a great amount of NH_3^+ ionic species, forming a nanocomposite with high catalytic activity on the electrode surface. As proof-of-concept, antibodies against the core hepatitis B virus were label-free and reagentless electrochemically detected by square wave voltammetry (SWV) through decrease on cathodic peaks. It was recently reported that hepatitis B core antigen antibodies (anti-HBc) is a powerful biomarker for hepatitis B virus (HBV) infection, being more specific than HBsAg due to the possibility of detecting the occult HBV infections. The nanostructured film was characterized by atomic force microscopy and electrochemical techniques. This immunosensor showed linear responses from 1.0 to 5.0 ng mL^{-1} and a limit of detection of 0.89 ng mL^{-1} anti-HBc. It was also tested in assays with negative and positive blood samples using 0.1 M KCl as electrolyte support on readings showing specific responses. This easy reagentless detection platform, showing a remarkable potential to development of bolder and simpler HBV assay for screening of blood bags, in attempting to circumvent point-of-care testing limitations.

1. Introduction

The hepatitis B virus (HBV) is a major global issue, prevalent in different continents including Asia, African and others. Potential complications from chronic HBV infection include cirrhosis of the liver, liver failure, liver cancer and premature death [1,2]. HBV infected individuals are commonly asymptomatic, unknowing that own the circulating virus, besides in many cases, symptoms can take two to five months to appear and about 70 percent of adults have subclinical or anicteric hepatitis. Thus, those unknowingly infected can powerfully spread the infection to others [3]. HBV infection has been frequently detected by two serological markers, hepatitis B surface antigen (HBsAg) and antibodies against the virus core (anti-HBc) [4]. In countries with limited resources that suffer from the lack of facilities in the serological tests, different strategies have been sought [5]. In recent studies, anti-HBc has been indicated as the most specific marker for blood donor screening compared to HBsAg, detecting also the occult hepatitis B infection [5–8]. Owing to HBV infection *via* blood transfusion to be a major concern in transfusion medicine [9], the development of simple screening tests to detect HBV in blood donors and prevent recipient HBV infection are really desirable.

On the last decade, point-of-care based-immunosensors have been proposed for several biomarkers and employing different transduction techniques, such as electrochemical [10,11], optical [12,13] and piezoelectric [14,15]. Electrochemical immunosensors based on the screen-printed technology have shown to be more attractive due to several advantages including low-cost, easy miniaturization and compatibility with enzymatic transducers, like the popular glucometers. Although electrochemical immunosensors have achieved great advances by reducing the time of analysis and time-consuming steps, do not requiring labeled antigen or antibody to detect the immunocomplex interactions by impedimetric or amperometric electrical signals [16], they still are limited for point-of-care diagnostics as compared with rapid immunochromatographic tests. This inconvenience is absolutely a limitation for a wide-scale practice and use by non-skilled personnel [17]. The idea reported here is a catalytic sensor surface capable to generate electroactive species as redox probe to the electrical signal, facilitating the measurements on the samples by square wave or differential pulse voltammetry transduction [18].

Polymers have been widely used to biosensor developments [12,19], specially containing alternated π-bonds jointly to aromatic ring resonance that leads to a high conductivity [20]. Conductivity of a

* Corresponding author.
E-mail address: rosa.dutra@ufpe.br (R.F. Dutra).

https://doi.org/10.1016/j.colsurfb.2018.08.050
Received 19 March 2018; Received in revised form 15 August 2018; Accepted 23 August 2018
Available online 24 August 2018
0927-7765/

polymer film electrochemically synthesized can be controlled by adjusting electrochemical techniques, counter ions and pH [21]. Polytyramine (PTy) is a derivative from the amino acid tyrosine and possess amine portion separated from the phenolic ring by two methylene groups [22]. In aqueous acid electrosynthesis, the PTy film is more conductive and thicker, being expected that only the phenol moiety be oxidized and a high surface concentration of reactive primary amines are formed [23–25]. Previous synthesis in perchlorate acid have demonstrated a reactive PTy film containing about 80% protonated amine (-NH3+) and 20% to neutral amine (-NH2) [19].

Carbon allotropes have been widely studied for biosensors due to their excellent electrical properties. Using the carbodiimide chemistry by amine moieties, vertical alignment of the carbon nanotubes have been achieved by their carboxylated anion head groups [26,27]. CNTs aligned on the electrode surface lead to higher electrocatalytic ability per unit area than CNTs randomly dispersed, phenomenon that can be attributed to the open ends be more electroactive than sidewalls [28]. Biomolecule immobilization steps are considered crucial to stable and reproducible biosensors. The carboxyl groups in CNTs served as a double purpose, anchoring the antigen (HBcAg) by its amine sites. Herein, PTy and CNTs were strategically joined to permit the immobilization and improvement on the electron transfer, detecting lower fluctuations on diffusion barrier induced by antigen-antibody interactions.

The great amount of amine groups derived from PTy-CNT composite are able to generate a faradaic current in a specific redox potential. This catalytic nanofilm had advantage to result an amperometric response, being simpler, without necessity of redox probe solution reading step, *i.e.* reagentless immunosensor. Similar reading mode were obtained by Sun et al. [29], using a composite containing polyaniline in which the faradaic current from anodic SWV peaks was ascribed to inherent redox activity from amine groups of polyaniline. Thus, this proposed immunosensor represents advances to label-free immunosensors that use SWV or other voltammetric or impedimetric transduction, since the readings can be performed at support electrolyte as KCl. This work represents new perspectives to overcome limitations of direct detection in blood samples.

2. Material and methods

2.1. Reagents and anti-HBc samples

The tyramine monomer (Ty, 97%), 1-ethyl-3-(3 dimethylaminopropyl) carbodiimide (EDC), *N*-hydroxysuccinimide (NHS), potassium ferricyanide (K_3 [Fe (CN) $_6$]), potassium ferrocyanide (K_4 [Fe (CN) $_6$]), and dimethylformamide (DMF) were obtained from Sigma-Aldrich (St. Louis, USA). Hepatitis B virus core antigen (HBcAg) and monoclonal Hepatitis B virus core antibodies (anti-HBc) were acquired from Abcam (Cambridge, UK). Carboxylated multi-walled carbon nanotubes (COOH–CNT) with 95% purity were obtained from Dropsens® (Oviedo, SPA). All other chemicals used were of analytical grade and solutions were prepared in ultra-pure water acquired from a Milli-Q station (Milli-Q, USA) with conductivity below 18 MΩ cm^{-1}.

Blood samples from negative hepatitis B (anti-HBc) individuals were collected after approval by Research Ethics Committee of Pernambuco University, Brazil. For all procedures, the blood was collected in 4 mL Vacutainer EDTA tube to avoid coagulation. All the blood pools used in experiments were freshly collected and the HBV positive was spiked with anti-HBc (1 ng mL^{-1}) for analytical measurements. The control was obtained by incubating non-spiked blood pool samples of healthy individuals.

2.2. Characterization of electrode surface and analytical measurements

Electrochemical measurements were performed in a three-electrode system containing a helical platinum wire as counter electrode, Ag/AgCl (3 M KCl Sat.) as reference and a gold electrode (GE) with 1 mm diameter, as working electrode. The electrochemical measurements were performed with a potentiostat/galvanostat IviumCompactStat (Eindhoven, Netherlands) coupled to a microcomputer and controlled by IviumSoft software.

To characterize the modifications of the electrode surface, electrochemical measurements was carried out by cyclic voltammetry (CV) and analytical responses by square wave voltammetry (SWV) techniques. CVs measurements were carried out at 50 mV s^{-1} scan rate in a potential between 0 and 0.5 V using 5 mM$K_3Fe(CN)_6$/$K_4Fe(CN)_6$ prepared in 100 mM KCl as redox probe. The SWVs were recorded at 10 Hz with 10 mV pulse amplitude, 10 mV step potential in a window potential from 0.8 to 0.5 V in 100 mM KCl. The analytical responses to anti-HBc were performed by SWV using the same characterization procedure. Calculations and graphs were made using the OriginPro 8.0 software.

The structural characterization of the HBcAg-GE was accomplished by a Fourier Transform Infrared in the Attenuated Total Reflectance mode (ATR FT-IR), through a Bruker IFS 66 model FT-IR spectrometer (Billerica, USA), using a range from 4000 to 500 cm^{-1} wavelengths. The measurements were collected from crystalline gold disks of approximately 0.8 cm diameter that were connected to an electrochemical cell by means of a conductive wire, in order to electropolymerize monomers of the Ty and prepare the HBcAg-electrode.

Atomic Force Microscopy (AFM) was used to perform morphological analyses of modifications on the GE surface made in noncontact mode, using Nanosurf Flex AFM equipped with a C3000 controller. The images obtained were treated and analyzed through software Gwydion.

2.3. Synthesis of catalytic PTy-3D carbon nanostructured surface

Prior to modification, the gold electrode (GE) was polished with alumina slurry (0.5 μm) to remove impurities present on the electrode surface, followed by rinsing with distilled water. The PTy film was electrochemically grown on the GE from a solution of 2.5 mM Ty prepared in 100 mM H_2SO_4. The working potential was swept at 50 mV s^{-1} and 10 cycles were applied between from – 0.6 to 1.1 V *vs.* Ag/AgCl.

Carboxylic groups of carbon nanotubes were bound to the PTy film by incubating an aliquot (5 μL) of COOH–CNT (1 mg mL^{-1}) dispersion on the electrode surface for 45 min. Prior to incubation, 1 mg of COOH–CNTs were dispersed in 1 mL of DMF in an ultrasonic bath for 2 h. In order to activate the carboxyl groups of COOH-CNT, this suspension was [1:1] pre-activated for 40 min with a mixture of 20 mM EDC and 50 mM NHS solution [1:1] prepared in 0.1 M sodium acetate buffer, pH 5.5) [30].

2.4. Immobilization of HBcAg and analytical measurements

In order to immobilize the antigen on the nanostructured electrode, an aliquot (5 μL) of the HBcAg solution (100 μg mL^{-1}) was pipetted onto the GE surface and incubated for 1 h at room temperature. Non-specific bindings were blocked using a solution of 50 mM glycine, prepared in PBS (10 mM, pH 7.2) that reacted for 45 min on the electrode surface. Glycine is an amino acid widely used in immunosensors for blocking of unspecific bonds since it is a very small molecule and contains amine and carboxylic moieties [31].

Analytical responses were obtained by incubating the HBcAg-nanostructured electrode surface with 5 μL of anti-HBc (1 ng mL^{-1}) samples for 15 min [32]. A schematic diagram of all steps involved on the synthesis of PTy/COOH-CNT/HBc/gold electrode and immunoassay is shown in Fig. 1.

3. Results and discussion

3.1. Synthesis of PTy/COOH-CNT electrode surface

Polymer electrode prepared by electropolymerization has been commonly used due to feasible controlling of electrochemical

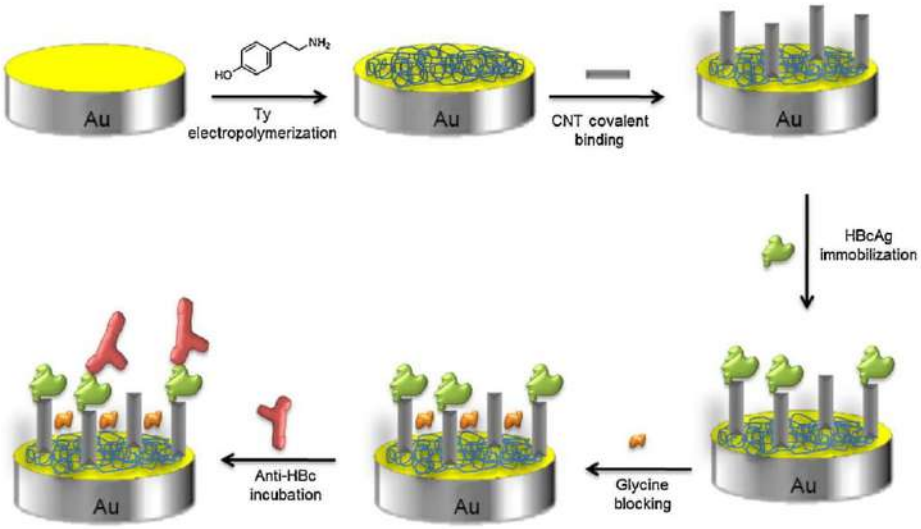

Fig. 1. Schematic diagram of steps performed on synthesis of the HBc gold electrode and immunoassay (anti-HBc incubation).

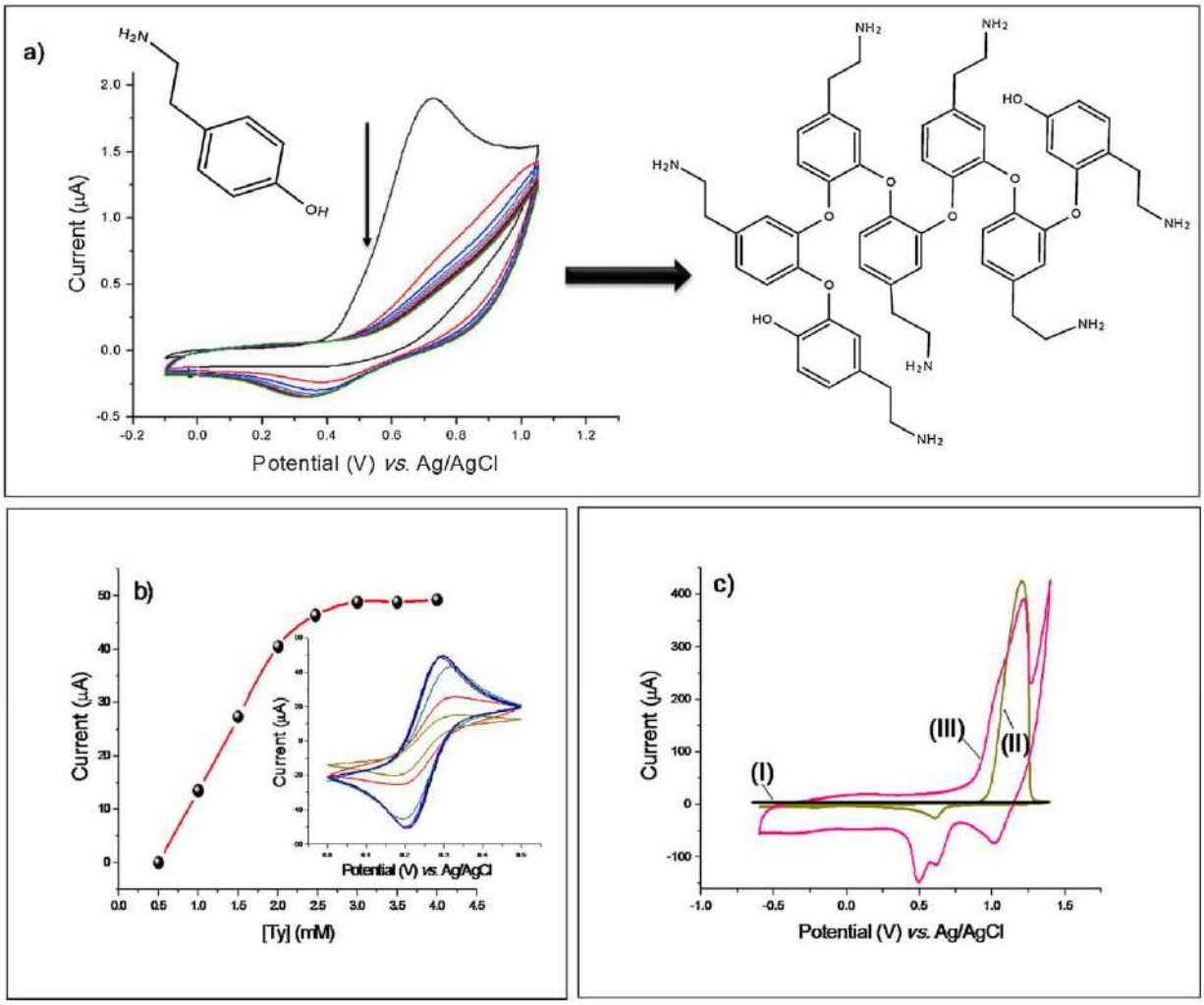

Fig. 2. Pty film synthesis (a) Electrosynthesis of PTy by continuous potential cycling (10 cycles) (b) Dependence of Ty concentrations according to cathodic peaks of CVs (*inset*: CVs of Ty at different concentrations, performed in 5 mM $K_3Fe(CN)_6/K_4Fe(CN)_6$), and (c) Typical CVs of (I) bare GE, (II) Pty/GE and (III) CNT/Pty/GE carried out in 100 mM KCl at 50 mV/s scan rate.

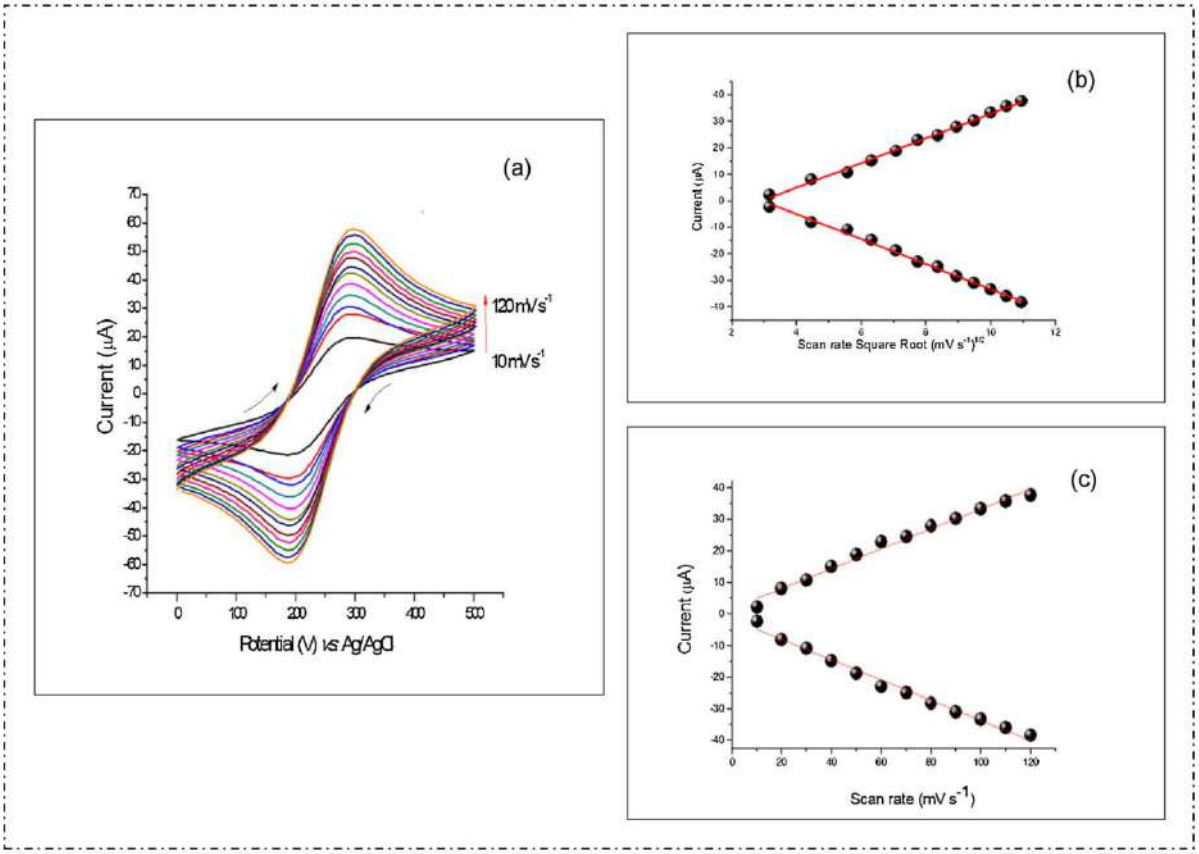

Fig. 3. (a) CVs obtained from the CNT/Pty/GE in presence of redox probe of 5 mM $K_3Fe(CN)_6/K_4Fe(CN)_6$ prepared in 100 mM KCl at scan rates (inner to outer) 10, 20, 30, 40, 50, 60, 70, 80, 90, 100, 110, 120 mV/s. (b): Plot of anodic and cathodic peak current from CVs *vs.* square root of scan rate and (c): Plot of anodic and cathodic peak current from CVs *vs.* scan rate.

conditions. A layer of polymer can be formed *in situ* on the electrode surface with controllable thickness, high conductivity and good stability [33]. Herein, the optimal conditions of Pty synthesis was established by irreversible oxidizing of Ty monomers at around 0.7 V of CV sweeping at 50mVs-1, in the potential window from −0.1 V to 1.4 V. Ty polymerization was achieved at 10 cycles, after that the redox current did not increase considerably with number of cycling (Fig. 2(a)). Conductivity dependence resulting from monomer concentration was also evaluated, varying the Ty concentrations prepared in acid medium (100 mM H2SO4) from 0.5 to 4.0 mM. Neutral or alkaline medium used in electropolymerization can generate less conductive PTy films [24]. Herein, the electropolymerization was chosen in acid medium to ensure a higher conductivity of PTy film. In this medium, it expected that Pty synthetized contains reactive amine groups with a great majority of protonated amine ($-NH_3+$) conversely a minimal amount of neutral amine ($-NH_2$) [19,34]. It was observed a prominent anodic current peak, at approximately 1.2 V that can be ascribed to protonated amine and cathodic peak at 0.6 V, probably due to the amine formed (Fig. 2(c)). The Ty optimal concentration was obtained at 2.5 mM, by observing a plateau represented by monomer concentrations *versus* cathodic peak currents extracted from CVs (Fig. 2(b)). Increase in polymer concentrations cause decrease or stabilization of peak currents, as it is related to the number of binding sites available [35].

Taking into account that one of the objectives of this study was obtain a catalytic electrode surface, which the ionic species would able to generate analytical responses by itself, *i.e.* by dispensing the use of redox probe readings, the analytical responses obtained here by SWV were based on these redox peaks. Nevertheless, the anodic peak potential was very high, close to 1 V, which is capable to oxide many substances present in samples. Thus, it is preferable that SWV performed by cathodic peaks because it has advantage of minimizing various blood interferents, especially those resultants of metabolites more abundant easier oxidized, such as ascorbic (AA) and uric acid (UA). AA and UA have oxidation peaks at +0.38 and + 0.44 mV, respectively, and their electrochemical reactions are irreversible, thus not having reduction peaks to interfere at measurements [36]. Hemoglobin is another important blood interferent, however Hb possess a reduction peak at approximately −0.2 mV [37]. A probable mechanism of reduction of NH_3^+ for cathodic peak in SWV measurements, and CNT charge transfer is proposed in Eq. (1). In this case, it was ascribed that protonated amine at 0.6 V is reduced to NH_2 and CNTs acted as electron mediator compounds. This behavior of electroactive species able to generate signals by SWV and mediate responses according to the electric transfer barrier on the electrode surface was also explored by other authors recently [19,29].

$$NH_3^+ + e^- \rightarrow NH_2 \leftrightarrow CNT^+ + e^- \rightarrow CNT \quad (1)$$

The interaction between COOH-CNT and PTy film was studied by CVs. Previous studies have shown that the vertical alignment of CNTs in comparison with the random alignment, improve the electron transfer rates from the electrolyte to the electrode [28]. Vertically aligned assemblies of the CNTs were achieved using several strategies onto different substrates, such as gold [38], silicon [27] and others [39]. One of the possibilities is the vertical alignment by amino-functionalized substrates through the end carboxyl group of the CNTs [40]. Herein, the protonated Pty polymer film promoted the highly stable and vertical

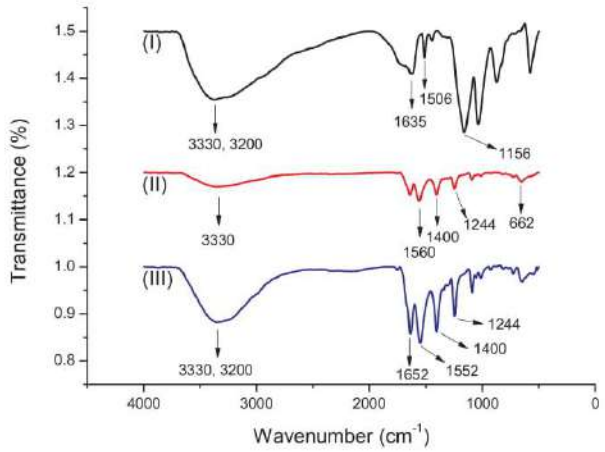

Fig. 4. ATR-FT-IR spectrum obtained from surface of: (I) Pty, (II) COOH–CNT/GE, and (III) COOH–CNT/PTy/GE.

anchoring of the CNTs *via* their carboxylated anion head groups, since carbodiimide chemistry was used to form amide linkages [41]. Deposition of CNTs on PTy film resulted in an increase of approximately 60% of electroactive area as compared with Pty/GE (Fig. 2(c)). This increase can be attributed to CNT-related increase in electron transfer [31,42] and the synergism between Pty and CNT [28]. The carboxyl groups in CNTs served here as a double purpose, also anchoring the antigen (HBcAg) by its amine sites.

Additionally, electrochemical stability of PTy/CNT matrix was evaluated by cycling the electrode to successive CVs. When the CNT/Pty/GE was submitted to 20 cycles, at 50 mV s^{-1} in 0 to 0.5 V using of 5 mM $K_3Fe(CN)_6/K_4Fe(CN)_6$ as redox probe, it was observed that the coefficient of variations of the redox current peaks were less than 1%, exhibiting a similar profiles of CVs. Mechanistic studies were performed changing the scan rates from 10 to 120 mV s^{-1} immersing the working electrode to the electrochemical cell filled with a 5 mM $K_3Fe(CN)_6/K_4Fe(CN)_6$ redox probe solution prepared in 100 mM KCl. It was observed that cathodic and anodic current peaks from CVs (Ipc and Ipa, respectively) proportionally increased with the square root of scan rates increase, exhibiting an adjusted R square ≥ 0.996 (Fig. 3(b), which is indicative that the process was diffusion controlled, as expected [43]. A discrete shift on redox peak potentials was detected meaning a possible interaction between nitrogen reactive species of Pty and iron species present in the ferrocyanide redox probe. Finally, the electrode surface reaction was also controlled since the current redox peaks increased proportionally with scan rates (Fig. 3(c)).

Study of pre-activation time of CNTs by EDC/NHS occurred previously to deposition onto Pty film electrode surface, varying the period at 10, 15, 20, 25, 30, 35, 40, 45 and 50 min demonstrated that 35 min was optimal, according to steady-state curve of anodic peaks from CVs of the CNT/Pty/GE *versus* activation-times of CNTs (Fig. S1). The optimal time-activation of CNTs corresponded to maximal electroactive area, implying in a major electron transfer rate. The carbodiimide group present in EDC/NHS promotes activation of the carboxylic group of CNT by formation of *o*-acylisourea intermediate. The EDC by-product is released as soluble urea derivative and the NHS is normally used along with EDC to create esters more stable than *o*-acylisourea intermediate, allowing the coupling of the amine with the carboxylic group [44].

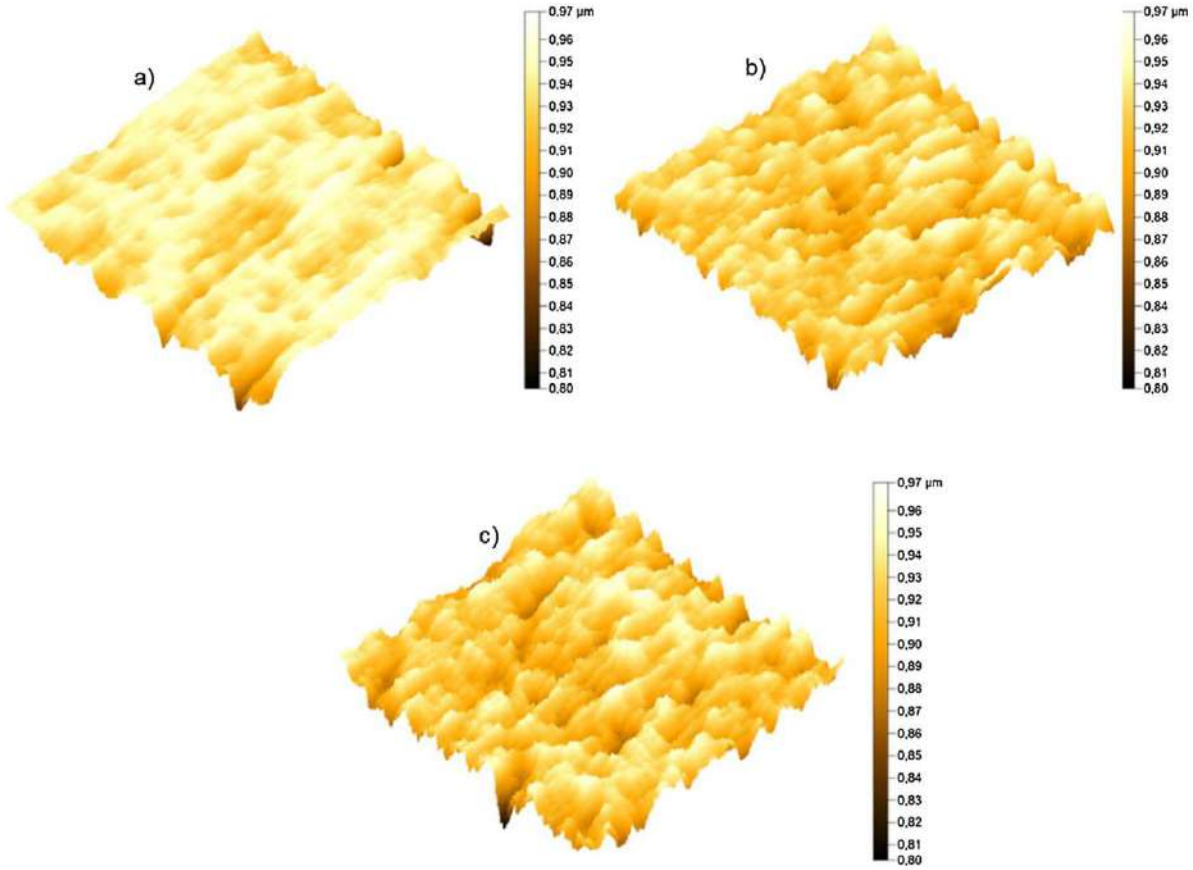

Fig. 5. Contact mode Atomic Force Microscopy (AFM) images of (a) bare electrode; (b) PTy/GE and (c) CNT/ PTy/GE.

In order to understand better of the CNT/PTy interactions, ATR-FT-IR spectra were performed (Fig. 4). The PTy film coating the gold electrode was confirmed at *spectrum (I)* by a large band at 3330 cm^{-1}that corresponded to the OH stretch in the presence of intramolecular hydrogen bonds [45,46]. PTy was also evidenced by an asymmetric band at 1635 cm^{-1} of NH_2, resulting from PTy amide I modes; at 1506 cm^{-1}, corresponding to C=C aromatic symmetric stretching; and at 1156 cm^{-1}, due to the C–O–C asymmetric stretching [46]. Additionally, it was observed the band 3330 overlapped with the 3200 cm^{-1} band being representative of an asymmetric stretch of NH_3^+, which is typically derived of the PTy electrosynthesis in acid medium due to the oxidation of Ty. Catalytic activity of PTy film was also confirmed by NH_3^+ at *spectrum (III)*, corresponding to Pty-CNT film that showed the same overlapped band at 3200 cm^{-1}. The catalytic activity is also corroborated by cyclic voltammogram that shows a prominent anodic peak and a cathodic peak at 0.6 V, in presence of inert electrolyte (0.1 M KCl). The strong and stable bond CNT-PTy is displayed at *spectrum (III)* by the presence of the amide I band at 1652 cm^{-1} and amide II bending at 1552 cm^{-1} [47]. The great electroactive area obtained, due to the high yield at CNT-PTy coupling is derived from EDC/NHS activation of CNT to form an *o*-acylisourea intermediate that is dependent of COO-. The bands characteristic of deprotonated carboxyl groups were found at 1560 and 1400 cm^{-1} at *spectrum (II)*, due to the asymmetric and symmetric stretch vibration of COO- [47]. The electrocatalytic activity of Pty polymer is derived from NH_3^+ that generates electroactive species at anodic and cathodic polarizations (*spectrum II)*.

AFM morphological analysis of Pty film on the electrode resulted in an average roughness of approximately 150 nm (Fig. 5(b)), which was significantly higher than the bare GE (71 nm), exhibiting a very smooth and regular morphology (Fig. 5(a)). These findings confirm the successful in electropolymerization of tyramine monomers onto the gold electrode surface. Average roughness also increased to 296 nm with CNT attachment, that was according to electroactive area increase (Fig. 5(c)) when compared with PTy only (b), demonstrating the synergic effect as resulted from the CNT adding to PTy film.

It is well-established that the CNTs exert an important role to the sensor response, since they are related with electron transfer rate on the interface electrolyte-electrode surface [10,48]. After analyses of FTIR and CVs profiles, it was possible ascribed that CNTs were covalently bound to PTy. Taking account that CNTs are EDC/NHS pre-activated and amide bonds are formed, and also that CNTs attached by simple adsorptions were removed with successive washes with a saline solution (PBS); certainly, the amount of CNTs present on the electrode surface are dependent of amine bonds of Pty.

3.2. Response to the Anti-HBc antibodies

The analytical responses of the immunosensor were evaluated by incubating the electrode to different concentrations of anti-HBc diluted in 10 mM PBS. The amperometric signals in responses to analytes decreased with the increase of anti-HBc. This behavior is ascribed to insulating nature of antibodies, preventing the barrier of diffusion (Fig. 6(b)). The incubation time of antigen-antibody exert influence on the immunosensor response. It was chosen 15 min of incubation time based on previous studies, in which is achieved approximately 100% of current response by antigen-antibody interactions [49,50].The immunosensor shows a good linear range from 1.0 to 5.0 ng mL^{-1}anti-HBc (square R equal to 0.961 and relative error < 1%), which is according to clinical range for anti-HBc [51,52].

As shown also in Fig. 6(b), up to 5 ng mL^{-1} anti-HBc, the calibration curve achieved a plateau, as response that the maximal antigen-antibody interactions were obtained. The limit of detection (LOD = 3.3 x standard deviation of y-intercepts (σ)/slope of the calibration curve (S)) was calculated according to fit linear regression equation of the calibration curve (ΔI = 77.3 – 4.28 [anti-HBc]), by data processing in the

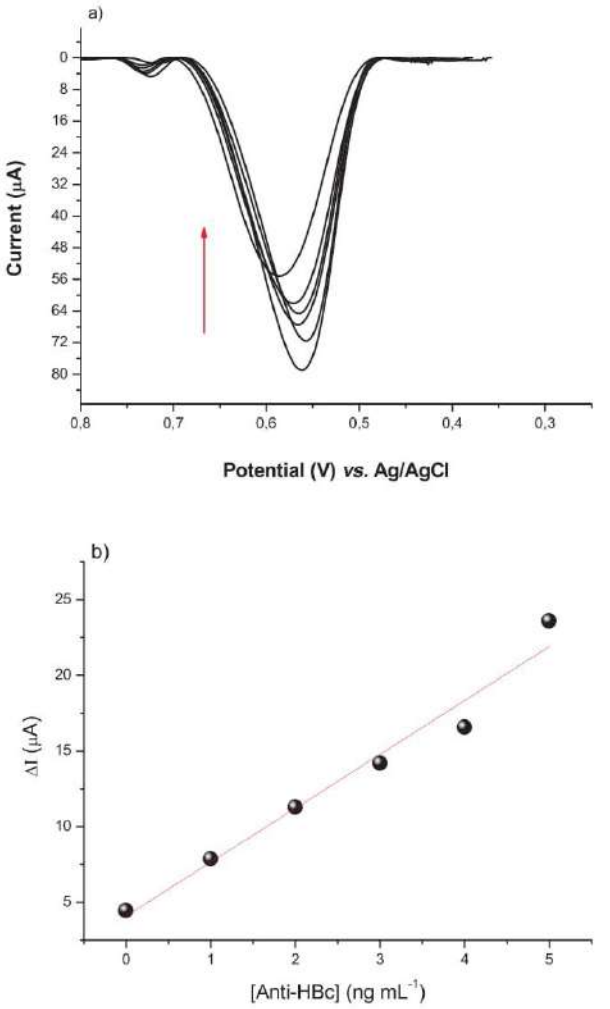

Fig. 6. (a) SWV curves in responses to different concentrations of anti-HBc with measurements performed in 100 mM KCl at 50 mV/s scan rate; **(b)** Cathodic current peaks in relation to the anti-HBc concentrations with adjusted linear fit (red line) (For interpretation of the references to colour in this figure legend, the reader is referred to the web version of this article).

Origin Pro SRO v8.0724. It was found a LOD = 0.89 ng mL^{-1} anti-HBc, similar to Cabral et al., [53], being suitable for clinical levels. However, this immunosensor has advantage of detecting without a redox probe solution, being more practical and easier than labeled and label-free immunosensors previously described [53,54].

The immunoelectrode was also evaluated regarding to repeatability and reproducibility. By using an incubation average concentration of anti-HBc (2 ng mL^{-1}) and submitting the same electrode to successive SWV readings, at 20 replicates, with attention of remove the electrode of electrochemical cell in each reading followed by PBS wash, it was found a good repeatability with a coefficient of variation (CV) lower 1%. The reproducibility study was performed by using 8 electrodes prepared in the same conditions, and by incubating with 2 ng mL^{-1} of anti-HBc. The measurements of cathodic peaks from SWVs of incubations subtracted from blank after normalized resulted in a CV = 6%.

3.2.1. Response to anti-HBc in real samples

The selectivity of the sensor platform was evaluated submitting the electrode to real samples. Blood samples were extracted from Vacutainer EDTA tubes and spiked with anti-HBc diluted in PBS,

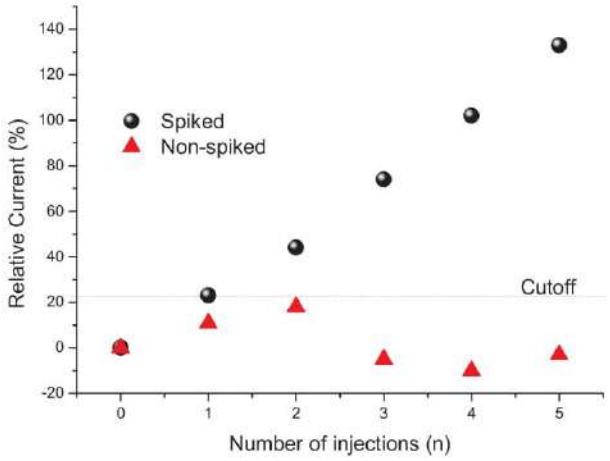

Fig. 7. Matrix effect study performed in samples of human blood pools of 1 ng mL^{-1} anti-HBc spiked and non-spiked. Plot represents the cathodic peak currents subtracted from the blank measured at 0.6 V from the successive SWVs.

resulting in aliquots with 1 ng mL^{-1} anti-HBc, and the negative samples were carefully prepared with the same volume of PBS, in order that the signal increment in response to incubations were exclusively due to the anti-HBc. The specificity of sensor could be studied since the blood is very complex matrix, containing several proteins, lipids, cells, debris, *etc.* and electroactive species, serving as good model to evaluated possible interferences [55]. According to Fig. 7, it was observed that difference of peak currents from the blank gradually increase with the anti-HBc concentrations, conversely to the non-spiked blood that was practically constant in all negative blood samples. The limit of reaction (cutoff) was found at 1.5 ng mL^{-1} anti-HBc, calculated according to the value obtained by mean from six negative samples plus twice their standard deviations. These results showed that this platform is reliable and present specificity to recognize negative from positive blood samples by SWV, without any use of redox probe solutions and with a similar analytical range to previous anti-HBc immunosensor [53]. This catalytic nanostructured surface has advantage of facilitating measurements directly on serological samples and reagentless, leading toward the point-of-care testing.

4. Conclusions

It was possible to detect antibodies against core of HBV with discrimination in blood samples. Amine groups of PTy showed a catalytic activity, allowing an electrochemical detection by SWV without requirements of redox probe solutions. This advantage reduces the inconvenient steps on the analysis, which are time-consuming and presents difficulties on detection. The reagentless detection with minimal steps by simple use of a catalytic sensor surface with electroactive species released for amperometric measurements was achieved. This approach is an attempt to circumvent the point-of-care testing limitations, allowing a future direct detection in blood samples.

Acknowledgments

The authors thankNational Council for Scientific and Technological Development (CNPq) for the financial support and the Foundation for Science and Technology of the State of Pernambuco (FACEPE) by scholarship's Trindade, E. during this work.

Appendix A. Supplementary data

Supplementary material related to this article can be found, in the online version, at doi:https://doi.org/10.1016/j.colsurfb.2018.08.050.

References

[1] S. Datta, S. Chatterjee, V. Veer, Recent advances in molecular diagnostics of hepatitis B virus, World J. Gastroenterol. 20 (2014) 14615, https://doi.org/10.3748/wjg.v20.i40.14615.
[2] E.M. El-Ghitany, A.G. Farghaly, Evaluation of commercialized rapid diagnostic testing for some Hepatitis B biomarkers in an area of intermediate endemicity, J. Virol. Methods 194 (2013) 190–193, https://doi.org/10.1016/j.jviromet.2013.08.026.
[3] C. Trépo, H.L.Y. Chan, A. Lok, Hepatitis B virus infection, Lancet 384 (2014) 2053–2063, https://doi.org/10.1016/S0140-6736(14)60220-8.
[4] G. Albertoni, M.J.B. Castelo Girão, N. Schor, Mini review: current molecular methods for the detection and quantification of hepatitis B virus, hepatitis C virus, and human immunodeficiency virus type 1, Int. J. Infect. Dis. 25 (2014) 145–149, https://doi.org/10.1016/j.ijid.2014.04.007.
[5] G. Karimi, M. Zadsar, N. Vafaei, Z. Sharifi, M. FalahTafti, Prevalence of antibody to Hepatitis B core antigen and Hepatitis B virus DNA in HBsAg negative healthy blood donors, Virol. J. 13 (2016) 36, https://doi.org/10.1186/s12985-016-0492-8.
[6] X. Ye, T. Li, X. Xu, P. Du, J. Zeng, W. Zhu, B. Yang, C. Li, J.-P. Allain, Characterisation and follow-up study of occult hepatitis B virus infection in anti-HBc-positive qualified blood donors in southern China, Blood Transfus. (2016) 1–7, https://doi.org/10.2450/2016.0268-15.
[7] M. Jahan, M.A. Islam, S.M.F. Akbar, K. Takahashi, S. Tabassum, A. Rahman, M.A. Haque, J. Biswas, S. Mishiro, M. Al-Mahtab, Anti-HBc screening of blood donors in Bangladesh: relevance to containment of HBV propagation, J. Clin. Exp. Hepatol. 6 (2016) 115–118, https://doi.org/10.1016/j.jceh.2016.05.002.
[8] M.-A. Mahtab, Epidemiology of viral hepatitis and liver diseases in Bangladesh, Euroasian J. Hepato-Gastroenterol. 5 (2015) 26–29, https://doi.org/10.5005/jp-journals-10018-1124.
[9] C. Niederhauser, Reducing the risk of hepatitis B virus transfusion-transmitted infection, J. Blood Med. 2 (2011) 91–102, https://doi.org/10.2147/JBM.S12899.
[10] M.M.S. Silva, A.C.M.S. Dias, B.V.M. Silva, S.L.R. Gomes-Filho, L.T. Kubota, M.O.F. Goulart, R.F. Dutra, Electrochemical detection of dengue virus NS1 protein with a poly(allylamine)/carbon nanotube layered immunoelectrode, J. Chem. Technol. Biotechnol. 90 (2015) 194–200.
[11] B. Zribi, E. Roy, A. Pallandre, S. Chebil, M. Koubaa, N. Mejri, H. Magdinier Gomez, C. Sola, H. Korri-Youssoufi, A.-M. Haghiri-Gosnet, A microfluidic electrochemical biosensor based on multiwall carbon nanotube/ferrocene for genomic DNA detection of Mycobacterium tuberculosis in clinical isolates, Biomicrofluidics 10 (2016) 14115, https://doi.org/10.1063/1.4940887.
[12] S. Chandra, R. Bharadwaj, S. Mukherji, Label free ultrasensitive optical sensor decorated with polyaniline nanofibers: characterization and immunosensing application, Sens. Actuators B Chem. 240 (2017) 443–450, https://doi.org/10.1016/j.snb.2016.08.103.
[13] S. Zeng, D. Baillargeat, H.-P. Ho, K.-T. Yong, Nanomaterials enhanced surface plasmon resonance for biological and chemical sensing applications, Chem. Soc. Rev. 43 (2014) 3426–3452, https://doi.org/10.1039/c3cs60479a.
[14] J. Ramos-Jesus, L.C. Pontes-de-Carvalho, S.M.B. Melo, N.M. Alcântara-Neves, R.F. Dutra, A gold nanoparticle piezoelectric immunosensor using a recombinant antigen for detecting Leishmania infantum antibodies in canine serum, Biochem. Eng. J. 110 (2016) 43–50, https://doi.org/10.1016/j.bej.2016.01.027.
[15] T. Xu, J. Miao, Z. Wang, L. Yu, C.M. Li, Micro-piezoelectric immunoassay chip for simultaneous detection of Hepatitis B virus and alpha-fetoprotein, Sens. Actuators B Chem. 151 (2011) 370–376, https://doi.org/10.1016/j.snb.2010.08.013.
[16] E. Sheikhzadeh, M. Chamsaz, A.P.F. Turner, E.W.H. Jager, V. Beni, Label-free impedimetric biosensor for Salmonella Typhimurium detection based on poly [pyrrole-co-3-carboxyl-pyrrole] copolymer supported aptamer, Biosens. Bioelectron. 80 (2016) 194–200, https://doi.org/10.1016/j.bios.2016.01.057.
[17] E.A. Obaje, G. Cummins, H. Schulze, S. Mahmood, M.P.Y. Desmulliez, T.T. Bachmann, Carbon screen-printed electrodes on ceramic substrates for label-free molecular detection of antibiotic resistance, J. Interdiscip. Nanomed. 1 (2016) 93–109, https://doi.org/10.1002/jin2.16.
[18] B. Yilmaz, Electrochemical behavior of atorvastatin at glassy carbon electrode and its direct determination in pharmaceutical preparations by square wave and differential pulse voltammetry, Indian J. Pharm. Sci. 78 (2016) 360–367.
[19] L.D. Tran, B. Piro, M.C. Pham, T. Ledoan, C. Angiari, L.H. Dao, F. Teston, A polytyramine film for covalent immobilization of oligonucleotides and hybridization, Synth. Met. 139 (2003) 251–262, https://doi.org/10.1016/S0379-6779(03)00131-0.
[20] H. Shirakawa, E.J. Louis, A.G. MacDiarmid, C.K. Chiang, A.J. Heeger, Synthesis of electrically conducting organic polymers: halogen derivatives of polyacetylene, (CH) x, J. Chem. Soc. Chem. Commun. (1977) 578, https://doi.org/10.1039/c39770000578.
[21] S. Cosnier, A. Karyakin, Electropolymerization: concepts, Mater. Appl. (2010), https://doi.org/10.1002/9783527630592.
[22] A. Ehsani, M.G. Mahjani, S. Adeli, S. Moradkhani, Electrosynthesis and physioelectrochemical properties of poly tyramine electroactive film in the presence of the surfactant: comparable study, Prog. Org. Coat. 77 (2014) 1674–1681, https://doi.org/10.1016/j.porgcoat.2014.05.027.
[23] a Tenreiro, C.M. Cordas, L.M. Abrantes, Oligonucleotide immobilisation on polytyramine-modified electrodes suitable for electrochemical DNA biosensors, Port. Electrochim. Acta 21 (2003) 361–370, https://doi.org/10.4152/pea.200304361.
[24] A. Ehsani, Influence of counter ions in electrochemical properties and kinetic parameters of poly tyramine electroactive film, Prog. Org. Coat. 78 (2015) 133–139, https://doi.org/10.1016/j.porgcoat.2014.09.015.

[25] C.M. De Castro, S.N. Vieira, R.A. Gonçalves, A.G. Brito-Madurro, J.M. Madurro, Electrochemical and morphologic studies of nickel incorporation on graphite electrodes modified with polytyramine, J. Mater. Sci. 43 (2008) 475–482, https://doi.org/10.1007/s10853-007-1880-7.
[26] T.I.W. Schnoor, G. Smith, D. Eder, K.K.K. Koziol, G. Tim Burstein, A.H. Windle, K. Schulte, The production of aligned MWCNT/polypyrrole composite films, Carbon N. Y. 60 (2013) 229–235, https://doi.org/10.1016/J.CARBON.2013.04.016.
[27] Y. Yan, J. Cui, Q. Zhang, Assembly of carbon nanotubes toward practical applications, in: Q. Zhang (Ed.), Carbon Nanotubes and Their Applications, CRC Press, 2012, pp. 73–120.
[28] Q. Zhang, Carbon Nanotubes and Their Applications, CRC Press, 2012.
[29] X. Sun, N. Hui, X. Luo, Reagentless and label-free voltammetric immunosensor for carcinoembryonic antigen based on polyaniline nanowires grown on porous conducting polymer composite, Microchimica Acta 184 (2017) 889–896, https://doi.org/10.1007/s00604-016-2068-0.
[30] A.C.M.S. Dias, S.L.R. Gomes-Filho, M.M.S. Silva, R.F. Dutra, A sensor tip based on carbon nanotube-ink printed electrode for the dengue virus NS1 protein, Biosens. Bioelectron. 44 (2013) 216–221, https://doi.org/10.1016/J.BIOS.2012.12.033.
[31] P.M.S. Silva, A.L.R. Lima, B.V.M. Silva, L.C.B.B. Coelho, R.F. Dutra, M.T.S. Correia, Cratylia mollis lectin nanoelectrode for differential diagnostic of prostate cancer and benign prostatic hyperplasia based on label-free detection, Biosens. Bioelectron. 85 (2016), https://doi.org/10.1016/j.bios.2016.05.004.
[32] F.Y. Wu, Y.W. Liao, J.F. Wu, H.L. Chen, H.Y. Hsu, M.H. Chang, Y.H. Ni, A simple and rapid test-card method to detect hepatitis B surface antigen and antibody: potential application in young children and infants, Pediatr. Neonatol. 57 (2016) 219–224, https://doi.org/10.1016/j.pedneo.2015.07.003.
[33] S. Li, Molecularly Imprinted Sensors: Overview and Applications, Elsevier, 2012.
[34] A. Ehsani, M.G. Mahjani, F. Babaei, H. Mostaanzadeh, Physioelectrochemical and DFT investigation of metal oxide/p-type conductive polymer nanoparticles as an efficient catalyst for the electrocatalytic oxidation of methanol, RSC Adv. 5 (2015) 30394–30404, https://doi.org/10.1039/C5RA02297E.
[35] M.L. Yola, T. Eren, N. Atar, Molecularly imprinted electrochemical biosensor based on Fe @ Au nanoparticles involved in 2-aminoethanethiol functionalized multi-walled carbon nanotubes for sensitive determination of cefexime in human plasma, Biosens. Bioelectron. 60 (2014) 277–285, https://doi.org/10.1016/j.bios.2014.04.045.
[36] L. Yang, D. Liu, J. Huang, T. You, Simultaneous determination of dopamine, ascorbic acid and uric acid at electrochemically reduced graphene oxide modified electrode, Sens. Actuators B Chem. 193 (2014) 166–172, https://doi.org/10.1016/j.snb.2013.11.104.
[37] W. Sun, S. Gong, F. Shi, L. Cao, L. Ling, W. Zheng, W. Wang, Direct electrochemistry and electrocatalysis of hemoglobin in graphene oxide and ionic liquid composite film, Mater. Sci. Eng. C 40 (2014) 235–241, https://doi.org/10.1016/j.msec.2014.03.035.
[38] B. Wu, J. Zhang, Z. Wei, S. Cai, Z. Liu, Chemical alignment of oxidatively shortened single-walled carbon nanotubes on silver surface, J. Phys. Chem. B 105 (2001) 5075–5078, https://doi.org/10.1021/JP0101256.
[39] C.N.R. Rao, R. Sen, Large aligned-nanotube bundles from ferrocene pyrolysis, Chem. Commun. 0 (1998) 1525–1526, https://doi.org/10.1039/a802258e.
[40] L. Dai, A. Patil, X. Gong, Z. Guo, L. Liu, Y. Liu, D. Zhu, Aligned nanotubes, ChemPhysChem 4 (2003) 1150–1169, https://doi.org/10.1002/cphc.200300770.
[41] Ö. Ertekin, S. Öztürk, Z.Z. Öztürk, Label free QCM immunobiosensor for AFB1 detection using monoclonal IgA antibody as recognition element, Sensors (Switzerland) 16 (2016) 1–12, https://doi.org/10.3390/s16081274.
[42] F.T.C. Moreira, B.A.G. Rodriguez, R.A.F. Dutra, M.G.F. Sales, Redox probe-free readings of a B-amyloid-42 plastic antibody sensory material assembled on copper@carbon nanotubes, Sens. Actuators B Chem. 264 (2018) 1–9, https://doi.org/10.1016/j.snb.2018.02.166.
[43] A.J. Bard, L.R. Faulkner, N. York, C. @bullet, W. Brisbane, S.E. Toronto, Electrochemical Methods Fundamentals and Applications, (1944), https://doi.org/10.1016/B978-0-12-381373-2.00056-9.
[44] G. Lai, H. Zhang, J. Yong, A. Yu, In situ deposition of gold nanoparticles on polydopamine functionalized silica nanosphere for ultrasensitive nonenzymatic electrochemical immunoassay, Biosens. Bioelectron. 47 (2013) 178–183, https://doi.org/10.1016/j.bios.2013.03.029.
[45] Y. Hishikawa, E. Togawa, T. Kondo, Characterization of individual hydrogen bonds in crystalline regenerated cellulose using resolved polarized FTIR spectra, ACS Omega 2 (2017) 1469–1476, https://doi.org/10.1021/acsomega.6b00364.
[46] M. Fan, D. Dai, B. Huang, Fourier transform infrared spectroscopy for natural fibres, Fourier Transform –Mater. Anal. (2012), pp. 46–68.
[47] R.J. Service, W. Hillier, R.J. Debus, Evidence from FTIR difference spectroscopy for an extensive network of hydrogen bonds near the oxygen-evolving Mn4Ca cluster of photosystem II involving D1-Glu65, D2-Glu312, and D1-Glu329, Biochemistry 49 (2010) 6655–6669, https://doi.org/10.1021/bi100730d.Evidence.
[48] Y. Hu, Z. Zhao, Q. Wan, Bioelectrochemistry Facile preparation of carbon nanotube-conducting polymer network for sensitive electrochemical immunoassay of Hepatitis B surface antigen in serum, Bioelectrochemistry 81 (2011) 59–64, https://doi.org/10.1016/j.bioelechem.2011.01.005.
[49] L. Talamini, N. Zanato, E. Zapp, D. Brondani, I.C. Vieira, Direct Electrochemical Nano-immunosensor for Microcystin-LR in Seawater, Electroanal 30 (2018) 819–827, https://doi.org/10.1002/elan.201700815.
[50] R.F. Dutra, L.T. Kubota, An SPR immunosensor for human cardiac troponin T using specific binding avidin to biotin at carboxymethyldextran-modified gold chip, Clin. Chim. Acta 376 (2007), https://doi.org/10.1016/j.cca.2006.07.029.
[51] R.S. Koff, Hepatitis B Vaccines in Clinical Practice, New York, (1992), https://doi.org/10.1002/hep.1840190141.
[52] Y.-W. Huang, C.-L. Lin, P.-J. Chen, M.-Y. Lai, J.-H. Kao, D.-S. Chen, Higher cut-off index value of immunoglobulin M antibody to hepatitis B core antigen in Taiwanese patients with hepatitis B, J. Gastroenterol. Hepatol. 21 (2006) 859–862, https://doi.org/10.1111/j.1440-1746.2006.04280.x.
[53] D.G.A. Cabral, E.C.S. Lima, P. Moura, R.F. Dutra, A label-free electrochemical immunosensor for hepatitis B based on hyaluronic acid–carbon nanotube hybrid film, Talanta 148 (2016) 209–215, https://doi.org/10.1016/j.talanta.2015.10.083.
[54] S. Patris, P. De Pauw, M. Vandeput, J. Huet, P. Van Antwerpen, S. Muyldermans, J.M. Kauffmann, Nanoimmunoassay onto a screen printed electrode for HER2 breast cancer biomarker determination, Talanta 130 (2014) 164–170, https://doi.org/10.1016/j.talanta.2014.06.069.
[55] A. de Moraes, L. Kubota, Recent trends in field-effect transistors-based immunosensors, Chemosensors 4 (2016) 20, https://doi.org/10.3390/chemosensors4040020.

APÊNDICE C – CAPÍTULO DE LIVRO PUBLICADO

NANOMATERIALS FOR ADVANCING THE HEALTH IMMUNOSENSOR

Blanca A.G. Rodriguez, Erika K.G. Trindade, Diego G.A. Cabral, Erika C.L. Soares, Cayo E.L. Menezes, Danielle C.M. Ferreira, Renata K. Mendes and Rosa F. Dutra

In: **Biosensors - Micro and Nanoscale Applications**

InTech, 2015

Chapter 12

Nanomaterials for Advancing the Health Immunosensor

Blanca A.G. Rodriguez, Erika K.G. Trindade,
Diego G.A. Cabral, Erika C.L. Soares,
Cayo E.L. Menezes, Danielle C.M. Ferreira,
Renata K. Mendes and Rosa F. Dutra

Additional information is available at the end of the chapter

http://dx.doi.org/10.5772/61149

Abstract

Nanotechnology has exerted a significant impact in the development of biosensors allowing more sensible analytical methods. In health applications, the main challenge of the immunoassay is to reach the suitable limit of detection, recognizing different analytes in complex samples like whole blood, serum, urine, and other biological fluids. Different nanomaterials, including metallic, silica and magnetic nanoparticles, quantum dots, carbon nanotubes, and graphene, have been applied, mainly to improve charge electron transfer, catalytic activity, amount of immobilized biomolecules, low-background current, signal-to-noise ratio that consequently increase the sensitivity of immunosensors. Given the great impact of nanotechnology, this chapter intends to discuss new aspects of nanomaterials relating to immunosensor advancement.

Keywords: Immunosensors, immunoassay, nanosensor, nanomaterial

1. Introduction

A major challenge faced by health programs is the maintenance and availability of diagnostic tests that are required not only in inpatient or outpatient hospital but also for an improved epidemiological survey. In many cases, the absence of laboratory testing or delay of diagnosis generates negative economic impacts, resulting in unnecessary hospitalization, intercurrence,

and in some cases implications on the global life quality of patients and underreporting of surveillance. In this context, the development of practical, fast, and reliable analytical methods is imperative.

Biosensors have been considered one of the more attractive analytical methods. They are biodevices capable of transforming an interaction with specific analytes into an electrical signal by a transducer, including a biorecognition element. [1] Pharmaceutical industries and users of rapid tests from the United States and Europe are unanimous in stating that biosensors, mainly those based on point-of-care testing (POCT), or bedside testings are a practical technology, regarded as a short-, medium-, and long-term trend. Among several advantages, POCT can provide immediate responses (results in few minutes or in real time), samples do not need to be transported to the analytical phase (in situ monitoring) and require generally small volumes of samples, and the users can be skilled or unskilled and present better cost-effective analyses compared with conventional technologies used in clinical diagnostic (user-friendly technology). One of the most widely useful POCT is the glucometer, which measures glucose levels with accuracy by requiring a single drop of blood. The rapid glucose measurement is very important in trials to avoid serious adverse effects stemming from diabetes, including seizures, coma, or even death. Worldwide, some diabetic outpatients have been benefited by POCTs.

Although there is a great promising market dedicated to health for the detection of diseases and therapeutic monitoring, biosensors are not yet entirely broadcast, especially those devoted to nonenzymatic reactions, i.e., biosensors based on the affinity between antigen–antibodies, DNA–RNA, DNA–DNA, etc. So far, there are focused studies to develop affinity biosensors for a wide number of applications. Some of these include environmental, agriculture, veterinary, safety food analysis, and health diagnostic in attempting to detect pesticides in water, in monitoring of environmental pollutants in soil, and in determining contaminants and pathogens in food and many others.[2]

Regarding the health diagnostic, affinity biosensors devoted to immunoserological diagnosis have demonstrated to be more accurate, feasible, practical, and advantageous for POCTs than nucleic acid biosensors. First, the levels of antibodies or antigens circulating in whole blood, serum, or other biological fluids are in higher amounts compared to RNA or DNA sequences. Second, blood samples of immunosensors do not need cell lysis before measurements to release the analytes. Third, antigen or antibody samples do not need pretreatment before measurements as amplification by polymerase chain reaction (PCR) or transcriptase reverse polymerase chain reaction (TR-PCR). Fourth, antibodies are more chemically stable than RNA or DNA sequences that are easily contaminated by attacking the RNases or DNases enzymes present in digital samples.

Due especially to nanotechnology, biosensors dedicated to immunoserological diagnosis have emerged, in the last decade, with the possibility of very promising point-of-care diagnosis. The contribution of nanomaterials has made possible the development of new immobilization matrices with improved features, increased sensor surface area, greater amount of biomolecules per area/volume, and major electrical conductivity, making it possible to achieve a lower limit of detection compared to existing bulk biosensors. Currently, several studies have

http://dx.doi.org/10.5772/61149

highlighted the following nanomaterials: metallic, silica and magnetic nanoparticles, quantum dots (semiconductor nanoparticle), carbon nanotubes, graphene, and nanostructured surface.

Selective monoclonal antibodies, recombinant antigens, fragments, and aptamers associated with the nanomaterial advancements to mediate the antigen–antibody responses have also allowed several nanostructured devices with optical, piezoelectric, and electrochemical improved transductions, besides the integration of microfluidics and portable approaches.

Given the great impact of nanotechnology, this chapter intends to discuss new aspects of nanomaterials concerning to the development of immunosensors that resulted in more accurate, reliable, and practical analytical methods for health.

2. Important aspects for immunosensor development

Immunosensor technology has shown an exponential growth in the number of publications over the last decade (Figure 1(a)). Although, there were significant advances in all the areas mainly in the food analyses, immunosensors devoted to health still have huge challenges to overcome in order to yield commercial uses (Figure 1(b)). Some difficulties can be attributed to the biomolecules specificity, immobilization matrix stability, transduction mode employed and pretreatment of complex samples like whole blood, serum, or other fluidic biologics for a reliable detection.

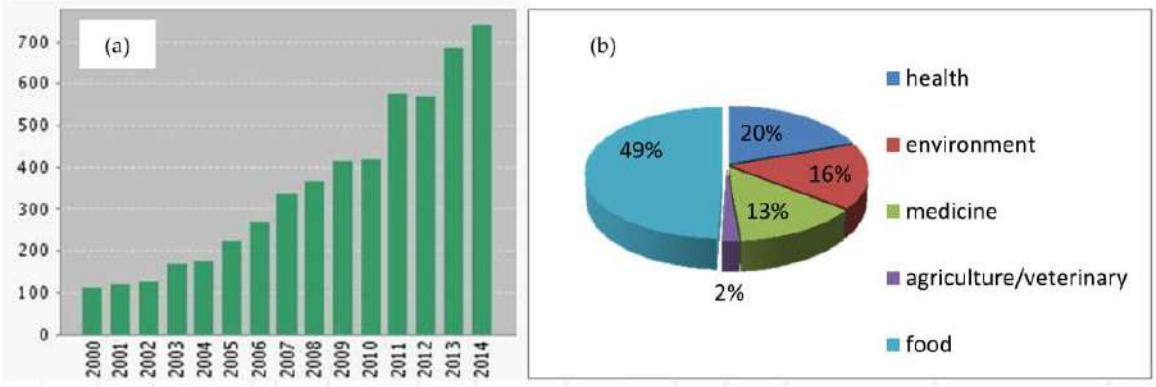

Figure 1. Immunosensors research published over the last decade (a) and main application areas (b). (Extracted from ISI of Knowledge base)

Three aspects are considered crucial in the development of an ideal immunosensor: (a) the bioreceptor, i.e., biomolecule used to recognize the antigen or antibodies in the sample; (b) the matrix assembled for immune compound immobilization; and (c) the transducer type employed.

The choosing of bioreceptors for analyte recognition is a fundamental aspect to ensure an optimal selectivity of immunosensor. Different immunomolecules have been used to detect antigens or antibodies in different samples, besides monoclonal or polyclonal antibodies, and

antigens, recently recombinant antibodies, [3] aptamers, [4] and antibody fragments [5] have been also assayed. Immunoglobulin classes IgG and IgM are the most commonly employed in immunosensors. IgG is a Y-shaped structure with two binding sites for antigens recognizing (two paratopes), with approximately 150 kDa. Meanwhile, IgM immunoglobulins are pentamers comprising of ten antigen sites, called natural antibodies. However, due to IgG being more prevalent and most abundant in the circulation (73%), this immunglobulin is more frequently used in all immunoassays. IgM immunoglobulins are detected in specific assays when is important to identify diseases in their acute Phase, Kidwai et al. [6] developed a rapid immunochromatographic (ICT) assay detection for IgM and IgG detection in serum.

Immunosensor performance is directly dependent on the immobilization matrix used and orientation and density of affinity biomolecules (antibodies and antigens) on the electrode surfaces. There are different strategies used to immobilize the recognition element, either directly on the electrode surface or on other solid supports. [7] Conventionally, there are noncovalent and covalent techniques employed to immobilize antibodies, which are based on adsorption, encapsulation, and entrapment in polymers, covalent binding, and cross-linking of antibodies aggregates (Figure 2). Developments in these techniques have great interest and potential application in other areas of biotechnology, including purification of proteins, [8] medicine and drug delivery, [9] regenerative medicine, tissue engineering, and many other applications. [10]

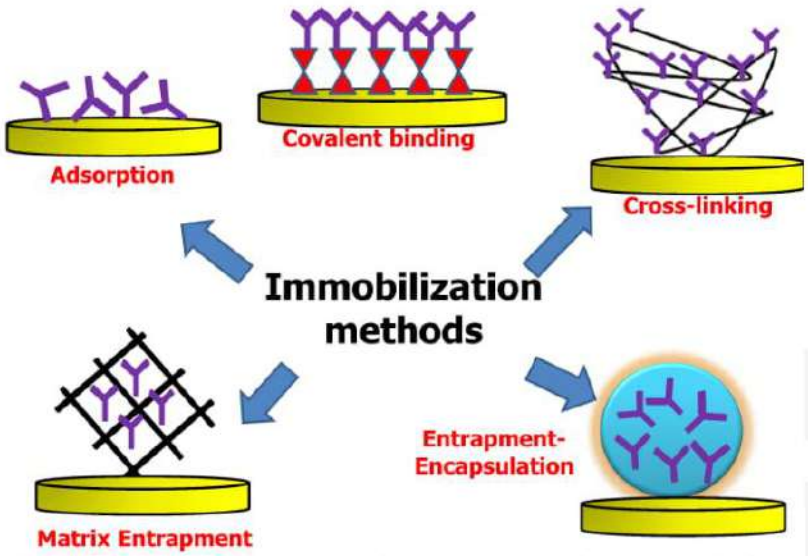

Figure 2. Illustration of different methods of antibodies immobilization.

Although sensor surfaces prepared with antibodies immobilized in a random manner yield satisfactory results, the site-directed immobilization of the sensing molecules significantly improves the immunosensor sensitivity. [11] In this sense, antibodies should be immobilized with optimal capability to recognize the antigens, while fully maintaining their preserved structures. The Fab region needs to be sufficiently free in order to be exposed to the medium,

i.e., epitopes of antigens. The best approach is to immobilize antibodies by their Fc regions. [12] This configuration has been achieved using different strategies, including by the use of protein A [13] or protein G, [14] via covalent immobilization through the oxidized sugar chains of the antibody, [15] and others. Besides orientation, it's important to consider antibody density on the electrode surface. A higher density increases the sensor response, however is likely to increase the steric hindrance on planar substrates causing a low immobilization efficiency and low assay sensitivity. To solve these problems, researchers are focused on modifying the substrates for forming the 3D network, which ensures high percentage availability of antibody binding sites. Nanomaterials contribute to increase the amount of protein immobilization because of their capability to form 3D nanostructured surfaces with innumerous cavities and valleys.

Choosing the transducer is another important and fundamental aspect to achieve the sensitivity and response time desired. Bioaffinity sensors (immunosensor) have been explored by using different transduction modes: optical, acoustic and electrochemical by using different approaches. Surface plasmon resonance, [16] localized surface plasmon resonance [17] and fluorescence resonance energy transfer (FRET) [18] are examples of optical transducers. Quartz crystal microbalance (QCM), also entitled mass-sensitive, is the most explored as acoustic transducer. Electrochemical transducers are comprised of different ways to generate an electrical signal, for instance, by amperometric, impedimetric, potentiometric and capacitive changes. [19] Regarding the response time, two classes of immunosensor operation mode are distinguished by, a) Label-free or nonlabeled immunosensors that readily convert the species interaction response with the complementary species into an electrical signal, denominated as direct transduction, and b) Labeled immunosensors that need a second antibody or antigen conjugated to chemical species to generate the analytical response, such as enzymes, fluorescent labels, etc. [20] Although labeled immunosensors are more time consuming than label-free immunosensors, they provide more specificity due to the second antibody which minimize the nonspecific binding negative effects.

The design of label-free affinity biosensors has been extensively studied in academy and industry. One source of stimulation is the demand of POCTs for health, which requires rapid response, lower cost-effective analyses and simplicity for potential analysis. The main technologies of label-free immunosensors currently in use or under development are: surface plasmon resonance (SPR) devices, mass-sensitive, field effect transistor (FET), and electrochemical sensors, including impedimetric and capacitive. Recently, due to advances of nanomaterial based-immunosensors, new categories of label-free amperometric sensors using screen printed electrodes have been successfully developed. [21, 22, 23, 24]

3. Immunosensor based on nanomaterials

Nanomaterial is composed of unique functional materials that display incomparable characteristics related to their shape, structure and size (in the order of 1 to 100 nm). Nanostructured materials are interesting because they can bridge the gap between the bulk and molecular

levels and lead to entirely new avenues for applications, especially in electronics, optoelectronics and biology. The contribution of nanomaterials has allowed powerful immunosensor assemblies, creating platforms with increasing detection limit. [25]

In recent years, various nanomaterials with different physical and chemical properties have been applied to achieve the immobilization of immunocompounds. They can modify the sensing surface, improving the immobilization of procedures and transduction properties of immunosensors. A great number of electrochemical advantages have been mentioned, such as possessing low-background current, high signal-to-noise ratio, and fast electron transfer, including an increased amount of immobilized biomolecules, with consequent increase on the sensitivity of sensors. Nanomaterials with zero-dimensional space (metallic, silica, and magnetic nanoparticles and quantum dots or semiconductor nanoparticles), one-dimensional space (carbon nanotubes), and two-dimensional space (graphene) have been show as potential for different transducers in many immunosensor applications.

3.1. Metallic, silica, and magnetic nanoparticles

Nanoparticles (NPs) obtained from commercial sources or properly produced in laboratories have attracted much attention in biological studies due to their low toxicity, biocompatibility, and unique optical properties. Nanoparticles and nanospheres can be divided into magnetic, metallic, semiconducting, or insulating nanoparticles based on their conductivity.

NPs have high surface areas and unique physical–chemical properties that can be easily tuned, making them ideal candidates for developing immunosensors devices. The basic function of nanoparticles in an immunosensor can be summarized as follows: immobilizing the biomolecules on the electrode surface, catalyzing electrochemical reaction, enhancing electron transfer charge, and acting as a reactant or labeling biomolecules for further experiments, among others. [26]

Biological tests measuring the presence or activity of selected analytes become quicker, more sensitive, and flexible when nanoscale particles are combined, with numerous advantages over more traditional procedures. In recent years, various nanomaterials with distinct physical and chemical properties have been applied to improve the immobilization of immunocompounds. [27] These have many electrochemical advantages, such as possessing low-background current, high signal-to-noise ratio, and fast electron transfer, besides increased amount of immobilized biomolecules, with consequent increase on the sensitivity of sensors. [28]

Surface modification using nanoparticles composites have shown an increase of sensitivity and help adsorb a large amount of antibodies on electrode surface. Lu et al. [29] constructed an immunosensor based on a nanocomposite formed with CeO_2 and gold nanoparticles on the Au electrode via cysteine to detect a cardiac marker, the myeloperoxidase.[29] Thereat, the nanoparticles enhanced the active surface area available for antibody binding. The high stability of this sensor was attributed to the good biocompatibility of the composite. Another study shows an increase in immunosensor response. Fe_2O_3 nanoparticles were used in the construction of an electrochemical device to detect cancer biomarker prostate antigen (PSA) via horseradish peroxidase (HRP) signal. The high amount of nitrodopamine (film coated on nanomaterial to

immobilize the anti-PSA) anchored onto Fe_3O_4 increased the loading of biomolecules onto the surface, which increased the electrochemical immunosensor sensitivity. [30]

The carcinoembryonic antigen (CEA) is a protein used as a tumor marker and has been frequently investigated in immunoreactions. An elevated CEA level in serum may be an early indication of lung cancer, ovarian carcinoma, colon cancer, breast cancer, and cystadenocarcinoma. Recently, an interesting work was reported involving this protein investigation using an immunosensor constructed by Pt hollow nanospheres modified with anti-CEA as label for a 3D Au-TiO_2 hybrid platform. [31] The immunoassay exhibited a high sensitivity and a low detection limit compared with conventional label methods. Another way to detect CEA antigen was developed by Gao et al. [32] using a label-free voltammetric sensor with chitosan and gold nanoparticles (AuNPs) to immobilize anti-CEA on carbon surface. The detection is based on the variation of current responses before and after the immunoreaction. When the immobilized antibodies have bounded with antigens, the antigen–antibody complex formed on the surface inhibited the electron transfer. Then a decrease of the electrochemical signal was verified as the concentration of antigen on surface increased. Another method also using a composite of chitosan and AuNPs for CEA determination, but with multiwalled carbon nanotubes, was described by Huang et al. [33] The nanocomposite film exhibited high current response intensity, good biocompatibility, and high stability. Similar CEA detection was also performed using a gold nanoparticle–thionine-reduced graphene oxide composite that possesses as advantage fast electron transfer kinetics and large specific surface area. [34] Another work for CEA analysis described the use of silver nanoparticles on SiO_2 surfaces. [35] The high stability of the immunosensor was assigned to the stable nanocomposite produced.

The sensitivity of electrochemical immunosensors can also be improved by using the association of AuNPs and dendrimers that are three-dimensional macromolecules, with hundreds of functional groups at the periphery, for surface modification. This architecture was employed by An et al. [36] to detect α-synuclein, a very important neuron protein. The dendrimer (PAMAM)-encapsulated AuNPs were covalently bound on the poly-o-aminobenzoic acid (ABA) electropolymerized on a glassy carbon electrode surface to achieve abundant carboxyl groups, which allowed a highly dense antigen immobilization and facilitated the improvement of electrochemical responses as well. Subsequently, the enhanced gold nanoparticle labels were fabricated by immobilizing a horseradish peroxidase secondary antibody (HRP-Ab_2) on the AuNPs surface. After an immunoassay process, the labels were introduced onto the electrode surface to produce an electrocatalytic response with hydrogen peroxide. The presence of dendrimer Au not only increased the covalent coupling of more protein but also accelerated electron transfer when compared to immunosensor without dual signal amplification strategy.

The picogram detection limit of estradiol was achieved using an immunosensor constructed with AuNPs and protein G scaffold to modify a gold electrode. [37] Coupled with the amperometric determination of the hormone in a flow system, the device exhibited superior linear range, sensitivity, and stability in blood serum samples spiked with estradiol.

Other applications for metallic nanoparticle have included optical transduction. Krishnan constructed an optical immunosensor in a quartz glass surface for the detection of *Escherichia*

coli, using core-shell nanoparticles (silver-silica) anchoring labeled antibodies. The results show that changes in photoluminescent standards are consistent with the immobilization of various species. Thus, the optical immunosensor demonstrated improved sensitivity and specificity in comparison to the usual methods, detecting as low as 5 CFU/mL.

Using a great number of luminescence molecules as stabilizers coated on the surface of the AuNPs, Shen et al. [40] developed an electrochemiluminescence immunosensor to detect human cardiac troponin, an important acute myocardial infarction biomarker. First, the sensor was constructed by using streptavidin-coated gold nanoparticles as the immobilization matrix for biotinylated antibody. Meanwhile, the three-dimensional nanostructures increased the surface-to-volume ratio, allowing more biomolecules to be immobilized. The sandwich-type immunosensor was fabricated by reacting with antigen and AuNPs modified with luminescence molecules labeled with the secondary antibody, forming a nanoprobe. The enhanced sensitivity of the proposed apparatus mainly derives from the novel nanoprobe, which achieves a large amount of luminescence molecules loading toward each sandwich immunological reaction event.

Another strategy in immunocomplex detection involves the use of magnetic nanoparticles as solid support for biomolecule immobilization. The magnetic particles offer the convenience of magnetic separation. These particles respond to a magnetic field but demagnetize completely when the field is removed. Thus, the nanoparticles can easily be separated from the liquid phase with a small magnet but can be dispersed again immediately after the magnet is removed. The use of magnetic nanoparticles as solid phase for the immunosensor development improves the bioreaction performance due to surface area increase and has better immunoassay kinetics because the particles are in suspension and the target species does not need to diffuse very far. [41]

An interesting work was described by Shen et al., [42] who developed a device to detect *E. coli*, an intestinal pathogenic bacterium, using a quartz crystal microbalance (QCM) immunosensor based on beacon magnetic nanoparticles. A polyclonal antibody was immobilized on iron nanoparticles with subsequent addition of *E. coli*. AuNPs were inserted in the system to amplify the signal. Weakly bound biomolecules were removed with a magnetic plate. Finally, the crystal was modified with protein A and monoclonal antibody. The frequency shift of the QCM immunosensor is amplified using *E. coli* immobilized on to magnetic particles and enlarged gold particles for the bacterium detection. The signal was amplified three times, and the crystal was regenerated without difficulty and could be used at least 10 times. In a recent work, the use of magnetic nanoparticles as an amplification means for QCM signal for avian influenza H5N1 virus detection has been reported. [43] Polyclonal antibodies against the virus were immobilized on the gold surface of the crystal through self-assembled monolayer (SAM). Target H5N1 viruses were then captured by the immobilized antibodies, resulting in a change in the frequency. Magnetic nanoparticles coated with anti-H5 antibodies were used for further amplification of the binding reaction between antibody and antigen (virus).

AuNPs have a remarkably high extinction coefficient and strong distance-dependent optical properties. Different aggregation states of AuNPs correspond to distinctive color, which can be appreciably discerned with the naked eye and be used in immunoassay. Based on this, Yuan

et al. [44] developed a label-free colorimetric immunoanalysis for the simple detection of neurogenin3, a marker for pancreatic endocrine precursor cells, using glutathione functionalized gold nanoparticles. The antibody-conjugated AuNPs were formed through electrostatic interaction upon the addition of the antibody to the modified AuNPs solution. The antigen positively charged to the negatively charged AuNP antibody will minimize the electrostatic repulsion between nanoparticles by neutralizing the surface charge and then agglomeration is induced by an increasing NaCl salt concentration, noticeably revealed by the color change of the solution from red to purple or blue. The concentration of neurogenin3 can be conveniently accessed by the optical absorption spectra. Another important property of the AuNPs is that they could catalyze silver reduction and act as the nuclei for silver precipitation. [45] In this interesting work, the core mechanism of the method to quantify cardiac troponin is that the catalytic capability of the AuNPs was inhibited by immunocompounds covering their surface. This covering is influenced by the amount of reduced silver of the reaction, resulting in a color difference.

In state-of-the-art improved sensor devices for health applications, the possibility of assembling nanoparticles and biomolecules in different ways by using different sizes, formats, and compound types allow more sensitive, simple, robust, and especially faster analysis.

3.2. Quantum dots

Quantum dots (QDs) represent one class of nanostructured materials. They are spherical nanocrystals of semiconductor, 1–10 nm in diameters, made of elements of the IIB–VIA or IIIA–VA groups. The use of QD properties requires sufficient control during their synthesis because their intrinsic properties are determined by different factors, such as size, shape, defect, impurities, and crystallinity. [46, 47] Two of the most widely used commercial QDs come with a core of CdSe or CdTe and a shell of ZnS and emissions from 405 to 805 nm. [48, 49] The shell stabilizes the structure, helping to overcome quenching compared to a QD made only from a core and provides a large surface area available for further modification.

Analogous dimensions of QD and biological materials, such as enzymes, antigens/antibodies, protein receptors, or nucleic acids, show great promise as photonic labels for bioanalytical applications and suggest that electronic communication between the QD and the specific recognition site or biocatalytic processes of the biomaterials can exist. These electronic interactions may lead to the optical or photoelectrochemical transduction of the biological events. [47, 50]

Generally, monodispersed QDs are developed by introducing organic molecules that adsorb on the surface and act as capping agents. The efficacy of QD in a biological application is critically dependent on coating properties. The liabilities of these initial methods require the continued development of QD coatings. Important criteria for an ideal QD coating include high-affinity for the QD surface, long-term colloidal stability across a broad range of pH and ionic strengths capacity for bioconjugation, minimization of hydrodynamic size, and biocompatibility with nonspecific binding. [51] However, the selection of organic ligands that bond with surface atoms of the QD is a very delicate issue. In general, phosphenes or mercaptans (-SH) are the most widely used ligands. [52]

In order to make QD suitable for biological imaging and use in a biological environment, they also have to be rendered water soluble. This is done by capping the shell with a polymer layer that contains a hydrophobic segment facing inward, the shell, and a hydrophilic segment facing outward. The hydrophilic layer can be modified to include functional groups such as –COOH and $-NH_2$ groups for further conjugation to proteins and antibodies or oligonulceotides. [49, 53] The single-step synthesis of thiolated cyclodextrin-modified CdSe/CdS core-shell QD resulted in a water-soluble QD, keeping the luminescence properties of the QD in aqueous systems. This is an important aspect since biorecognition events require aqueous environments for reaction. [54]

Thiol ligands and amphiphilic polymers are the most common types of QD coating available. They allow two essential design elements: a moiety that anchors to the QD surface and a hydrophilic functionality for aqueous dispersion. The selection of these groups determines the degree to which a QD coating can approach the ligand/amphiphilic polymer structures. [51] For example, small molecules with thiol groups can bind to the quantum dot surface, and distal carboxylated group provides aqueous colloidal stability. [55] Another strategy for QD coating that provides aqueous dispersion, improves the biocompatibility, and minimizes nonspecific binding was developed by Mattoussi et al. (2000). They combined dihydrolipoic acid, a dithiol ligand that binds the QD more closely, which is attached to a poly(ethylene glycol) oligomer.

Biomolecule conjugation on to the QD is achieved by different ways like electrostatic binding, noncovalent biotin–streptavidin bonding, or covalent bonding. The most widely used conjugation technique of all is the covalent bond formation between the QD surface and the biomolecules. Surface modifications on QD allow easier covalent bond formation. In one of the most widely used methods, amine-terminated QDs are used for conjugating antibodies. The amine-terminated QDs are activated with maleimide containing a cross-linker molecule, which can then be conjugated to a fragment or whole antibody molecule. Some of the most commonly employed QD conjugation methods are based on cross-linking reactions between amine and sulfhydryl groups, carboxylic acid, and amine and aldehyde and hydrazide groups. The carboxylic-amine bond has one advantage over all other methods, seeing as this method does not require any antibody modification before QD conjugation. In the case of amine and sulfhydryl bond formation, the antibody should be reduced to expose their interchain -SH bonds. In relation to aldehyde and hydrazide bonds, carbohydrate groups on the antibody Fc portion are oxidized. These modifications on antibodies may affect their performance to a certain extent. [56]

Functionalized semiconductor quantum dots have been used as fluorescence labels in numerous biorecognition events. For example, Liu et al. (2004) developed an immunosensor with simultaneous measurements of four proteins based on antibodies linked to the inorganic nanocrystal. Stripping voltammetric immunoassay was used to observe the response of a mixture containing microglobulin, IgG, bovine serum albumin, and C-reactive protein connected with ZnS-, CdS-, PbS-, and CuS-labeled antibodies, respectively. The system was obtained by using carbamate linkage for conjugating the hydroxyl-terminated nanocrystal with the secondary antibody. [57]

Li et al. (2011) [58] used a novel strategy to modify the surface of graphene quantum dots composites. A layer-by-layer assembling process was employed via electrostatic interactions

between negatively charged thioglycolic acid modified CdSe QD and positively charged graphene, which was noncovalently functionalized with poly (diallyldimethylammonium chloride) (PDDA) via an exfoliation in situ reduction of graphene oxide in the presence of PDDA. This process allowed excellent conductivity, extraordinary electron transport properties, and large specific surface area, which resulted in high electroluminescence (ECL) intensity and excellent film-forming ability and made it a promising candidate for the development of ECL immunosensors.

Luminescent quantum dots are viable optical markers and have been used in a direct assay for IgG. Protein A was labeled with CdSe/Zn QD (λ_{max} of 655 nm) and then was immobilized at the tip of an optical fiber. Once the immunoreaction with IgG occurs, a decrease in fluorescence intensity is observed as a result of the fluorescence resonance energy transfer from the QD to the bound protein. [59] Lingerfelt et al. [60] reported the preparation of QD-biotin conjugates and their use in immunochromatographic assays. The detection of immunoglobulin G was carried out on a glass chip through a sandwich assay approach using a secondary antibody conjugated to the QD. [61] A sandwich immunoassay for the detection of staphylococcal enterotoxin B was run using polyclonal sheep anti-staphylococcal enterotoxin B antibody conjugated with QD and microtiter plates coated with monoclonal staphylococcal enterotoxin B antibody. [62]

Kerman et al. (2007) applied conjugated QD streptavidin in a model immunoassay system for the detection of a total prostate-specific antigen cancer marker from the spiked and undiluted serum samples. Immunorecognition was carried out on a carbon substrate using a sandwich assay approach. After the recognition event, the substrate was exposed to the biotinylated secondary antibodies and, subsequently, fluorescence imaging of the substrate surface illuminated the QD. [63]

QDs based on narrow photoemission spectra, with high resistance to photobleaching and broad excitation spectra, are widely used as tags in immunoassay. A carcinoembryonic antigen immunosensor was fabricated using biofunctionalized QD probes. This immunosensor array was designed to detect a wide range of analytes using the inherent characteristics of QD and the flexibility of engineered elastin-like polypeptides. [64]

There are some studies based on thioalkyl-functionalized QD, which are pH sensitive, [65] suggesting many different biological applications. In this context, mercaptoacetic acid-CdSe/ZnSe/ZnS QDs have been used as an intracellular pH sensor by observing a quenching of fluorescent QDs in acidic pH. [66]

Another approach was based on the direct conjugation of CdSe/ZnS QD–IgG complexes using a genetically engineered tripartite fusion protein. This fusion protein was made up of a histidine tag for QD conjugation, an elastin-like peptide for stimuli-responsive purification and the protein L (cell-wall component of *Peptostreptococcus magnus*) that has high affinity to IgG. The functionality of this sensitive immunofluorescent probe was demonstrated in the detection of a representative tumor antigen. [64]

Despite recent progress, more work still needs to be done to achieve reproducible and robust surface functionalization and develop flexible bioconjugation techniques. The potential of QD in biology has just begun.

3.3. Carbon nanotubes

Carbon nanotubes (CNTs) can be highlighted as the most important nanomaterials for biosensors. Their excellent optical and mechanical conductivity, high surface-to-volume ratio, good chemical stability, biocompatibility, and easy functionality have revolutionized the biosensors area for the last decade.

Since their discovery by Ijima in 1991, CNTs are being used in large volumes for different purposes in many industrial areas, i.e., in nanocomposites for sporting materials, as a battery in supercapacitors, transparent films, and liquid crystal displays. Other limited-volume carbon applications include their use as components in wind turbine blades, scanning probe tips, membrane filters and sorbents, flat panel displays, memory devices, transistors, drug delivery systems, and other medical and analytical chemistry applications. [67]

Carbon nanotubes can be described as hollow cylindrical tubes of graphene sheets with high aspect ratios (length/diameter). [68] The structure of graphene is a planar atomic sheet consisting of covalently bonded carbon atoms. The atoms in graphene are sp^2 carbon units, forming a two-dimensional (2D) network with a hexagonal lattice. A graphene layer wrapped as a cylinder forms a single-walled carbon nanotube (SWNT). A multiwalled carbon nanotube (MWNT) is nothing more than multiple SWNTs packed in a tight concentric frame. All the carbon nanotubes have several nanometers in diameter and many microns in length. SWNTs have the smallest diameter (0.8–5 nm), whereas MWNTs have a larger diameter (~3 to >100 nm), both variable in length (from millimeters to tens of nanometers). The proper architecture is reflected in the highly anisotropic properties. Most of the extraordinary electrical, thermal, and mechanical characteristics are localized specifically along the axial direction. The strong sp^2 bonding between the carbon atoms in CNTs yields remarkable mechanical strength, making them one of the most resilient materials. Moreover, it is known that an SWNT presents metallic and semiconducting properties where such electronic features depend on its chirality. [69] They have three different structures: armchair, zigzag, and chiral. [70]

The applications of CNTs in biosensors have been hindered for a long time due to the drawback of insolubility. CNTs present a high molecular weight, an ability to entangle (tendency to individually interact with each other through van der Waals forces), aggregating into bundles and ropes. However, these bundles can be quite large that they become insoluble in any solvent; thereby, it can be difficult to disperse them in either aqueous or nonaqueous medium. [71]

Ultrasonication is an effective method to disperse CNTs in liquids that have low viscosity, such as water, acetone, and ethanol. However, most polymers are either in a solid or viscous liquid state, which require the polymer to be dissolved or diluted using a solvent to reduce the viscosity before dispersion of CNTs. [72] The simplest stable dispersions have been achieved by using a solvent able to efficiently interact with CNTs, such as phenylethyl alcohol, *N*-methylpyrrolidone (NMP), *N*,*N*-dimethylformamide (DMF), and *N*,*N*-diethylacetamide (DEA). An additional strategy to favor dispersion in organic solvents is to coat CNTs with a molecule characterized by a high affinity toward nanotube sidewalls and at the same time soluble in the selected solvent. Both small molecules and polymers formed by repetitive units

http://dx.doi.org/10.5772/61149

of alkyl chains and aromatic compounds have been used as dispersants. Thus, the adsorption of different polycyclic aromatic hydrocarbons such as pyrene, anthracene, tetracene, and phenanthrene on SWCNTs has been extensively investigated. In order to favor the dispersion of CNTs in water, the widely and most used approach is the adsorption of surfactants. These small molecules typically have a hydrophobic tail and a hydrophilic head group—the former is intended to favor adsorption onto the hydrophobic carbon nanotube and the latter to promote affinity with the aqueous solvent. Over the years, stable aqueous CNT dispersions were obtained with differently charged and nonionic surfactants such as sodium dodecylbenzene sulfonate (SDBS), cetyltrimethylammonium p-toluenesulfonate (CTAT), cetyltrimethylammonium bromide (CTAB), and sodium cholate (SC) enhanced by sonication. Additionally, polymers have been employed for CNT dispersion in water. The majority of polymers and block copolymers have been used to wrap CNT by exposing their polar domains toward the aqueous environments while favoring the contact of their hydrophobic domains with the nanotube surface. [73]

Strategies for the immobilization of biomolecules on CNTs have been widely explored aiming to improve sensitivity on an immunosensor. The high aspect-ratio of CNT allows a great amount of anchored biomolecules by noncovalent and covalent functionalization for different types of transduction (Figure 3).

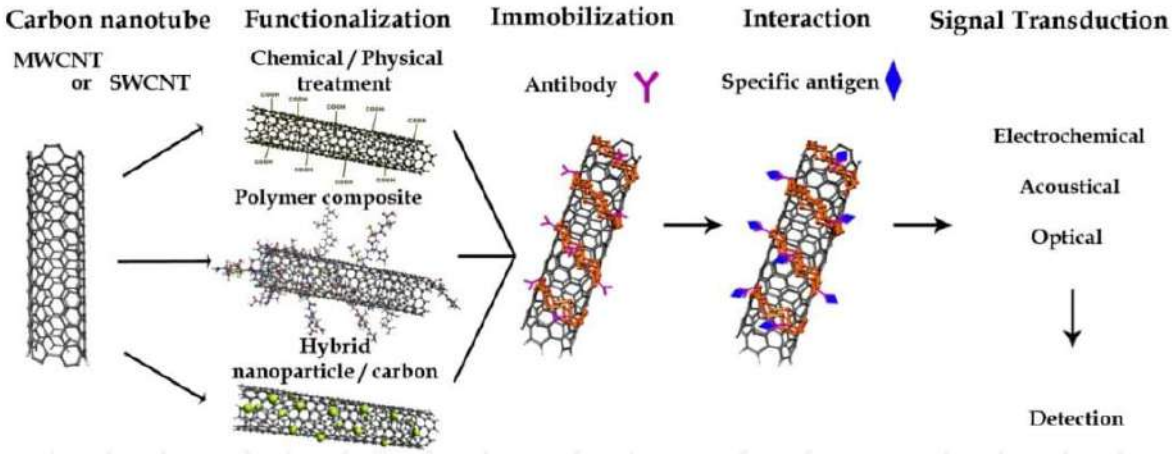

Figure 3. The schematic diagram steps and transducer types of immunosensors based on carbon nanotubes.

Noncovalent functionalization enables reversible adsorption of biomolecules on the CNT surface. For this purpose, CNTs are added to a dispersant solution, and the mixture is agitated in an ultrasound bath. The CNTs are mechanically debundled and then stabilized by dispersant molecules through noncovalent interactions. This does not cause changes in the chemical structures, electronic, and mechanical properties of the carbon nanotubes, and therefore it is a very attractive method. Surfactants, biomolecules, and polymers are widely used as dispersants and noncovalent modifiers. Among them, the polymers are quite efficient dispersants because of their long chain structure that can wrap themselves around CNTs by disrupting the van der Waals interactions between the walls of nanotubes. In biosensors, polymers are

particularly interesting and have been widely employed to prepare CNT composites for electrochemical detection, especially for conductive polymers due to their native electron trans-mediation, high conductivity, good environmental stability, and specific organic groups. Furthermore, they can be overoxidized to create an electrically insulating layer. Many reports have demonstrated that CNTs coated with polymers, including polypyrrole, poly(methylene blue), poly(neutral red), poly(acrylic acid), and poly(3-methylthiophene) have become a popular strategy [74]

The covalent chemical functionalization arises mainly from organic molecules reacting with carboxyl groups of CNTs treated by oxidation, which depends on the hydrophilicity/hydrophobicity of the species attached, which can make carbon nanotubes soluble in water or organic solvents. The modification of carbon nanotube surfaces by covalent attachments of soluble groups usually alters intrinsic properties such as conductivity, mechanical strength, and optical properties. [73, 75] Nevertheless, the functionalization involving the introduction of carboxyl, amine, thiol, and other reactive groups are attractive strategies because antibodies or antigens can be covalently immobilized, improving the stability and, in some cases, the sensitivity and selectivity of the immunosensors. Figure 4 exhibits different covalent and noncovalent methods of functionalization of the carbon nanotubes.

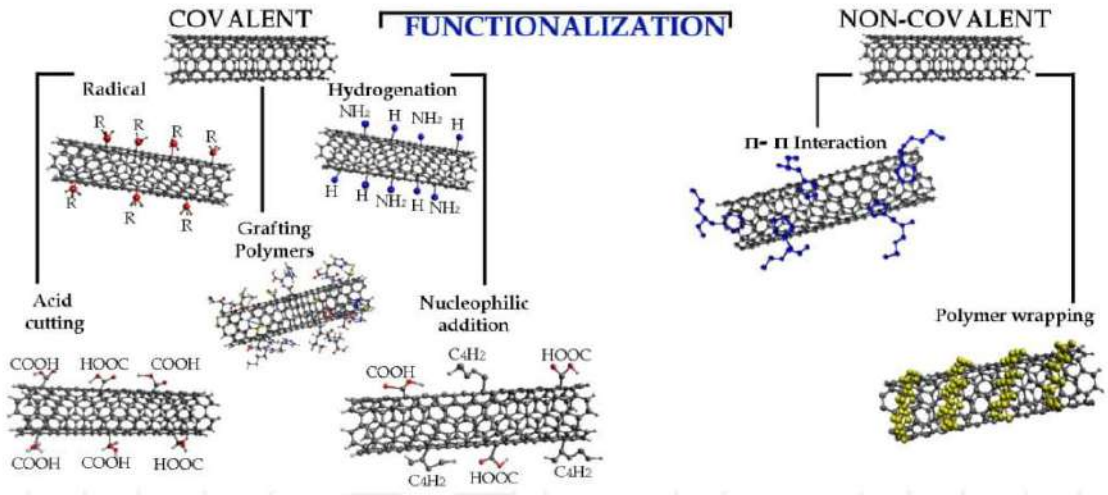

Figure 4. Illustration of different carbon nanotube functionalization methods.

In some practical applications, Sánchez and coworkers [76] have constructed immunosensors where the biomolecules are immobilized on an MWCNT–polysulfone composite film. The layer was applied onto screen printed working electrodes to provide a suitable immunosensor for the rapid determination of human chorionic gonadotropin hormone. The detection limit was 14.6 mIU/mL with a linear range up to 600 mIU/mL. Viswanathan et al. [77] developed another disposable electrochemical immunosensor based on CNTs for the detection of carcinoembryonic antigen with a detection limit of 1 pg/mL in saliva and serum.

For better detecting performance toward interleukin-6, in cases of oral cancer, Malhotra et al. [78] made an ultrasensitive immunosensor sandwich assay on an electrically conductive and

http://dx.doi.org/10.5772/61149

high surface area platform, featuring densely packed and upright SWCNTs with capture antibodies attached to their ends. This biosensor had the highest sensitivity at 19.3 nA/mL (pg IL-6)$^{-1}$ cm^{-2} and the best detection limit (DL) of 0.5 pg/mL (25 fM) for IL-6 in 10 μL of calf serum. Similarly, Munge et al. [79] have presented a novel electrochemical sensor using a sandwich immunoassay for the detection of metalloproteinase-3, a cancer biomarker, based on vertically aligned SWCNT arrays. The multilabeled polymeric bead amplification method demonstrated a detection limit of 0.4 ng/mL in 10 μL of calf serum. This showed great potential for these elements in future cancer diagnostics.

The self-assembly of oxidative SWCNTs on gold was attempted for the detection of bovine serum albumin, BSA, by cyclic voltammetry. This sensor has shown excellent sensitivity and dynamic linear response at the range of 0.1 to 1.2 μM. [80] A conductive multilayer composed of Nafion-coated MWCNTs, thionine (Thi), and AuNPs was prepared using an innovative self-assembly strategy to form an immunosensor for α-1-fetoprotein. This reagentless amperometric sensor presented broader linear response in two ranges between 0.5–20 ng/mL and 20–200 ng/mL with a detection limit of 0.26 ng/mL. [81]

There are many studies demonstrating that CNTs can provide high electrocatalytic activity to the electrochemical devices and minimize surface fouling effect. Their unique properties enable them to promote a fast electron transfer, play the role of a biomolecular immobilization platform, and be compatible with different materials for construction of different electrodes. The sensitivity of electrochemical sensors has been greatly enhanced due to these materials, which promotes high active surface area and conductivity. CNTs play an important role in recent trends for immunosensor fabrication. They can function as transducers, act as carriers and labels of immunoassay due to the transfer of large amounts of electroactive species for amplifying electrochemical signals, and also offer an easy way to protect and stabilize these bioactive species. [82] In this section, different strategies were described like the easy adsorption of CNT on the electrode surface, biomolecule immobilization by simple adsorptions and covalent binding, and preparation of screen printed electrode.

Based on a simple amino-functionalization method for MWCNT, Dutra's group developed an electrochemical immunosensor for the detection of human cardiac troponin T (cTnT), an important marker for acute myocardial infarction. It showed a broad linear range (0.02 to 0.32 ng/mL) and a low limit of detection, 0.016 ng/mL. [83] Another sandwich-type immunosensor for the detection of cTnT based on carbon nanotubes supported by a conductive polyethyleneimine film has achieved a low limit of the detection of 0.033 ng/mL and a linear range between 0.1 and 10 ng/mL. [24] Amperometric response is generated by peroxidase reaction with substrate in chronoamperometry detection. The high electronic transfer and catalytic response helped by the CNT was essentially important to dispense the mediator in order to generate the analytical responses. Due to the high conductivity achieved by incorporation of CNTs in screen printed electrodes, a label-free amperometric immunosensor was fabricated, presenting new strategies based on differential pulse amperometry. The immunosensing device for cTnT, with amine-functionalized carbon nanotubes incorporated in screen-printed

electrode ink, reached a lower detection limit of 0.0035 ng/Ml, better than any previously described immunologic sensors. [21]

3.4. Graphene

Graphene is a two-dimensional material, formed by carbon atoms that are densely packed in a regular sp^2-bonded atomic scale as a hexagonal pattern, [84] which was produced in laboratory for the first time in 2004. [85] This is the base construction block for other carbon allotropes such as fullerene, carbon nanotubes, graphite, nanoribbons, and others. [86] It is a transparent (optical transmittance of ~97.7%), very thin sheet with large theoretical surface area (2630 $m^2 g^{-1}$), one atom thick, stronger than steel (mechanical stiffness of 1TPa). In addition, it is a good heat conductor (thermal conductivity of 500 W m^{-1} K^{-1}), chemically inert, and a semimetal with high electron transfer (charge-carrier mobility of 250 000 cm^2 V^{-1} s^{-1} at room temperature). [87, 88] These properties make them attractive for many applications. [84] There are a variety of synthesis methods for obtaining graphene such as chemical vapor deposition, chemical vapor deposition by plasma, the graphite intercalation of metal sheets, mechanical or thermal exfoliation of graphite oxide, intercalation, and exfoliation of graphite, among other variants of these. Despite all these syntheses methods, the mass production is still difficult, making it hard to develop some applications. [88]

Graphene oxide (GO) synthesis has been an alternative to graphene mass production. It is produced from the oxidation of graphite and has polar oxygen functional groups. GO is rich in carboxylic acids at its edges, and epoxy and hydroxyl groups at basal planes, which grants many functionalization routes and good dispersion in water. [89] Furthermore, the functional groups are responsible for the exfoliation of graphite, seeing as they increase the interplanar distance due to the formation of hydrogen bonds between the graphite sheets. The hydrogen bonds are weak and can be easily broken by ultrasound bath, resulting in monolayer or a few sheets of carbon, known as GO. This is an excellent material for biological applications attributed to the functional groups that readily interact with nucleic acids, proteins, cells, and other organic molecules. However, GO is not a good electrical conductor because of the disruption of its sp^2 bonding as functional groups increase, which can narrow its nanobiotechnology applications. To overcome these difficulties, the reduced form of GO has been chosen as an alternative.

Reduced graphene oxide (RGO) has more commonly been used to form nanocomposites with nanoparticles or polymers to develop biomedical applications such as biosensors, controlled drug delivery, therapeutic modalities for cancer treatment, substrates for antibacterial effects, scaffolds for mammalian cell culture, and gene delivery among others. [90]

In the RGO synthesis, functional groups are removed, and the conductivity is increased again. This removal can be done in different ways such as electrochemical, optical, hydrothermal, microwave, or heating procedures. These methods for removing the functional groups form different shapes and therefore the conductivity recovery is variable. Also, they form different functional groups, becoming favorable in a wide number of applications. [91]

http://dx.doi.org/10.5772/61149

The most common method for obtaining RGO is chemical reduction, which is used in colloidal dispersing of GO. Hydrazine monohydrate is the most used reduction agent, seeing as it does not react with water, which makes it attractive for aqueous dispersions. The reduction process mediated by hydrazine normally occurs through the addition of H_2 groups and removal of N_2, and it is gentle enough not to affect the cyano and nitro groups. The second most used reducing agent is sodium borohydride ($NaBH_4$), which is more effective than hydrazine and easily hydrolyzed in water. The hydrolysis process should be slow enough so it does not affect the reduction process. The $NaBH_4$ reduces C=O species and has a low effect in epoxy and carboxylic acid groups. Other reduction agents such as hydroquinone, alkaline solutions, and gaseous hydrogen are also being described as mediators. [92]

Another low-cost mean of producing RGO is by thermally reducing GO, heating it in a furnace at 1050 °C, which creates thermodynamically stable oxide carbon species. Electrochemistry can also be used in the reduction process of GO, removing oxygen functionalities. Thermal and electrochemical reduction techniques have the advantage of avoiding dangerous reducers and the problem with their disposal, but they are still less used than chemical reduction. The reduction processes frequently provide RGO with functional groups, but in some cases, its functionalization is still necessary prior to use. Covalent and noncovalent methods for functionalization of RGO have been studied, whereas noncovalent bonds are the most common used, for instance, the physical adsorption of both polymers and small molecules via van der Waals interactions onto the basal planes of RGO sheets. [92]

An initial and successful approach using RGO to create biosensors was its combination with nanoparticles. An example is the work of Shan et al., [93] who used Au nanoparticles associated with RGO and chitosan as a nanocomposite film onto a gold electrode for developing an electrochemical glucose sensor obtaining a linear response range from 2 to 10 mM. Copper nanoparticles were also used to modify RGO sheets to create an electrochemical sensor for glucose obtaining a detection limit of 0.5 μM. [94]

Afterward, RGO was applied to the production of immunosensors, with and without nanoparticles. An example is the work of Mao et al., [95] who reported the use of RGO sheets coated with Au nanoparticles, which were initially functionalized with human immunoglobulin G (IgG) to create conjugates. These conjugates were immobilized onto a field effect transistors (FETs) biosensor platform for the detection of human proteins.

A developing area for immunosensors is the detection of cancer markers. It is a recent and very attractive field, with growing publication numbers, including the use of RGO for these. An example is the work of Zhong et al., [96] who used a gold nanoparticle enwrapped graphene nanocomposite on a glassy carbon electrode in a sandwich-type immunoassay format. The detection limit obtained for this assay was 10.0 pg mL^{-1}. Another CEA immunosensor was developed by Huang et al. [97] using Ag/Au nanoparticles coated with RGO in a clinical immunoassay for the detection of carcinoembryonic antigen (CEA). The nanoparticles were used as means for amplification of the signal and the method showed a detection limit of 8.0pg mL^{-1} in human serum.

Different cancer markers were the focus of other works, such as the one developed by Tang et al., [98] which aimed to create an electrochemical immunosensor for the simultaneous detection of alpha fetoprotein (AFP) and carcinoembryonic antigen (CEA), using biofunctionalized magnetic RGO nanosheets (MGO) coated with iron oxide nanoparticles as immunosensing probes, obtaining detection limits of 1 pg mL^{-1} for CEA and 1 pg mL^{-1} for AFP. Also, Teixeira et al. [99] created a chemically modified epitaxial graphene diagnostic sensor for the detection of human chorionic gonadotropin, which is a main marker for pregnancy and can also indicate some types of tumors. They obtained a detection limit of 0.62 ng/mL.

For optical transductors in cancer marker detection, RGO was used by Xu et al. [100] in a modified glassy carbon electrode using luminol to create a electrogenerated chemiluminescence (ECL) immunosensor for prostate specific antigen, using two antibodies in a sandwich immunoassay, which achieved a detection limit 8.0pg mL^{-1}. RGO was also used in the development of an ECL immunosensor using CdTe quantum dots (semiconductor nanocrystals) along with Au nanoparticles for signal amplification in the detection of human IgG with detection limit of 0.005 pg/mL. [101]

4. Conclusions

The different concepts of nanomaterials applied to immunosensors have been discussed. Nanomaterials can be utilized for a wide variety of immobilization matrices intending to improve the immunosensor sensitivity, allowing lower limit of detection. The potential of nanomaterials on immunosensors has resulted in a positive impact on the clinical outcome of various diseases, including cancer, cardiac injuries, parasitic infections, and viruses, among others. It is well known that carbon nanotubes and grapheme nanostructures are more favorable to amperometric transducers due to their electrochemical proprieties, which increase the electronic transfer charge and electrocatalytic activity. Metallic and magnetic nanoparticles have successfully been applied to different transducers, especially electrochemical, by enlarging the electroactive surface area. Quantum dots, a semiconductor nanoparticle, present a promising potential for many transducers mainly due to their photostability and luminescence characteristics. Nevertheless, more challenging studies involving nanomaterial sciences, biochemistry, electronic, and molecular engineering should be done in attempting to achieve faster, more practical, and more reliable biosensors. More specifically, biomolecules and a deeper knowledge in nanomaterial science associated to new electronic designs represent a promising field in the development of portable and integrated point of care devices for health applications and other areas of diagnostic.

Acknowledgements

The authors thank the financial support of the National Council for Scientific and Technological Development (CNPq), CAPES (Coordination for the Improvement of Higher Level Personnel), and the Foundation for Research of the State of Pernambuco (FACEPE).

Author details

Blanca A.G. Rodriguez[1], Erika K.G. Trindade[1], Diego G.A. Cabral[1], Erika C.L. Soares[1], Cayo E.L. Menezes[1], Danielle C.M. Ferreira[2], Renata K. Mendes[3] and Rosa F. Dutra[1*]

*Address all correspondence to: rosa.dutra@ufpe.br

1 Laboratory of Biomedical Engineering, Federal University of Pernambuco, Recife, Brazil

2 National Center for Research in Energy and Materials (CNPEM), Campinas, Brazil

3 Pontifical Catholic University of Campinas, São Paulo, Brazil

References

[1] Morgan, C.; Newman, D.; Price, C., Immunosensors: technology and opportunities in laboratory medicine. *Clinical Chemistry* 1996, *42* (2), 193–209.

[2] Holford, T. R. J.; Davis, F.; Higson, S. P. J., Recent trends in antibody based sensors. *Biosensors and Bioelectronics* 2012, *34* (1), 12–24.

[3] Zeng, X. Q.; Shen, Z. H.; Mernaugh, R., Recombinant antibodies and their use in biosensors. *Analytical and Bioanalytical Chemistry* 2012, *402* (10), 3027–3038.

[4] Lim, Y. C.; Kouzani, A. Z.; Duan, W., Aptasensors: a review. *Journal of Biomedical Nanotechnology* 2010, *6* (2), 93–105.

[5] Rousseaux, J.; Rousseaux-Prevost, R.; Bazin, H., Optimal conditions for the preparation of Fab and F(ab)2 fragments from monoclonal IgG of different rat IgG subclasses. *Journal of Immunological Methods* 1983, 64, 141–146.

[6] Kidwai, A. A.; Jamal, Q.; Mehrunnisa, S.; Farooqi, F. U. R.; Saleem, U., Serodiagnosis of dengue infection using rapid immunochromatography test in patients with probable dengue infection. *Journal of the Pakistan Medical Association* 2010, *60* (11), 936–939.

[7] Pei, X.; Zhang, B.; Tang, J.; Liu, B.; Lai, W.; Tang, D., Sandwich-type immunosensors and immunoassays exploiting nanostructure labels: a review. *Analytica Chimica Acta* 2013, *758*, 1–18.

[8] Pfaunmiller, E.; Moser, A. C.; Hage, D. S., Biointeraction analysis of immobilized antibodies and related agents by high-performance immunoaffinity chromatography. *Methods* 2012, *56* (2), 130–135.

[9] Sanchez-Moreno, P.; Ortega-Vinuesa, J. L.; Boulaiz, H.; Marchal, J. A.; Peula-Garcia, J. M., Synthesis and characterization of lipid immuno-nanocapsules for directed drug

delivery: selective antitumor activity against HER2 positive breast-cancer cells. *Biomacromolecules* 2013, *14* (12), 4248–4259.

[10] Shalumon, K. T.; Chen, J. P., Scaffold-based drug delivery for cartilage tissue regeneration. *Current Pharmaceutical Design* 2015.

[11] Makaraviciute, A.; Ramanaviciene, A., Site-directed antibody immobilization techniques for immunosensors. *Biosensors and Bioelectronics* 2013, *50*, 460–471.

[12] Bergstrom, G.; Mandenius, C.-F., Orientation and capturing of antibody affinity ligands: applications to surface plasmon resonance biochips. *Sensors and Actuators B: Chemical* 2011, *158* (1), 265–270.

[13] Cavalcanti, I. T.; Silva, B. V. M.; Peres, N. G.; Moura, P.; Sotomayor, M. D. P. T.; Guedes, M. I. F.; Dutra, R. F., A disposable chitosan-modified carbon fiber electrode for dengue virus envelope protein detection. *Talanta* 2012, *91*, 41–46.

[14] Lee, J.; Park, H.; Jung, Y.; Kim, J.; Jung, S.; Chung, B., Direct immobilization of protein G variants with various numbers of cysteine residues on a gold surface. *Analytical Chemistry* 2007, *79* (7), 2680–2687.

[15] Batalla, P.; Fuentes, M.; Grazu, V.; Mateo, C.; Fernandez-Lafuente, R.; Guisan, J. M., Oriented covalent immobilization of antibodies on physically inert and hydrophilic support surfaces through their glycosidic chains. *Biomacromolecules* 2008, *9* (2), 719–723.

[16] Dutra, R. F.; Kubota, L. T., An SPR immunosensor for human cardiac troponin T using specific binding avidin to biotin at carboxymethyldextran-modified gold chip. *Clin Chim Acta* 2007, *376* (1–2), 114–120.

[17] Lee, J. H.; Kim, B. C.; Oh, B. K.; Choi, J. W., Highly sensitive localized surface plasmon resonance immunosensor for label-free detection of HIV-1. *Nanomedicine* 2013, *9* (7), 1018–1026.

[18] Grant, S. A.; Pierce, M. E.; Lichlyter, D. J.; Grant, D. A., Effects of immobilization on a FRET immunosensor for the detection of myocardial infarction. *Analytical and Bioanalytical Chemistry* 2005, *381* (5), 1012–1028.

[19] Mehrvar, M.; Abdi, M., Recent developments, characteristics, and potential applications of electrochemical biosensors. *Analytical Sciences* 2004, *20* (8), 1113–1126.

[20] Mistry, K. K.; Layek, K.; Mahapatra, A.; RoyChaudhuri, C.; Saha, H., A review on amperometric-type immunosensors based on screen-printed electrodes. *Analyst* 2014, *139* (10), 2289–2311.

[21] Silva, B.; Cavalcanti, I.; Silva, M.; Dutra, R., A carbon nanotube screen-printed electrode for label-free detection of the human cardiac troponin T. *Talanta* 2013, *117*, 431–437.

[22] Qi, T.; Liao, J.; Li, Y.; Peng, J.; Li, W.; Chu, B.; Li, H.; Wei, Y.; Qian, Z., Label-free alpha fetoprotein immunosensor established by the facile synthesis of a palladium-graphene nanocomposite. *Biosens Bioelectron* 2014, *61*, 245–250.

[23] Pandiaraj, M.; Sethy, N. K.; Bhargava, K.; Kameswararao, V.; Karunakaran, C., Designing label-free electrochemical immunosensors for cytochrome *c* using nanocomposites functionalized screen printed electrodes. *Biosensors and Bioelectronics* 2014, *54*, 115–121.

[24] Gomes-Filho, S. L. R.; Dias, A. C. M. S.; Silva, M. M. S.; Silva, B. V. M.; Dutra, R. F., A carbon nanotube-based electrochemical immunosensor for cardiac troponin T. *Microchemical Journal* 2013, *109*, 10–15.

[25] Dolatabadi, J.; de la Guardia, M., Nanomaterial-based electrochemical immunosensors as advanced diagnostic tools. *Analytical Methods* 2014, *6* (12), 3891–3900.

[26] Luo, X.; Morrin, A.; Killard, A. J.; Smyth, M. R., Application of Nanoparticles in Electrochemical Sensors and Biosensors. 2006; *319*–326.

[27] Vidotti, M.; Carvalhal, R. F.; Mendes, R. K.; Ferreira, D. C. M.; Kubota, L. T., Biosensors based on gold nanostructures. *Journal of the Brazilian Chemical Society* 2011, *22* (1), 3–20.

[28] Campbell, F.; Compton, R., The use of nanoparticles in electroanalysis: an updated review. *Analytical and Bioanalytical Chemistry* 2010, *396* (1), 241–259.

[29] Lu, L.; Liu, B.; Li, S.; Zhang, W.; Xie, G., Improved electrochemical immunosensor for myeloperoxidase in human serum based on nanogold/cerium dioxide-BMIMPF6/L-Cysteine composite film. *Colloids and Surfaces B: Biointerfaces* 2011, *86* (2), 339–344.

[30] Li, H.; Wei, Q.; Wang, G.; Yang, M.; Qu, F.; Qian, Z., Sensitive electrochemical immunosensor for cancer biomarker with signal enhancement based on nitrodopamine-functionalized iron oxide nanoparticles. *Biosensors and Bioelectronics* 2015, *26* (6), 3044–3049.

[31] Yang, H.; Yuan, R.; Chai, Y.; Mao, L.; Su, H.; Jiang, W.; Liang, M., Electrochemical immunosensor for detecting carcinoembryonic antigen using hollow Pt nanospheres-labeled multiple enzyme-linked antibodies as labels for signal amplification. *Biochemical Engineering Journal* 2011, *56* (3), 116–124.

[32] Gao, X.; Zhang, Y.; Wu, Q.; Chen, H.; Chen, Z.; Lin, X., One step electrochemically deposited nanocomposite film of chitosan-carbon nanotubes-gold nanoparticles for carcinoembryonic antigen immunosensor application. *Talanta* 2011, *85* (4), 1980–1985.

[33] Huang, K.; Niu, D.; Xie, W.; Wang, W., A disposable electrochemical immunosensor for carcinoembryonic antigen based on nano-Au/multi-walled carbon nanotubes-chitosans nanocomposite film modified glassy carbon electrode. *Analytica Chimica Acta* 2010, *659* (1–2), 102–108.

[34] Kong, F.; Xu, M.; Xu, J.; Chen, H., A novel label-free electrochemical immunosensor for carcinoembryonic antigen based on gold nanoparticles-thionine-reduced graphene oxide nanocomposite film modified glassy carbon electrode. *Talanta* 2011, *85* (5), 2620–2625.

[35] Yuan, Y.; Yuan, R.; Chai, Y.; Zhuo, Y.; Mao, L.; Yuan, S., A novel label-free electrochemical immunosensor for carcinoembryonic antigen detection based on the [Ag-Ag2O]/SiO2 nanocomposite material as a redox probe. *Journal of Electroanalytical Chemistry* 2010, *643* (1–2), 15–19.

[36] An, Y.; Jiang, X.; Bi, W.; Chen, H.; Jin, L.; Zhang, S.; Wang, C.; Zhang, W., Sensitive electrochemical immunosensor for alpha-synuclein based on dual signal amplification using PAMAM dendrimer-encapsulated Au and enhanced gold nanoparticle labels. *Biosensors and Bioelectronics* 2012, *32* (1), 224–230.

[37] Liu, X.; Wong, D., Picogram-detection of estradiol at an electrochemical immunosensor with a gold nanoparticle vertical bar protein G-(LC-SPDP)-scaffold. *Talanta* 2009, *77* (4), 1437–1443.

[38] Krishnan, S.; Chinnasamy, T.; Veerappan, S.; Senthilkumar, K.; Kannaiyan, D., Dual labeled Ag@SiO2 core-shell nanoparticle based optical immunosensor for sensitive detection of *E. coli*. *Materials Science and Engineering C: Materials for Biological Applications* 2014, *45*, 337–342.

[39] Zhang, S.; Ma, H.; Yan, L.; Cao, W.; Yan, T.; Wei, Q.; Du, B., Copper-doped titanium dioxide nanoparticles as dual-functional labels for fabrication of electrochemical immunosensors. *Biosensors and Bioelectronics* 2014, *59*, 335–341.

[40] Shen, W.; Tian, D.; Cui, H.; Yang, D.; Bian, Z., Nanoparticle-based electrochemiluminescence immunosensor with enhanced sensitivity for cardiac troponin I using *N*-(aminobutyl)-*N*-(ethylisoluminol)-functionalized gold nanoparticles as labels. *Biosensors and Bioelectronics* 2011, *27* (1), 18–24.

[41] Mendes, R.; Laschi, S.; Stach-Machado, D.; Kubota, L.; Marrazza, G., A disposable voltammetric immunosensor based on magnetic beads for early diagnosis of soybean rust. *Sensors and Actuators B-Chemical* 2012, *166*, 135–140.

[42] Shen, Z.; Wang, J.; Qiu, Z.; Jin, M.; Wang, X.; Chen, Z.; Li, J.; Cao, F., QCM immunosensor detection of *Escherichia coli* O157:H7 based on beacon immunomagnetic nanoparticles and catalytic growth of colloidal gold. *Biosensors and Bioelectronics* 2011, *26* (7), 3376–3381.

[43] Li, D.; Wang, J.; Wang, R.; Li, Y.; Abi-Ghanem, D.; Berghman, L.; Hargis, B.; Lu, H., A nanobeads amplified QCM immunosensor for the detection of avian influenza virus H5N1. *Biosensors and Bioelectronics* 2011, *26* (10), 4146–4154.

[44] Yuan, Y.; Zhang, J.; Zhang, H.; Yang, X., Label-free colorimetric immunoassay for the simple and sensitive detection of neurogenin3 using gold nanoparticles. *Biosensors and Bioelectronics* 2011, *26* (10), 4245–4248.

[45] Wu, W.; Bian, Z.; Wang, W.; Zhu, J., PDMS gold nanoparticle composite film-based silver enhanced colorimetric detection of cardiac troponin I. *Sensors and Actuators B: Chemical* 2010, *147* (1), 298–303.

[46] Bera, D.; Qian, L.; Tseng, T.; Holloway, P., Quantum dots and their multimodal applications: a review. *Materials* 2010, *3* (4), 2260–2345.

[47] Gill, R.; Zayats, M.; Willner, I., Semiconductor quantum dots for bioanalysis. *Angewandte Chemie-International Edition* 2008, *47* (40), 7602–7625.

[48] Medintz, I.; Uyeda, H.; Goldman, E.; Mattoussi, H., Quantum dot bioconjugates for imaging, labelling and sensing. *Nature Materials* 2005, *4* (6), 435–446.

[49] Chan, W.; Nie, S., Quantum dot bioconjugates for ultrasensitive nonisotopic detection. *Science* 1998, *281* (5385), 2016–2018.

[50] Somers, R.; Bawendi, M.; Nocera, D., CdSe nanocrystal based chem-/bio-sensors. *Chemical Society Reviews* 2007, *36* (4), 579–591.

[51] Algar, W.; Susumu, K.; Delehanty, J.; Medintz, I., Semiconductor quantum dots in bioanalysis: crossing the valley of death. *Analytical Chemistry* 2011, *83* (23), 8826–8837.

[52] Colvin, V.; Goldstein, A.; Alivisatos, A., Semiconductor nanocrystals covalently bound to metal-surfaces with self-assembled monolayers. *Journal of the American Chemical Society* 1992, *114* (13), 5221–5230.

[53] Lidke, D.; Nagy, P.; Heintzmann, R.; Arndt-Jovin, D.; Post, J.; Grecco, H.; Jares-Erijman, E.; Jovin, T., Quantum dot ligands provide new insights into erbB/HER receptor-mediated signal transduction. *Nature Biotechnology* 2004, *22* (2), 198–203.

[54] Palaniappan, K.; Xue, C.; Arumugam, G.; Hackney, S.; Liu, J., Water-soluble, cyclodextrin-modified CdSe-CdS core-shell structured quantum dots. *Chemistry of Materials* 2006, *18* (5), 1275–1280.

[55] Mattoussi, H.; Mauro, J.; Goldman, E.; Anderson, G.; Sundar, V.; Mikulec, F.; Bawendi, M., Self-assembly of CdSe-ZnS quantum dot bioconjugates using an engineered recombinant protein. *Journal of the American Chemical Society* 2000, *122* (49), 12142–12150.

[56] Xing, Y.; Chaudry, Q.; Shen, C.; Kong, K.; Zhau, H.; Chung, L.; Petros, J.; O'Regan, R.; Yezhelyev, M.; Simons, J.; Wang, M.; Nie, S., Bioconjugated quantum dots for multiplexed and quantitative immunohistochemistry. *Nature Protocols* 2007, *2* (5), 1152–1165.

[57] Liu, G.; Wang, J.; Kim, J.; Jan, M.; Collins, G., Electrochemical coding for multiplexed immunoassays of proteins. *Analytical Chemistry* 2004, *76* (23), 7126–7130.

[58] Li, L.; Liu, K.; Yang, G.; Wang, C.; Zhang, J.; Zhu, J., Fabrication of graphene-quantum dots composites for sensitive electrogenerated chemiluminescence immunosensing. *Advanced Functional Materials* 2011, *21* (5), 869–878.

[59] Aoyagi, S.; Kudo, M., Observation of fluorescence-labeled protein A on a biosensor surface by means of TOF-SIMS. *Sensors and Actuators B-Chemical* 2005, *108* (1–2), 708–712.

[60] Lingerfelt, B.; Mattoussi, H.; Goldman, E.; Mauro, J.; Anderson, G., Preparation of quantum dot-biotin conjugates and their use in immunochromatography assays. *Analytical Chemistry* 2003, *75* (16), 4043–4049.

[61] Sun, B.; Xie, W.; Yi, G.; Chen, D.; Zhou, Y.; Cheng, J., Microminiaturized immunoassays using quantum dots as fluorescent label by laser confocal scanning fluorescence detection. *Journal of Immunological Methods* 2001, *249* (1–2), 85–89.

[62] Goldman, E.; Balighian, E.; Mattoussi, H.; Kuno, M.; Mauro, J.; Tran, P.; Anderson, G., Avidin: a natural bridge for quantum dot-antibody conjugates. *Journal of the American Chemical Society* 2002, *124* (22), 6378–6382.

[63] Kerman, K.; Endo, T.; Tsukamoto, M.; Chikae, M.; Takamura, Y.; Tamiya, E., Quantum dot-based immunosensor for the detection of prostate-specific antigen using fluorescence microscopy. *Talanta* 2007, *71* (4), 1494–1499.

[64] Lao, U.; Mulchandani, A.; Chen, W., Simple conjugation and purification of quantum dot-antibody complexes using a thermally responsive elastin-protein L scaffold as immunofluorescent agents. *Journal of the American Chemical Society* 2006, *128* (46), 14756–14757.

[65] Susha, A.; Javier, A.; Parak, W.; Rogach, A., Luminescent CdTe nanocrystals as ion probes and pH sensors in aqueous solutions. *Colloids and Surfaces A: Physicochemical and Engineering Aspects* 2006, *281* (1–3), 40–43.

[66] Liu, Y.; Sun, Y.; Vernier, P.; Liang, C.; Chong, S.; Gundersen, M., pH-sensitive photoluminescence of CdSe/ZnSe/ZnS quantum dots in human ovarian cancer cells. *Journal of Physical Chemistry C* 2007, *111* (7), 2872–2878.

[67] Herrero-Latorre, C.; Alvarez-Mendez, J.; Barciela-Garcia, J.; Garcia-Martin, S.; Pena-Crecente, R. M., Characterization of carbon nanotubes and analytical methods for their determination in environmental and biological samples: a review. *Analytica Chimica Acta* 2015, *853*, 77–94.

[68] Vashist, S.; Zheng, D.; Al-Rubeaan, K.; Luong, J.; Sheu, F., Advances in carbon nanotube based electrochemical sensors for bioanalytical applications. *Biotechnology Advances* 2011, *29* (2), 169–188.

[69] Li, J.; Pandey, G. P., Advanced physical chemistry of carbon nanotubes. *Annual Review of Physical Chemistry* 2015.

[70] Yang, N.; Chen, X. P.; Ren, T. L.; Zhang, P.; Yang, D. G., Carbon nanotube based biosensors. *Sensors and Actuators B: Chemical* 2015, *207*, 690–715.

[71] Girifalco, L.; Hodak, M.; Lee, R., Carbon nanotubes, buckyballs, ropes, and a universal graphitic potential. *Physical Review B* 2000, *62* (19), 13104–13110.

[72] Peng-Cheng Maa, N. A. S., Gad Maromb, Jang-Kyo Kima, Dispersion and functionalization of carbon nanotubes for polymer-based nanocomposites: a review. 2010, *41* (10), 1345–1367.

[73] Di Crescenzo, A.; Ettorre, V.; Fontana, A., Non-covalent and reversible functionalization of carbon nanotubes. *Beilstein Journal of Nanotechnology* 2014, *5*, 1675–1690.

[74] Gao, C.; Guo, Z.; Liu, J.; Huang, X., The new age of carbon nanotubes: an updated review of functionalized carbon nanotubes in electrochemical sensors. *Nanoscale* 2012, *4* (6), 1948–1963.

[75] Tuncel, D., Non-covalent interactions between carbon nanotubes and conjugated polymers. *Nanoscale* 2011, *3* (9), 3545–3554.

[76] Sanchez, S.; Roldan, M.; Perez, S.; Fabregas, E., Toward a fast, easy, and versatile immobilization of biomolecules into carbon nanotube/polysulfone-based biosensors for the detection of hCG hormone. *Analytical Chemistry* 2008, *80* (17), 6508–6514.

[77] Viswanathan, S.; Rani, C.; Anand, A.; Ho, J., Disposable electrochemical immunosensor for carcinoembryonic antigen using ferrocene liposomes and MWCNT screen-printed electrode. *Biosensors and Bioelectronics* 2009, *24* (7), 1984–1989.

[78] Malhotra, R.; Patel, V.; Vaque, J.; Gutkind, J.; Rusling, J., Ultrasensitive electrochemical immunosensor for oral cancer biomarker IL-6 using carbon nanotube forest electrodes and multilabel amplification. *Analytical Chemistry* 2010, *82* (8), 3118–3123.

[79] Munge, B.; Fisher, J.; Millord, L.; Krause, C.; Dowd, R.; Rusling, J., Sensitive electrochemical immunosensor for matrix metalloproteinase-3 based on single-wall carbon nanotubes. *Analyst* 2010, *135* (6), 1345–1350.

[80] Chen, Y.; Huang, J., Electrochemical sensing of bovine serum albumin at self-assembled SWCNTs on gold. *Diamond and Related Materials* 2009, *18* (2–3), 516–519.

[81] Su, H.; Yuan, R.; Chai, Y.; Zhuo, Y.; Hong, C.; Liu, Z.; Yang, X., Multilayer structured amperometric immunosensor built by self-assembly of a redox multi-wall carbon nanotube composite. *Electrochimica Acta* 2009, *54* (17), 4149–4154.

[82] Jacobs, C.; Peairs, M.; Venton, B., Review: carbon nanotube based electrochemical sensors for biomolecules. *Analytica Chimica Acta* 2010, *662* (2), 105–127.

[83] Freitas, T.; Mattos, A.; Silva, B.; Dutra, R., Amino-functionalization of carbon nanotubes by using a factorial design: human cardiac troponin T immunosensing application. *Biomed Research International* 2014.

[84] Yao, J.; Sun, Y.; Yang, M.; Duan, Y. X., Chemistry, physics and biology of graphene-based nanomaterials: new horizons for sensing, imaging and medicine. *Journal of Materials Chemistry* 2012, *22* (29), 14313–14329.

[85] Novoselov, K. S.; Geim, A. K.; Morozov, S. V.; Jiang, D.; Zhang, Y.; Dubonos, S. V.; Grigorieva, I. V.; Firsov, A. A., Electric field effect in atomically thin carbon films. *Science* 2004, *306* (5696), 666–669.

[86] Zhang, L.; Zhou, R.; Zhao, X., Graphene-based materials as supercapacitor electrodes. *Journal of Materials Chemistry* 2010, *20* (29), 5983–5992.

[87] Lawal, A. T., Synthesis and utilisation of graphene for fabrication of electrochemical sensors. *Talanta* 2015, *131*, 424–443.

[88] Zhu, Y.; Murali, S.; Cai, W.; Li, X.; Suk, J.; Potts, J.; Ruoff, R., Graphene and graphene oxide: synthesis, properties, and applications. *Advanced Materials* 2010, *22* (46), 5226–5226.

[89] Zhu, Y.; Murali, S.; Cai, W.; Li, X.; Suk, J.; Potts, J.; Ruoff, R., Graphene and graphene oxide: synthesis, properties, and applications. *Advanced Materials* 2010, *22* (35), 3906–3924.

[90] Chung, C.; Kim, Y.; Shin, D.; Ryoo, S.; Hong, B.; Min, D., Biomedical applications of graphene and graphene oxide. *Accounts of Chemical Research* 2013, *46* (10), 2211–2224.

[91] Chen, D.; Feng, H. B.; Li, J. H., Graphene oxide: preparation, functionalization, and electrochemical applications. *Chemical Reviews* 2012, *112* (11), 6027–6053.

[92] Dreyer, D.; Park, S.; Bielawski, C.; Ruoff, R., The chemistry of graphene oxide. *Chemical Society Reviews* 2010, *39* (1), 228–240.

[93] Shan, C.; Yang, H.; Han, D.; Zhang, Q.; Ivaska, A.; Niu, L., Graphene/AuNPs/chitosan nanocomposites film for glucose biosensing. *Biosensors and Bioelectronics* 2010, *25* (5), 1070–1074.

[94] Luo, J.; Jiang, S. S.; Zhang, H. Y.; Jiang, J. Q.; Liu, X. Y., A novel non-enzymatic glucose sensor based on Cu nanoparticle modified graphene sheets electrode. *Analytica Chimica Acta* 2012, *709*, 47–53.

[95] Mao, S.; Lu, G.; Yu, K.; Bo, Z.; Chen, J., Specific protein detection using thermally reduced graphene oxide sheet decorated with gold nanoparticle-antibody conjugates. *Advanced Materials* 2010, *22* (32), 3521–+.

[96] Zhong, Z.; Wu, W.; Wang, D.; Wang, D.; Shan, J.; Qing, Y.; Zhang, Z., Nanogold-enwrapped graphene nanocomposites as trace labels for sensitivity enhancement of electrochemical immunosensors in clinical immunoassays: carcinoembryonic antigen as a model. *Biosensors and Bioelectronics* 2010, *25* (10), 2379–2383.

[97] Huang, J. L.; Tian, J. N.; Zhao, Y. C.; Zhao, S. L., Ag/Au nanoparticles coated graphene electrochemical sensor for ultrasensitive analysis of carcinoembryonic antigen in clinical immunoassay. *Sensors and Actuators B: Chemical* 2015, *206*, 570–576.

[98] Tang, J.; Tang, D.; Niessner, R.; Chen, G.; Knopp, D., Magneto-controlled graphene immunosensing platform for simultaneous multiplexed electrochemical immunoassay using distinguishable signal tags. *Analytical Chemistry* 2011, *83* (13), 5407–5414.

[99] Teixeira, S.; Burwell, G.; Castaing, A.; Gonzalez, D.; Conlan, R. S.; Guy, O. J., Epitaxial graphene immunosensor for human chorionic gonadotropin. *Sensors and Actuators B-Chemical* 2014, *190*, 723–729.

[100] Xu, S.; Liu, Y.; Wang, T.; Li, J., Positive potential operation of a cathodic electrogenerated chemiluminescence immunosensor based on luminol and graphene for cancer biomarker detection. *Analytical Chemistry* 2011, *83* (10), 3817–3823.

[101] Li, L. L.; Liu, K. P.; Yang, G. H.; Wang, C. M.; Zhang, J. R.; Zhu, J. J., Fabrication of graphene-quantum dots composites for sensitive electrogenerated chemiluminescence immunosensing. *Advanced Functional Materials* 2011, *21* (5), 869–878.

APÊNDICE D – CAPÍTULO DE LIVRO PUBLICADO

POINT-OF-CARE ELECTROCHEMICAL IMMUNOSENSORS APPLIED TO DIAGNOSTIC IN HEALTH

Diego G. A. Cabral, Gilvânia M. de Santana, Paula A. B. Ferreira, Anne K. S. Silva, Erika K. G. Trindade and Rosa F. Dutra

In: **Advances in Biosensors: Reviews Volume 2**

IFSA Publishing, 2018

Chapter 2

Point-of-Care Electrochemical Immunosensors Applied to Diagnostic in Health

Diego G. A. Cabral, Gilvânia M. de Santana, Paula A. B. Ferreira, Anne K. S. Silva, Erika K. G. Trindade and Rosa F. Dutra

2.1. Introduction

Point-of-care testing (PoCT) have been recognized as one of the most attractive methods for decentralization of analytical practices, being mainly developed to diagnostics that require rapid interventions, such as cardiovascular diseases, drug intoxication, emergency preparedness in surgical procedures, containment of transmissibility, spread of infectious diseases, and surveys in endemic or epidemic outbreaks [1]. Another interesting application of PoCTs devices is in continuous monitoring of markers that require recurrent evaluations, glycemic or mostly in therapies and prolonged treatments of diseases like the cancer, being also benefit for treatment and monitoring of patients that live in areas far from central laboratories. In these situations, the conventional laboratorial testing become impracticable, since samples should be transported, processed and results returned to the doctors. Challenges in developing of PoCTs for medical diagnostics involve to combine the advantages of fast results, low cost and user friendly processing, without loss of diagnostic sensibility and specificity, when they are compared to laboratorial analyses.

PoCTs are analytical devices designed to be used near the bedside, reducing the turnaround time of the diagnostic cycle, usually processed

Rosa F. Dutra
Biomedical Engineering Laboratory, Federal University of Pernambuco, Brazil

outside hospital or laboratory that do not require skilled personnel for managements [2]. Currently, PoCT tests are considered practical and economical methods, being nowadays considered as one of the most attractive analytical possibilities, compared to the chemical analyzers, immunoanalyzers, PCR (polymerase chain reaction) and others [2]. Among PoCT devices, lateral flow assays (LFA) and biosensors addressed to immunoassays are more economically profitable than enzyme-linked immunosorbent assay (ELISA) or Electro-chemiluminescence immunoassay (ECLIA), especially regarding to time of analyzes.

Lateral flow assays (LFA) based on immunochromatographic tests are paper assays that use immobilized antibodies or antigens to capture target analytes in samples. A color band resulted on a paper-strip from molecule (antigen or antibody) or material labeling reveals this reaction, usually supplying qualitative results. However, additional image resources can be used to produce quantitative data based in contrast and brightness of color band [3]. A typical LFA is formed by overlapping membranes mounted on a rigid support, which confers stability and facilitates the handling [4]. Tip of the strip has a sample pad made of adsorbent material, where the sample is applied. The samples are transported by capillarity to the conjugation pad containing the labeled antibodies for biorecognition. The interaction between the target analytes and these antibodies form complexes that migrate to the reaction zone, usually formed by a nitrocellulose membrane. In this zone, there are two lines of immobilized antibodies, one to the target molecule and the control to define the results [8]. A schematic design of a LFA is shown in Fig. 2.1.

On the last few decades, advances of nanotechnology has allowed incorporation of gold nanoparticles to LFA, improving the sensitive of the analytical testing [7] Currently, LFA immunoassay have been developed for several applications, allowing the screening of infectious diseases (HIV, viral hepatitis, tuberculosis and herpes simplex virus and others) [8]. LFA has also been applied to PoCTs of cardiac markers such as troponin, H-FABP, hepatitis and others, possibility a semi-quantitative analysis; however it is quite limited, because the results are color band-dependents, thus the results are subject of human misinterpretation [9].

In attempting to overcome the limitations denoted by LFA, immunosensors can supply a quantifiable signal, as greater as well as

higher the analyte concentrations, independently of detected species: antibodies, antigens, enzymes, or other chemical species. The interest for immunosensors has been exponentially growing on the last decades due to combine advantages of high sensitivity, user-friendly processing and portability, beside to present a low cost per analyses (Fig. 2.2).

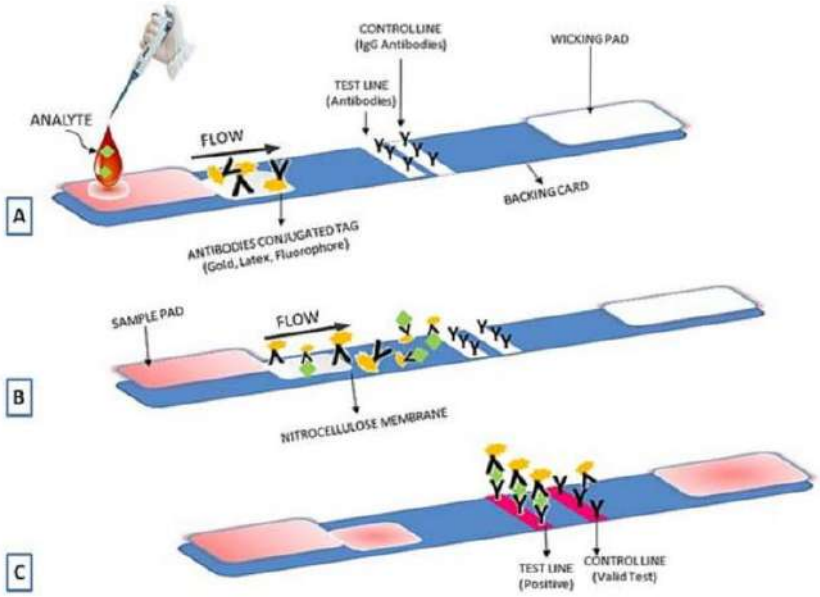

Fig. 2.1. Schematic design of a typical Lateral Flow Immunoassay at different steps: (A) adding the samples containing antigens and immunoglobulins; (B) migration of antigens with labelled antibodies, and (C) immunocomplex formed and immunoglobulis are positioned by affinity on the paper regions where labelled antibodies are exhibited by a color band.

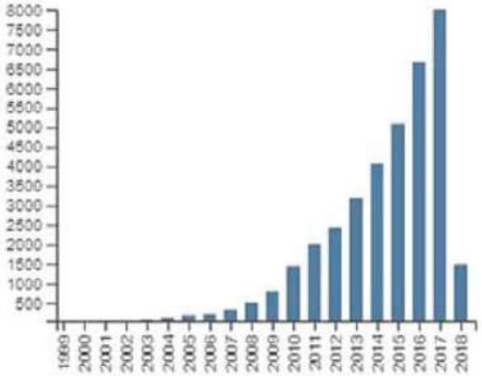

Fig. 2.2. Number of citation over the last decades (Extracted from Web of Science base: ["immunosensor" OR "electrode" OR "biosensor"] AND ["point-of-care"] in March 2018).

2.2. PoCT Electrochemical Immunosensor

Immunosensors are based on the specific antigen-antibody interactions causing a perturbation on the electrode surface by molecule capturing by immobilized antigens or antibodies; this perturbation is converted into measurable signals by a transducer. In general, signal is amplified, processed and readout in output display [10]. Specificity of immunosensors is mainly dependent of affinity between antigen-antibody. Monoclonal and polyclonal antibodies can be used in immobilization technique developments, nevertheless monoclonal antibodies are more attractive due to recognize only a one epitope of an antigen, being more specific, although commonly have a higher cost [11] Recombinant antigens have been more recently used to produce antibodies with more selectively, in order to recognize only one epitope region.

Screen-printed electrode (SPE) has significantly contributed for PoCT developments. The layer-by-layer printing of commercial or self-made inks onto different types of rigid and flexible substrates. Conventionally, SPE comprises one sensing unit with three printed electrodes, including a working electrode, a counter electrode and a reference electrode. The composition of the inks chosen in the printing process is essential to the selective determination intended for each analysis [12]. Commonly, SPE uses voltammetric techniques, measuring changes on current responses produced by a controlled potential (constant or periodic). Current responses are generated by diffusion of redox species from electrolyte/electrode interface, being proportional to the binding events, i.e. antigens or antibodies captured.

In numerous point-of-care immunosensors using amperometric transduction have been developed for clinical diagnostics, such as for HIV [13], prostate specific antigen (PSA) [14], celiac disease [15], cardiac troponin T [16] and cardiac troponin I [17]. Other transducer types using the SPE have also been described for impedance [18] or capacitance [19] measurements.

Recent advances in the SPE development for clinical diagnostic were obtained with progress derived from synthesis of nanostructured electrode surfaces. Metallic nanoparticles, nanowires, carbon nanotubes, graphene, and their respective nanocomposites have been widely used combining with pastes, or forming film on the working electrodes [20]. Using nanocomposites or nanofilms was possible to increase the amount

of immobilized biomolecules on the surface sensor due to greater of working electrode area. Additionally, nanomaterials have also contributed to increase the sensitivity of biosensors, due to their electrical, optics, acoustic and other interesting proprieties, particularly indispensable and individuals of each nanomaterial that are capable to produce devices with more reproducible results and robustness [21].

2.3. Advances on PoCT Immunosensors

Nanomaterials have improved specially the efficiency and reliability of electrochemical PoCT immunosensors, allowing a lower limit of detection in the concentrations of antigens or antibodies present in biologic fluid samples that was not previously possible. Nanomaterials can be defined based on size parameter(s), being under 100 nm sized in, at least, one dimension. Commonly, in nanoscale, these materials present new properties that are not normally observed, when they are in bulk. These alterations are obtained by the quantum effects of size, being especially evident in carbon allotropes and metal nanoparticle [22, 23]. For this reason, it is clear that the progress of bioanalytical assays will rely heavily on innovations in nanotechnology [24, 25].

Several nanomaterials have contributed to electrochemical immunosensor developments, among them metal nanoparticles, metal oxides nanoparticles, carbon nanotubes, graphene, their corresponding nanocomposites and quantum dots (Fig. 2.3) [26].

2.3.1. PoCT Immunosensors Based on Carbon Allotropes

Carbon allotropes contribution in electrochemical immuno-PoCTs has gained prominence due to their small size of the carbon atoms and the number of electrons they can share, allowing the formation of several bonding patterns and stable versatile materials with excellent intrinsic properties such as high electrical conductivity, large surface area, ease of functionalization and biocompatibility [27].

Carbon nanotube

Among the nanostructures synthesized from carbon allotropes should be highlighted the carbon nanotubes (CNT) that were discovered in 1991 by Iijima, enabling interaction with biomolecules for biosensor

applications [28]. CNTs can be described as hexagonal arrangements in cylindrical format, held by Van der Waals interactions in the adjacent layers. They promote a rapid electron transfer, increasing the reaction rate of many electroactive species, and then decreasing the electrode response time of the Immuno-PoCTs, thereby achieving high sensitivity with low detection limits [29]. With respect to the structure the CNT can be classified in two forms: single wall nanotubes (SWCNT), formed by a single layer of carbon atoms arranged in a hexagonal way, and multiple wall nanotubes (MWCNT), which consists of multiple layers of carbon atoms arranged in a hexagonal way arranged around a central area. The length of a CNT can range from nanometers to centimeters, but the diameter varies in the order of nanometers, depending on the type of CNT; so it possesses a high aspect ratio, or the length-to-diameter ratio, can be as high as 132,000,000:1, which is unequalled by any other material [30]. Activation or functionalization of CNTs by oxidation treatment introduces chemical functional groups, including alcoholic, carboxylic, aldehydic, ketonic, and esteric oxygenated functional groups [31]. These groups allow a greater interaction between CNTs and biomolecules, enabling an oriented immobilization, as example by the Fc portion of antibodies and by exposing their binding sites or antigenic regions to the specific epitopes (Fig. 2.4) [32].

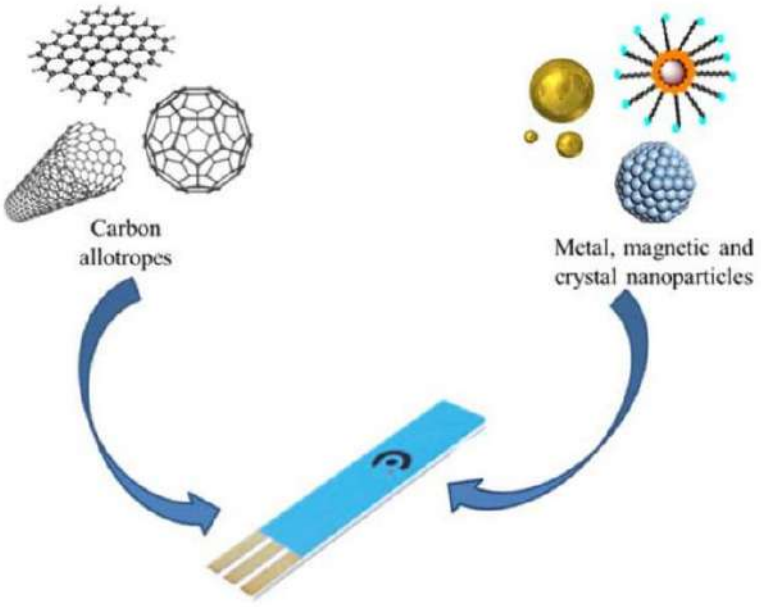

Fig. 2.3. Nanomaterials with potential applications in SPE based-PoCTs. Illustrating of CNTs as carriers or reporters for signal generation and powerful amplifiers for electrochemical transduction.

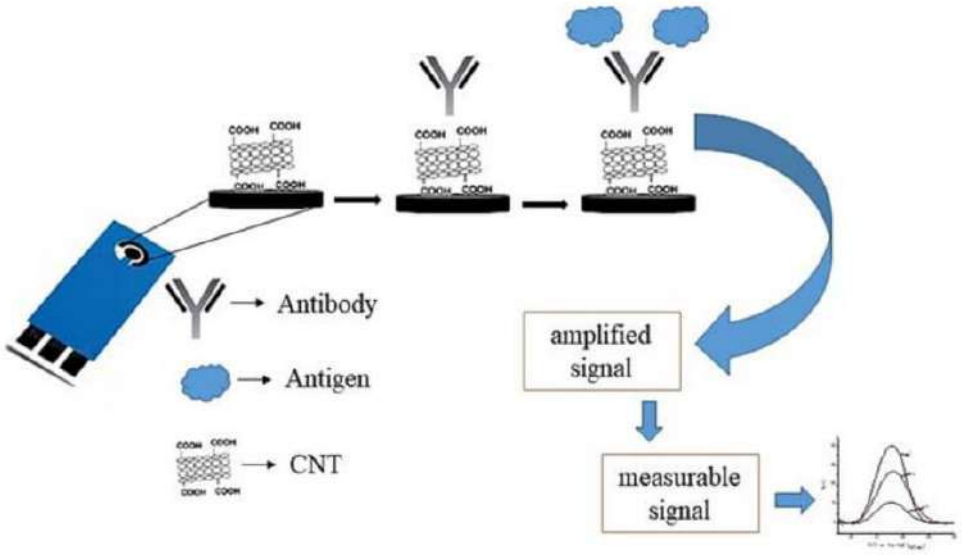

Fig. 2.4. Use of CNTs to detect the interaction between antigen-antibody in PoCT.

Studies have shown that CNTs interact with other materials, improving the intrinsic qualities of the PoCTs immunosensor. Dias et al. [33], (2013) produced a dengue virus for NS1 detection based on a homogeneous mixture consisting of carboxylated CNTs dispersed in carbon ink as a printed working electrode. The effect of the matrix, as well as the performance of the assays, was successfully evaluated using the spiked blood serum sample, obtaining excellent recovery values in the results. The carbon nanotubes incorporated into the carbon paint improved the reproducibility and sensitivity of the CNT-SPE immunosensor. In another work, Silva et al. [34] (2013) developed a label-free immunosensor based on printed electrodes for CNTs functionalized with amine groups to detect the cardiac troponin T. PoCT was developed by the homogenization between the carbon ink and the amine carbon nanotubes forming a thin film on a polyethylene terephthalate substrate. The use of NH_2-CNTs increased the reproducibility and stability of the sensor, and the amine groups allowed an oriented immobilization of antibodies against cardiac troponin T.

Aiming to allow the allignment of CNTs on sensor surface, polymer films have been commonly employed. The polymers interact with the CNT through the functional groups (-COOH, -OH, $-NH_2$) and may form nanocomposites or nanohybrids. As examples we

can cite the work of Sanchez-Tirado et al. [35], (2017) where dual screen-printed carbon electrodes modified with 4-carboxyphenyl-functionalized double-walled carbon nanotubes were used for the preparation of electrochemical immunosensors for the simultaneous determination of the cytokines Interleukin-1β (IL-1β) and factor necrosis tumor α (TNF-α). In addition, the dual immunosensor exhibits excellent reproducibility of the measurements, storage stability and selectivity as well as negligible crosstalking. In recent years, studies have shown that the use of CNT combined with conductive polymers can improve sensitivity and increase electron transfer on the sensor platform. In another study Gomes et al. [36], (2013) produced a nanostructured SPE immunosensor based on carbon nanotubes supported by a conductive polymer film for detection of cardiac Troponin T (cTnT). The combined use of polyethyleneimine (PEI) film and CNT provided important advantages for obtaining a highly sensitive analytical method for cTnT.

Graphene

Another prominent carbon nanomaterial is graphene (G). It is a 2D material of atomic thickness, formed by carbon atoms with sp2 hybridization, forming a structure of hexagonal shape similar to a hive. The characterization and identification of graphene was first performed in 2004, after synthesis obtained by successive exfoliation steps of graphite oxide using an adhesive tapes [37]. Among its remarkable properties, it is cited the transparency of the sheet (optical transmittance of ~97.7 %) and large surface area (2630 m^2 g^{-1}). Furthermore, it is a good heat conductor (thermal conductivity of 500 W m^{-1} K^{-1}), chemically inert and a semimetal with high electron transfer (charge mobility of 250 000 cm^2 V^{-1} s^{-1} in room temperature) [38].

According to physical and chemical characteristics, different forms of graphene are shown, among them Graphene Oxide (GO) and Reduced Graphene Oxide (RGO), which, because of their particularities, are highly attractive for the assembly of sensor surfaces [39]. GO has two dimensions, consisting of a hexagonal network of Sp2 bonds between carbon atoms (CC) and by Sp3 bonds with oxygen atoms (CO) forming carboxyl groups (-COOH), hydroxyls (-OH) or epoxy (-O-). This makes GO an excellent material for biological applications, since its functional groups readily interact with nucleic acids, proteins, cells, and other organic molecules [40]. Yukird et al. [41], (2017) developed an electrochemical immunosensor based on a nanohybrid formed by graphene and polyaniline (G/PANI). Electrospraying of G/PANI

increased the electrode surface area while electropolymerization of aniline increased the number of amino groups ($-NH_2$) for antibody immobilization.

Reduced graphene oxide (rGO) is another material that has been widely used in electrochemical analysis, due to its high effective surface area and high electrical conductivity [42]. rGO is produced from reduction of GO via thermal, chemical, electrochemical and laser-scribing methods. In rGO synthesis, functional groups are removed and the conductivity is increased again [40]. As examples of the use of graphene for the production of Immuno-PoCTs we can mention the work of Silva et al., (2016) [43], that produced a biomimetic sensor for the detection of Troponin T based on a nanocomposite formed by the conjugation of rGO and Polypyrrole. Another example is Lee et al. [44] (2017), who developed an electrochemical immunosensor for the detection of carcinoembryonic antigen. In this method, silver nanoparticles were mixed with rGO to modify the surface of screen-printed carbon electrode.

2.3.2. PoCT Immunosensors Based on Metal Nanoparticles

Metal nanomaterials have been aroused interest due to their special optical and electrocatalytic properties. They are often incorporated by adhesion or binding to the modified transduction platforms. Robust devices for health applications were fabricated with enhanced performance using nanoparticles [45]. Metal nanoparticles have been used to immobilize antibodies or antigens, and or have served as electronic conduction vehicles in electrochemical biosensors [46]. Metal nanoestructures, semiconductor nanoparticles and metal oxide nanostructures have been considered as potential signal labels when attached to secondary antibodies to stimulate the development of signal amplification strategy for immunosensing [47].

Gold nanoparticles

Gold is an inert metal in macroscale, but gold nanoparticles (GNPs) are adopted nanomaterial often explored as detectable labels to enhance a suitable signal, thereby providing an intense, pronounced and vivid mark. The color change of GNPs are observable with bare eye. This optical property of revelation in visible color is valuable especially in colorimetric assays [48]. Although they have a higher cost, they present

high conductivity, excellent biocompatibility, superior stability, low toxicity, relatively simple production and modification [49]. Thus, colloidal GNPs have been used to modify solid electrodes and has shown advantages in feasibly attachment of the immunological molecules and the electron transfer that increase the electrochemical signals. The strong affinity for the amino groups is explored and gold provide a microenvironment compatible with biomolecules, remaining their activity even after immobilization [50]. Moreover, the formation of self-assembled monolayers (SAMs) through oriented Au-S bonds affords great attention to gold toward SPEs for adhesion of more components. Gold SPE helps to deposit antibody in close vicinity with transducer and GNPs help to cast antibody in close vicinity with the antigen and hence results in the increase of sensitivity until femtogram level [51]. Also, Jacobs and coworkers [52] have proposed an 52immunosensors for ultrasensitive detection of troponin-T based on antibody conjugated to GNPs. Using electrochemical impedance spectroscopy, the interdigitated sensor was able to detect concentrations in femtogram per milliliter (fg/mL) of this cardiac marker. Recently, Sabouri et al. [53] have developed a sensitive 52 immunosensors for detection of Hepatitis B virus based on GNPs. HbsAg was targeted by a primary antibody and a secondary antibody co-immobilized on luminol-GNPs, with detection limit of 14 pg/mL.

Silver nanoparticles

Silver is a relatively cheap noble metal that exhibit superior properties over gold on the nanoscale, mainly of optical nature [54]. Its optical profile exhibits the sharpest and most intense bands among metals [55]. Consequently, for convenience, colorimetric assays are prevalent with silver nanoparticles (SNPs) by the straightforward color change discrimination. They can be oxidized more easily and offer improved electrochemical activity, making them good candidates for detection tags in electrochemical sensing. The utilization either naked or conjugated with recognition probes as signal transduction elements for analyte detection in biosensors was shown to improve the detection limits and enhance their diagnostic performance [56]. For this, silver nanostructures need to be associated with recognition molecules that can selectively detect and capture the analyte of interest. However, the functionalization still is a challenging process. They are less stable in aqueous dispersions and are susceptible to oxidation and etching by chloride ions. By their limited stability and difficulty to functionalize, SNPs have become less popular [57]. Considering practical situations,

Hao et al. [58] have developed a direct electrochemical detection approach to assay generically proteins by using SNPs labels coupled covalently with antibody on a SPE. The detection limit found was 0.4 ng/mL. Now, Felici and colleagues [59] have described a novel prototype of label-free 53 immunosensors using SPE and exploiting SNPs as a backing material and electrochemical tracker. Che and coworkers [60] have constructed an amperometric 53 immunosensors for the determination of α-1-fetoprotein, a tumor marker found in several malignant diseases. Multiwalled carbon nanotube-silver nanoparticle composite modified on the surface of a glassy carbon electrode leading a detection limit of 0.08 ng/m. Similarly, Ibupoto and colleagues [61] have described a new potentiometric 53 immunosensors for the selective detection of d-dimer using SNPs decorated ZnO nanotubes anchored to antibodies. D-dimer is a biomarker found at high levels in deep vein thrombosis disorders. It was found a detection limit of 1.00×10^{-6} μg/mL.

Magnetic nanoparticle

Comparatively, magnetic nanoparticles (MNPs) are cheaper to produce, being considered physically and chemically stable, biocompatible and environmentally safe. Magnetic labels have certain peculiarities for biosensing applications, like absence of pre-processing stage for sample purification, since biological entities do not show any magnetic behavior or susceptibility and therefore, no interferences or noise is to expect during signal capturing [62]. Hence, they are also important items for biomedical applications involved in LFA systems as a colored reagent, possessing strong brown coloration. One promising utility is magnetic preconcentration before the detection event. MNPs conjugated to bioreceptor unit can simply be mixed in solution to interact specifically with the analyte. They offer the convenience of separation via external magnetic field, permitting them easily be attracted with a small magnet, losing their magnetic effect when the field is removed. This way, these nanoparticles can be efficiently separated and isolated from the solution [56]. However, the main strategy is the integration of MNPs into the transducer element or the modification of the sensor surface. Despite a wide range of ferromagnetic materials, iron oxides (Fe_2O_3 and Fe_3O_4) are most commonly used for generation or amplification of analytical signal [63]. Employing proper functionalization methods, some notable benefits are achieved such as rapid analysis process, better stability and low detection limit. Besides, they are fluorescent alternatives that offer ease of handling, low production cost and smaller size of final fabricated

device when compared to fluorophores [64]. For instance, combining the aforementioned trends, a novel amperometric magnetoimmunoassay based on MNPs pulled by magnetic field on the screen-printed carbon electrodes surface was developed for the selective determination of Legionella pneumophila. The achieved limit of detection by Martín et al. was 104 Colony Forming Units (CFUs)/mL [65]. Singh and Krishnan achieved the first serum insulin voltammetric immunosensor for clinical diagnosis of type 1 and type 2 diabetic disorders. It was reported a lower detection limit of 5 pM for free insulin present in serum using functionalized magnetite nanoparticles [66].

Metal oxide nanoparticles

Zinc oxide (ZnO) also belong group of elite nanomaterials with inherent optical, and piezoelectric properties. It is a semiconducting material that exhibits biomimetic, high catalytic efficiency, little toxicity, low biodegradability, and stable immobilization of proteins due to high isoelectric point without distorting their bioactivity [67]. Beside good electron transfer, this metal oxide nanoparticle denotes a strong adsorption capability, offering numerous sites to antibodies, enzymes and proteins which make them choice for biosensors. It should be conjugated with biological molecules without losing the integrity [68]. For example, a glucose electrochemical sensor based on ZnO nanorods was investigated by Marie and coworkers [69]. The lower limit of detection was 0.22 μM. And a microfluidic immunosensor applied in congenital hypothyroidism screening was presented by Seia and colleagues [70]. ZnO nanobeads were employed as platform for monoclonal antibody immobilization to specifically capture thyrotropin hormone. The electrochemical detection limit of glass microchip was 0.00087 μUI mL.

2.4. Lab-On-A-Chip Based Immunosensors

Due to the in-depth knowledge of nanomaterials, great advances were achieved, making it possible to implement confined labs on a single chip or laboratory analysis system. Lab-on-a-chip combines analysis, reaction and processing in a single microchip, i.e., the ability to gather multiple key functions of a size reduced laboratory on an electronic device with a few square centimeters, which typically manipulates human fluids in the order of microliters to nanoliters [26]. This approach have been extensively applied in point of care devices due to advantages such as

compactness, mobility, integrability, modularity, reconfigurability, embedded computing, limited power consumption and minimum need to sample and reagent when enormous amounts of volume are not available [71]. Additionally, lab-on-chip platforms are hermetically enclosed with precise control conditions, avoiding evaporation and minimizing the risk of contamination by potentially infectious biological specimens [72]. Regarding personalized healthcare, the multiple detection by a single PoCT is an important trend which could replace time-consuming laboratory analyses [73]. In addition to releasing results in minutes, they play an important role in management and early investigation of diseases and outbreaks [74]. One of the purposes is the development of a chip-based, miniaturized and portable system that allows for the assay of different analytes in complex samples. In this way, many researches in the scientific community have focused on paper-based and printed electrode technologies as approaches for fabricating these diagnostic systems. These technologies are affordable, user-friendly, rapid, and scalable for manufacturing. Moreover, the association with nanomaterials provides a path for the development of highly sensitive and selective biosensors for prospective generation PoCT tools [21].

Paper-based microfluidics or lab on paper is a novel system for handling and analysis of fluid extracellular for a variety of medical applications, such as healthcare and screening [75]. This technology presents simplicity, portability, disposability, low-cost and allows the automation of multi-step processes [76]. Nitrocellulose membrane, chromatography paper and filter paper are attractive substrates for fabricating microfluidic device, because they are natural, porous, ubiquitous and inexpensive materials. Confining solvents and reagents in specific points, paper can drive and regulate aqueous movement passively using capillary forces without supplying of some kind of external energy, and the migration perform the sorting, mixing and uniform separation of the liquid samples diffused [77]. Furthermore, the chemical composition of paper permits the covalent bonding of bioactive compounds onto the surface. On the other hand, some obstacles to become an ideal PoCT are liquid evaporation, sample retention and nonspecific adsorption. These adversities could lead to false response errors and decreased sensitivity [21]. Its mode of construction is creating a set of microchannels bounded by hydrophobic barriers patterned on paper substrates witch the flow is conducted within the hydrophilic channels and consequently, fluid can be coordinated of a controlled mode. Two-dimensional (2D) and three-dimensional 3D microfluidic channels have been already built on

paper, being able to transport biological liquids injected separately by pathways for performing assays and quantifying concentrations of distinct analytes [78]. Printing is the one of the most commonly used techniques to achieve minimal consumption of hydrophobic material [79]. A wave of advancements in 3D printing technology to simplify in agile designing and fabrication supports the durability, flexibility and performance of PoCT microfluidic [80].

Different detection methods have been employed for a semi-quantitative detection, analytical assays based on colorimetric analysis. The results can be visually verified to the unaided eye or interpreted by a reader [81]. Nevertheless, fluorescence or electrochemical methods have become more widespread and attractive because of their high accuracy, sensitivity and lower limit of detection. Further, electrochemistry is less subject to the interference compounds exposed in the biological specimens, because it is not affected by ambient lighting conditions [21]. Colorimetric revealing has been expansively applied due to its simplicity and compatibility with cameras. Mobile phones are accessories widely available, allowing be coupled, and so, they are very suitable for incorporation into portable microfluidic devices. Their rapid improvement of hardware and software, high-resolution cameras, processing power and worldwide coverage of wireless internet network connection can facilitate diagnostic access, permit continuous monitoring of health parameters and promote increased surveillance notifications. This way, it is possible to do geo-timed reports and tracking of data automated providing governments with statistical information for clinical and epidemiological impact evaluation and counter-measures policies implementation. In fact, 3D printers and smartphones are instruments that are revolutionizing the future of lab-on-chip platform [82].

Other innovative actuation principle is centrifugal microfluidic that taking advantage of the forces acting on liquids in rotating chips. A spindle motor is necessary to press the fluid in the microfluidic chip. The centrifugal systems are particularly important for tasks involving separation of particles in suspension, as even small differences in density between solid parts and surrounding medium will result in sedimentation. It allows to perform the fluid manipulation within operational cartridges without the need of external micropumps and microvalves or previous sample preparation, as in the case to extract cell free plasma from whole blood [83]. Many challenges have been solved requiring only little of user interaction. These emergent microfluidic

systems with integrated sensing, also termed lab-on-a-disc, are typically based on optical techniques, for example, absorbance, fluorescence or imaging. Optical readout with movable instrumentation are a successful detection and ensures several advantages: non-contact, high sensitivity, and the availability of optical components such as lasers and photo detectors or even constituents developed for optical disc drives [84].

2.5. Conclusions

Although great advances have been achieved in the development of PoCT immunosensors applied to health that facilitated the diagnosis of many diseases, control and handling more effectively, allowing analysis or multi-analysis more quickly, more remains to be done to make PoCT a practical devices for clinical routine. Carbon nanotubes, graphene metallic and magnetic nanoparticles nanostructures are examples of nanomaterials that have been widely used for electrochemical PoCTs, improving the amperometric transductions by promoting increase on the electron transfer and offer better electrocatalytic activity. Additionally, due to the large superficial area of nanomaterials, they are able result in increase on electroactive surface area, implying a high sensitivity for PoCTs. While many challenges still need to be overcome, the focus on PoCT immunosensor researches have grown exponentially on the last few decades. Many advantages make them ideal analytical methods: the phlebotomy step is avoided and replaced by a simpler and safer procedure; the collection of capillary blood with a few microliters can be performed on bedside; turnaround time of the diagnostic cycle is dramatically reduced and the results can be immediately informed to the patient, possibiliting the decentralization of outpatient services; and also the coupling with technologies for mobile phones and similar devices is possible.

Acknowledgments

Authors thank the National Council of Technological and Scientific Development (CNPq), Brazilian agency. Diego G. A. Cabral, Gilvânia M. de Santana, Paula A. B. Ferreira, Anne K. S. Silva, Erika K. G. Trindade, postgraduate students are grateful to FACEPE (Brazil) for their scholarships.

References

[1]. E. C. Rama, A. Costa-García, Screen-printed Electrochemical Immunosensors for the Detection of Cancer and Cardiovascular Biomarkers, *Electroanalysis*, Vol. 28, Issue 8, Aug. 2016, pp. 1700-1715.

[2]. C. Florkowski, A. Don-Wauchope, N. Gimenez, K. Rodriguez-Capote, J. Wils, A. Zemlin, Point-of-care testing (POCT) and evidence-based laboratory medicine (EBLM) – does it leverage any advantage in clinical decision making?, *Crit. Rev. Clin. Lab. Sci.*, Vol. 54, Issue 7-8, November 2017, pp. 471-494.

[3]. X. Fu, Z. Cheng, J. Yu, P. Choo, L. Chen, J. Choo, A SERS-based lateral flow assay biosensor for highly sensitive detection of HIV-1 DNA, *Biosens. Bioelectron.*, Vol. 78, 2016, pp. 530-537.

[4]. K. M. Koczula, A. Gallotta, Lateral flow assays, *Essays Biochem.*, Vol. 60, Issue 1, 2016, pp. 111-120.

[5]. M. Sajid, A. N. Kawde, M. Daud, Designs, formats and applications of lateral flow assay: A literature review, *J. Saudi Chem. Soc.*, Vol. 19, Issue 6, 2015, pp. 689-705.

[6]. E. B. Bahadır, M. K. Sezgintürk, Lateral flow assays: Principles, designs and labels, *TrAC – Trends Anal. Chem.*, Vol. 82, 2016, pp. 286-306.

[7]. D. Quesada-González, A. Merkoçi, Nanoparticle-based lateral flow biosensors, *Biosens. Bioelectron.*, Vol. 73, Nov. 2015, pp. 47-63.

[8]. J.-H. Lee, *et al.*, Multiplex diagnosis of viral infectious diseases (AIDS, hepatitis C, and hepatitis A) based on point of care lateral flow assay using engineered proteinticles, *Biosens. Bioelectron.*, Vol. 69, July 2015, pp. 213-225.

[9]. X. Gong, *et al.*, A review of fluorescent signal-based lateral flow immunochromatographic strips, *J. Mater. Chem. B*, Vol. 5, Issue 26, July 2017, pp. 5079-5091.

[10]. C. Kokkinos, A. Economou, M. I. Prodromidis, Electrochemical immunosensors: Critical survey of different architectures and transduction strategies, *Trends Anal. Chem.*, Vol. 79, May 2016, pp. 88-105.

[11]. N. S. Lipman, L. R. Jackson, L. J. Trudel, F. Weis-Garcia, Monoclonal versus polyclonal antibodies: Distinguishing characteristics, applications, and information resources, *ILAR J.*, Vol. 46, Issue 3, January 2005, pp. 258-268.

[12]. R. A. S. Couto, J. L. F. C. Lima, M. B. Quinaz, Recent developments, characteristics and potential applications of screen-printed electrodes in pharmaceutical and biological analysis, *Talanta*, Vol. 146, January 2016, pp. 801-814.

[13]. N. Gan, X. Du, Y. Cao, F. Hu, T. Li, Q. Jiang, An Ultrasensitive electrochemical immunosensor for HIV p24 based on Fe_3O_4@SiO_2 nanomagnetic probes and nanogold colloid-labeled enzyme-antibody copolymer as signal tag, *Materials (Basel).*, Vol. 6, Issue 4, March 2013, pp. 1255-1269.

[14]. L. Suresh, P. K. Brahman, K. R. Reddy, J. S. Bondili, Development of an electrochemical immunosensor based on gold nanoparticles incorporated chitosan biopolymer nanocomposite film for the detection of prostate cancer using PSA as biomarker, *Enzyme Microb. Technol.*, Vol. 112, May 2018, pp. 43-51.

[15]. M. M. P. S. Neves, M. B. González-García, H. P. A. Nouws, A. Costa-García, Celiac disease detection using a transglutaminase electrochemical immunosensor fabricated on nanohybrid screen-printed carbon electrodes, *Biosens. Bioelectron.*, Vol. 31, Issue 1, January 2012, pp. 95-100.

[16]. B. V. M. Silva, B. A. G. Rodríguez, G. F. Sales, M. P. T. Sotomayor, R. F. Dutra, An ultrasensitive human cardiac troponin T graphene screen-printed electrode based on electropolymerized-molecularly imprinted conducting polymer, *Biosens. Bioelectron.*, Vol. 77, 2016, pp. 978-985.

[17]. Y. Xu, S. Yang, W. Shi, Fabrication of an immunosensor for cardiac troponin I determination, *Int. J. Electrochem. Sci.*, Vol. 12, Issue 9, 2017, pp. 7931-7940.

[18]. A. Afkhami, P. Hashemi, H. Bagheri, J. Salimian, A. Ahmadi, T. Madrakian, Impedimetric immunosensor for the label-free and direct detection of botulinum neurotoxin serotype A using Au nanoparticles/graphene-chitosan composite, *Biosens. Bioelectron.*, Vol. 93, Jul. 2017, pp. 124-131.

[19]. E. A. de Vasconcelos, N. G. Peres, C. O. Pereira, V. L. da Silva, E. F. da Silva, R. F. Dutra, Potential of a simplified measurement scheme and device structure for a low cost label-free point-of-care capacitive biosensor, *Biosens. Bioelectron.*, Vol. 25, Issue 4, December 2009, pp. 870-876.

[20]. Z. Taleat, A. Khoshroo, M. Mazloum-Ardakani, Screen-printed electrodes for biosensing: A review (2008-2013), *Microchim. Acta*, Vol. 181, Issue 9-10, July 2014, pp. 865-891.

[21]. L. Syedmoradi, M. Daneshpour, M. Alvandipour, F. A. Gomez, H. Hajghassem, K. Omidfar, Point of care testing: The impact of nanotechnology, *Biosens. Bioelectron.*, Vol. 87, January 2017, pp. 373-387.

[22]. M. Vidotti, R. Torresi, S. I. Córdoba De Torresi, Eletrodos modificados por hidróxido de níquel: Um estudo de revisão sobre suas propriedades estruturais e eletroquímicas visando suas aplicações em eletrocatálise, Eletrocromismo E baterias secundárias, *Quim. Nov.*, Vol. 33, Issue 10, 2010, pp. 2176-2186.

[23]. Q. Huang, *et al.*, Nanotechnology-based strategies for early cancer diagnosis using circulating tumor cells as a liquid biopsy, *Nanotheranostics*, Vol. 2, Issue 1, 2018, pp. 21-41.

[24]. Z. Farka, T. Juřík, D. Kovář, L. Trnková, P. Skládal, Nanoparticle-based immunochemical biosensors and assays: Recent advances and challenges, *Chem. Rev.*, Vol. 117, Issue 15, August 2017, pp. 9973-10042.

[25]. N. J. Wittenberg, C. L. Haynes, Using nanoparticles to push the limits of detection, *Wiley Interdiscip. Rev. Nanomedicine Nanobiotechnology*, Vol. 1, Issue 2, March 2009, pp. 237-254.

[26]. K. S. Krishna, Y. Li, S. Li, C. S. S. R. Kumar, Lab-on-a-chip synthesis of inorganic nanomaterials and quantum dots for biomedical applications, *Adv. Drug Deliv. Rev.*, Vol. 65, Issue 11-12, November 2013, pp. 1470-1495.

[27]. Z. Wang, Z. Dai, Carbon nanomaterial-based electrochemical biosensors: An overview, *Nanoscale*, Vol. 7, Issue 15, 2015, pp. 6420-6431.

[28]. A. Ghasemi, *et al.*, Carbon nanotubes in microfluidic lab-on-a-chip technology: Current trends and future perspectives, *Microfluid. Nanofluidics*, Vol. 21, Issue 9, 2017, pp. 1-19.

[29]. C.-M. Tîlmaciu, M. C. Morris, Carbon nanotube biosensors, *Front. Chem.*, Vol. 3, 2015, pp. 1-21.

[30]. A. Dasgupta, L. P. Rajukumar, C. Rotella, Y. Lei, M. Terrones, Covalent three-dimensional networks of graphene and carbon nanotubes: Synthesis and environmental applications, *Nano Today*, Vol. 12, 2017, pp. 116-135.

[31]. Z. Zhu, An overview of carbon nanotubes and graphene for biosensing applications, *Nano-Micro Lett.*, Vol. 9, Issue 3, 2017, pp. 1-24.

[32]. J. Seo, *et al.*, Immunosensor employing stable, Solid 1-amino-2-naphthyl phosphate and ammonia-borane toward ultrasensitive and simple point-of-care testing, *ACS Sensors*, Vol. 2, Issue 8, 2017, pp. 1240-1246.

[33]. A. C. M. S. Dias, S. L. R. Gomes-Filho, M. M. S. Silva, R. F. Dutra, A sensor tip based on carbon nanotube-ink printed electrode for the dengue virus NS1 protein, *Biosens. Bioelectron.*, Vol. 44, Issue 1, 2013, pp. 216-221.

[34]. B. V. M. Silva, I. T. Cavalcanti, M. M. S. Silva, R. F. Dutra, A carbon nanotube screen-printed electrode for label-free detection of the human cardiac troponin T, *Talanta*, Vol. 117, 2013, pp. 431-437.

[35]. E. Sánchez-Tirado, C. Salvo, A. González-Cortés, P. Yáñez-Sedeño, F. Langa, J. M. Pingarrón, Electrochemical immunosensor for simultaneous determination of interleukin-1 beta and tumor necrosis factor alpha in serum and saliva using dual screen printed electrodes modified with functionalized double-walled carbon nanotubes, *Anal. Chim. Acta*, Vol. 959, 2017, pp. 66-73.

[36]. S. L. R. Gomes-Filho, A. C. M. S. Dias, M. M. S. Silva, B. V. M. Silva, R. F. Dutra, A carbon nanotube-based electrochemical immunosensor for cardiac troponin T, *Microchem. J.*, Vol. 109, 2013, pp. 10-15.

[37]. S. Ma, *et al.*, Interaction processes of ciprofloxacin with graphene oxide and reduced graphene oxide in the presence of montmorillonite in simulated gastrointestinal fluids, *Sci. Rep.*, Vol. 7, Issue 1, 2017, pp. 1-11.

[38]. R. Raccichini, A. Varzi, S. Passerini, B. Scrosati, The role of graphene for electrochemical energy storage, *Nat. Mater.*, Vol. 14, Issue 3, 2015, pp. 271-279.

[39]. H. Sadegh, Development of graphene oxide from graphite: A review on synthesis, characterization and its application in wastewater treatment, *Rev. Adv. Mater. Sci.*, Vol. 49, 2017, pp. 38-43.

[40]. L. G. Guex, *et al.*, Experimental review: Chemical reduction of graphene oxide (GO) to reduced graphene oxide (rGO) by aqueous chemistry, *Nanoscale*, Vol. 9, Issue 27, 2017, pp. 9562-9571.

[41]. J. Yukird, T. Wongtangprasert, R. Rangkupan, O. Chailapakul, T. Pisitkun, N. Rodthongkum, Label-free immunosensor based on graphene/polyaniline nanocomposite for neutrophil gelatinase-associated lipocalin detection, *Biosens. Bioelectron.*, Vol. 87, 2017, pp. 249-255.

[42]. P. K. Drain, *et al.*, Diagnostic point-of-care tests in resource-limited settings., *Lancet. Infect. Dis.*, Vol. 14, Issue 3, March 2014, pp. 239-249.

[43]. B. V. M. Silva, B. A. G. Rodríguez, G. F. Sales, M. D. P. T. Sotomayor, R. F. Dutra, An ultrasensitive human cardiac troponin T graphene screen-printed electrode based on electropolymerized-molecularly imprinted conducting polymer, *Biosens. Bioelectron.*, Vol. 77, 2016, pp. 978-985.

[44]. S. X. Lee, H. N. Lim, I. Ibrahim, A. Jamil, A. Pandikumar, N. M. Huang, Horseradish peroxidase-labeled silver/reduced graphene oxide thin film-modified screen-printed electrode for detection of carcinoembryonic antigen, *Biosens. Bioelectron.*, Vol. 89, 2017, pp. 673-680.

[45]. G. Doria, *et al.*, Noble metal nanoparticles for biosensing applications, *Sensors*, Vol. 12, Issue 12, Feb. 2012, pp. 1657-1687.

[46]. Y. Li, H. J. Schluesener, S. Xu, Gold nanoparticle-based biosensors, *Gold Bull.*, Vol. 43, Issue 1, March 2010, pp. 29-41.

[47]. H. Malekzad, P. Sahandi Zangabad, H. Mirshekari, M. Karimi, M. R. Hamblin, Noble metal nanoparticles in biosensors: recent studies and applications, *Nanotechnol. Rev.*, Vol. 6, Issue 3, January 2017, pp. 301-329.

[48]. M. Holzinger, A. Le Goff, S. Cosnier, Nanomaterials for biosensing applications: A review, *Front. Chem.*, Vol. 2, 2014, 63.

[49]. N. Li, P. Zhao, D. Astruc, Anisotropic gold nanoparticles: synthesis, properties, applications, and toxicity, *Angew. Chemie Int. Ed.*, Vol. 53, Issue 7, February 2014, pp. 1756-1789.

[50]. F. Inci, *et al.*, Multitarget, quantitative nanoplasmonic electrical field-enhanced resonating device (NE ^{2} RD) for diagnostics, *Proceedings of Natl. Acad. Sci.*, Vol. 112, Issue 32, August 2015, pp. E4354-E4363.

[51]. S. Kumar, W. Ahlawat, R. Kumar, N. Dilbaghi, Graphene, carbon nanotubes, zinc oxide and gold as elite nanomaterials for fabrication of biosensors for healthcare, *Biosens. Bioelectron.*, Vol. 70, August 2015, pp. 498-503.

[52]. M. Jacobs, A. Panneer Selvam, J. E. Craven, S. Prasad, Antibody-conjugated gold nanoparticle-based immunosensor for ultra-sensitive detection of troponin-T, *J. Lab. Autom.*, Vol. 19, Issue 6, December 2014, pp. 546-554.

[53]. S. Sabouri, H. Ghourchian, M. Shourian, M. Boutorabi, A gold nanoparticle-based immunosensor for the chemiluminescence detection of the hepatitis B surface antigen, *Anal. Methods*, Vol. 6, Issue 14, June 2014, pp. 5059-5066.

[54]. R. El-Dessouky, M. Georges, H. M. E. Azzazy, Silver nanostructures: Properties, synthesis, and biosensor applications, *ACS Symposium Series*, Vol. 1112, 2012, pp. 359-404.

[55]. X. Lu, M. Rycenga, S. E. Skrabalak, B. Wiley, Y. Xia, Chemical synthesis of novel plasmonic nanoparticles, *Annu. Rev. Phys. Chem.*, Vol. 60, 2009, pp. 167-192.

[56]. Z. Farka, T. Juřík, D. Kovář, L. Trnková, P. Skládal, Nanoparticle-based immunochemical biosensors and assays: Recent advances and challenges, *Chem. Rev.*, Vol. 117, Issue 15, August 2017, pp. 9973-10042.

[57]. N. Hao, *et al.*, An electrochemical immunosensing method based on silver nanoparticles, *J. Electroanal. Chem.*, Vol. 656, Issues 1-2, 2011, pp. 50-54.

[58]. S. Felici, *et al.*, Towards a model of electrochemical immunosensor using silver nanoparticles, *Procedia Technol.*, Vol. 27, January 2017, pp. 155-156.

[59]. X. Che, R. Yuan, Y. Chai, J. Li, Z. Song, J. Wang, Amperometric immunosensor for the determination of α-1-fetoprotein based on multiwalled carbon nanotube-silver nanoparticle composite, *J. Colloid Interface Sci.*, Vol. 345, Issue 2, May 2010, pp. 174-180.

[60]. Z. H. Ibupoto, N. Jamal, K. Khun, X. Liu, M. Willander, A potentiometric immunosensor based on silver nanoparticles decorated ZnO nanotubes, for the selective detection of d-dimer, *Sensors Actuators B Chem.*, Vol. 182, June 2013, pp. 104-111.

[61]. J. B. Haun, T.-J. Yoon, H. Lee, R. Weissleder, Magnetic nanoparticle biosensors, *Wiley Interdiscip. Rev. Nanomedicine Nanobiotechnology*, Vol. 2, Issue 3, May 2010, pp. 291-304.

[62]. J. B. Haun, T.-J. Yoon, H. Lee, R. Weissleder, Magnetic nanoparticle biosensors, *Wiley Interdiscip. Rev. Nanomedicine Nanobiotechnology*, Vol. 2, Issue 3, May 2010, pp. 291-304.

[63]. L. Syedmoradi, M. Daneshpour, M. Alvandipour, F. A. Gomez, H. Hajghassem, K. Omidfar, Point of care testing: The impact of nanotechnology, *Biosens. Bioelectron.*, Vol. 87, January 2017, pp. 373-387.

[64]. M. Martín, *et al.*, Rapid Legionella pneumophila determination based on a disposable core-shell Fe_3O_4 @poly(dopamine) magnetic nanoparticles immunoplatform, *Anal. Chim. Acta*, Vol. 887, August 2015, pp. 51-58.

[65]. V. Singh, S. Krishnan, Voltammetric Immunosensor Assembled on carbon-pyrenyl nanostructures for clinical diagnosis of type of diabetes, *Anal. Chem.*, Vol. 87, Issue 5, March 2015, pp. 2648-2654.

[66]. Y. Zhang, T. R. Nayak, H. Hong, W. Cai, Biomedical applications of zinc oxide nanomaterials, *Curr. Mol. Med.*, Vol. 13, Issue 10, December 2013, pp. 1633-1645.

[67]. S. Kumar, W. Ahlawat, R. Kumar, N. Dilbaghi, Graphene, carbon nanotubes, zinc oxide and gold as elite nanomaterials for fabrication of biosensors for healthcare, *Biosens. Bioelectron.*, Vol. 70, August 2015, pp. 498-503.

[68]. M. Marie, S. Mandal, O. Manasreh, An electrochemical glucose sensor based on zinc oxide nanorods, *Sensors*, Vol. 15, Issue 12, July 2015, pp. 18714-18723.

[69]. M. A. Seia, S. V. Pereira, M. A. Fernández-Baldo, I. E. De Vito, J. Raba, G. A. Messina, Zinc oxide nanoparticles based microfluidic immunosensor applied in congenital hypothyroidism screening, *Anal. Bioanal. Chem.*, Vol. 406, Issue 19, July 2014, pp. 4677-4684.

[70]. A. T. Giannitsis, Microfabrication of biomedical lab-on-chip devices. A review, *Est. J. Eng.*, Vol. 17, Issue 2, 2011, pp. 109-139.

[71]. Y. Temiz, R. D. Lovchik, G. V. Kaigala, E. Delamarche, Lab-on-a-chip devices: How to close and plug the lab?, *Microelectron. Eng.*, Vol. 132, January 2015, pp. 156-175.

[72]. M. Zarei, Advances in point-of-care technologies for molecular diagnostics, *Biosens. Bioelectron.*, Vol. 98, December 2017, pp. 494-506.

[73]. P. K. Drain, *et al.*, Diagnostic point-of-care tests in resource-limited settings., *Lancet. Infect. Dis.*, Vol. 14, Issue 3, March 2014, pp. 239-249.

[74]. F. A. Gomez, Paper microfluidics in bioanalysis, *Bioanalysis*, Vol. 6, Issue 21, November 2014, pp. 2911-2914.

[75]. R. Amin, *et al.*, 3D-printed microfluidic devices, *Biofabrication*, Vol. 8, Issue 2, June 2016, 22001.

[76]. J. Hu, *et al.*, Advances in paper-based point-of-care diagnostics, *Biosens. Bioelectron.*, Vol. 54, April 2014, pp. 585-597.

[77]. C. M. B. Ho, S. H. Ng, K. H. H. Li, Y.-J. Yoon, 3D printed microfluidics for biological applications., *Lab Chip*, Vol. 15, Issue 18, 2015, pp. 3627-3637.

[78]. K. Yamada, T. G. Henares, K. Suzuki, D. Citterio, Paper-based inkjet-printed microfluidic analytical devices, *Angew. Chemie Int. Ed.*, Vol. 54, Issue 18, April 2015, pp. 5294-5310.

[79]. M. Zarei, Advances in point-of-care technologies for molecular diagnostics, *Biosens. Bioelectron.*, Vol. 98, December 2017, pp. 494-506.

[80]. O. Strohmeier, *et al.*, Centrifugal microfluidic platforms: Advanced unit operations and applications, *Chem. Soc. Rev.*, Vol. 44, Issue 17, August 2015, pp. 6187-6229.

[81]. R. Burger, L. Amato, A. Boisen, Detection methods for centrifugal microfluidic platforms, *Biosens. Bioelectron.*, Vol. 76, February 2016, pp. 54-67.

APÊNDICE E – CURRÍCULO LATTES DA AUTORA

Erika Ketlem Gomes Trindade
Naturalidade: Recife - PE
Data de nascimento: 01/09/1990

Formação acadêmica/titulação

2015 Doutorado em CIÊNCIAS BIOLÓGICAS.
Universidade Federal de Pernambuco, UFPE, Recife, Brasil
Título: Desenvolvimento de nanoimunossensores para detecção da cistatina C como alternativa para o diagnóstico de doenças renais
Orientador: Rosa Amália Fireman Dutra
Bolsista do(a): Fundação de Amparo à Ciência e Tecnologia do Estado de Pernambuco

2013 - 2015 Mestrado em ENGENHARIA BIOMÉDICA.
Universidade Federal de Pernambuco, UFPE, Recife, Brasil
Título: Desenvolvimento de Nanoimunossensor para Identificação de Anticorpos contra o Vírus da Hepatite B, Ano de obtenção: 2015
Orientador: Profª Drª Rosa Amália Fireman Dutra
Co-orientador: Prof Dr Eduardo Fontana
Bolsista do(a): Fundação de Amparo à Ciência e Tecnologia do Estado de Pernambuco

2008 - 2011 Graduação em BIOMEDICINA.
Universidade Federal de Pernambuco, UFPE, Recife, Brasil
Título: Pesquisa da Deficiência de Glicose-6-Fosfato Desidrogenase em Estudantes da Universidade Federal de Pernambuco
Orientador: Prof. Dr. Marcos André Cavalcanti Bezerra

Atuação profissional

1. Faculdade de Tecnologia Gestão e Marketing - FGM/IBGM

Vínculo institucional

2015 - 2015 Vínculo: Professor Substituto, Enquadramento funcional: Professor de nível superior , Carga horária: 20, Regime: Parcial

2. Fundação de Amparo à Ciência e Tecnologia do Estado de Pernambuco – FACEPE

Vínculo institucional

2015 - Atual Vínculo: Bolsista , Enquadramento funcional: Doutoranda , Carga horária: 40, Regime: Dedicação exclusiva

2013 - 2015 Vínculo: Bolsista , Enquadramento funcional: Mestranda , Carga horária: 40, Regime: Dedicação exclusiva

3. Conselho Nacional de Desenvolvimento Científico e Tecnológico - CNPq

Vínculo institucional

2015 - 2015 Vínculo: Bolsista , Enquadramento funcional: Pesquisadora , Carga horária: 40, Regime: Integral

4. Universidade Federal de Pernambuco - UFPE

Vínculo institucional

2015 - Atual Vínculo: Bolsista , Enquadramento funcional: Doutoranda , Carga horária: 40, Regime: Dedicação exclusiva
Outras informações:
Bolsista FACEPE

2013 - 2015 Vínculo: Bolsista , Enquadramento funcional: Mestranda , Carga horária: 40, Regime: Dedicação exclusiva
Outras informações:
Bolsista FACEPE

2010 - 2011 Vínculo: Bolsista , Enquadramento funcional: Iniciação Científica , Carga horária: 20, Regime: Dedicação exclusiva
Outras informações:
Aluna de iniciação científica na área de Biofísica de membranas de células-troncoBolsista FACEPE

2010 - 2010 Vínculo: Voluntário , Enquadramento funcional: Tutor , Carga horária: 40, Regime: Integral
Outras informações:
Curso de Férias "Escalas da Vida: da molécula ao organismo", realizado pelo Espaço Ciência e pelo Departamento de Fisiologia e Farmacologia da UFPE, com o objetivo de iniciar os alunos de escolas da rede pública de ensino na rotina laboratorial e incentivar a busca de conhecimento por parte deles.

2009 - 2010 Vínculo: Voluntário , Enquadramento funcional: Monitora , Carga horária: 12, Regime: Parcial
Outras informações:

Monitora na disciplina de Física e Biofísica

5. Hospital Barão de Lucena - HBL

Vínculo institucional

2011 - 2012 Vínculo: Estágio curricular , Enquadramento funcional: Estagiária , Carga horária: 25, Regime: Parcial
Outras informações:
Estágio curricular em Analises Clinicas coordenado pela Farmacêutica Mary Clere Alencar F. Lopes no Laboratório de Patologia Clinica do Hospital Barão de Lucena.

Produção

Produção bibliográfica

Artigos completos publicados em periódicos

1. **Trindade, Erika K.G.**; SILVA, BÁRBARA V.M.; Dutra, Rosa F.
A probeless and label-free electrochemical immunosensor for cystatin C detection based on ferrocene functionalized-graphene platform. BIOSENSORS & BIOELECTRONICS. , v.138, p.111311 - , 2019.
Palavras-chave: Redox probe-free, Cystatin C, Renal Failure, Immunosensor, Ferrocene, Graphene

2. **Trindade, Erika K.G.**; Dutra, Rosa F.
A label-free and reagentless immunoelectrode for antibodies against hepatitis B core antigen (anti-HBc) detection. COLLOIDS AND SURFACES B-BIOINTERFACES. , v.172, p.272 - 279, 2018.
Palavras-chave: Immunosensor, Nanosensor, Polytyramine, Anti-HBc, Reagentless, Hepatitis B

Capítulos de livros publicados

1. CABRAL, D. G. A.; SANTANA, G. M.; FERREIRA, P. A. B.; SILVA, A. K. S.; **Trindade, Erika K.G.**; DUTRA, R. A. F.
Point-of-Care Electrochemical Immunosensors Applied to Diagnostic in Health In: Advances in Biosensors: Reviews Volume 2.1 ed.Barcelona, Spain : IFSA Publishing, S. L., 2018, v.2, p. 43-64.
Palavras-chave: Immunosensors, Point-of-care, Health, Diagnostic, Electrochemical

2. Rodriguez, Blanca A.G.; **Trindade, Erika K. G.**; Cabral, Diego G.A.; Soares, Erika C.L.; Menezes, Cayo E.L.; Ferreira, Danielle C.M.; Mendes, Renata K.; Dutra, Rosa F. Nanomaterials for Advancing the Health Immunosensor In: Biosensors - Micro and

Nanoscale Applications.1 ed.Rijeka, Croatia : InTech, 2015, v.1, p. 347-373.
Palavras-chave: Immunosensors, Immunoassay, Nanosensor, Nanomateriais

Trabalhos publicados em anais de eventos (resumo)

1. SANTANA, G. M.; CABRAL, D. G. A.; MENDONCA, P. D.; SILVA, A. K. S.; **Trindade, Erika K.G.**; SILVA, B. V. M.; DUTRA, R. A. F.
Genosensor eletroquímico para a detecção da hepatite C baseado em nanocompósito In: 54º Congresso da Sociedade Brasileira de Medicina Tropical (Medtrop), 2018, Olinda.
Anais do Medtrop. , 2018.

2. **Trindade, Erika K.G.**; SILVA, B. V. M.; SANTANA, G. M.; DUTRA, R. A. F.
Graphene oxide and aminoferrocene nanoplatform for cystatin C detection in renal failure patients In: XVII Brazil MRS Meeting, 2018, Natal.
Anais do XVII Brazil MRS Meeting. , 2018.

3. **Trindade, Erika K.G.**; DUTRA, R. A. F.
Desenvolvimento de Plataforma Nanoestruturada para Teste Rápido de Hidronefrose In: XXI Simpósio Brasileiro de Eletroquímica e Eletroanalítica, 2017, Natal - RN.
Anais do XXI SIBEE. , 2017.
Palavras-chave: PLATAFORMA, NANOESTRUTURADA, HIDRONEFROSE
Áreas do conhecimento : Nanotecnologia,Biossensores,Nanosensores

4. GOMES, R. M. S.; **Trindade, Erika K.G.**; VAZ, E. C. R.; SANTANA, G. M.; DUTRA, R. A. F.
Fulerenos quimicamente modificados para desenvolvimento de sensores eletroquímicos In: XXI Simpósio Brasileiro de Eletroquímica e Eletroanalítica, 2017, Natal - RN.
Anais do XXI SIBEE. , 2017.
Palavras-chave: Fulereno, Sensor

5. SILVA, A. K. S.; **Trindade, Erika K.G.**; GERMINIO, J. E. S.; VAZ, E. C. R.; RODRIGUES, B. A. G.; DUTRA, R. A. F.
Nanobiossensor eletroquímico preparado em uma única etapa para imunodiagnóstico In: XXI Simpósio Brasileiro de Eletroquímica e Eletroanalítica, 2017, Natal - RN.
Anais do XXI SIBEE. , 2017.
Palavras-chave: Nanobiossensor, Imunodiagnóstico

6. **Trindade, Erika K.G.**; DUTRA, R. A. F.
DESENVOLVIMENTO DE MATRIZ ELETROQUÍMICA PARA DETECÇÃO DE ANTI-HBC In: 10º Congresso de HIV/AIDS e 3º Congresso de Hepatites Virais, 2015, João Pessoa - PB.
Anais do 10º Congresso de HIV/AIDS e 3º Congresso de Hepatites Virais. , 2015.
Palavras-chave: Hepatite B, Nanoimunossensor

7. Menezes, C. E. L.; **TRINDADE, E. K. G.**; DUTRA, R. A. F.
Desenvolvimento de nanoimunossensor para detecção de anticorpos contra o

nucleocapsídeo do vírus da hepatite B (Anti-HBc) In: 51º CONGRESSO DA SOCIEDADE BRASILEIRA DE MEDICINA TROPICAL, 2015, Fortaleza.
Anais Medtrop 2015. , 2015.
Palavras-chave: Hepatite B, Eletrodos Interdigitados, Imunossensor, Nanomateriais
Áreas do conhecimento : Nanomateriais,Nanotecnologia,Biossensores

8. **TRINDADE, E. K. G.**; SOARES, E. C. L.; CABRAL, D. G. A.; DUTRA, R. A. F.
Detecção eletroquímica de anticorpos anti-HBc para Hepatite B In: 51º CONGRESSO DA SOCIEDADE BRASILEIRA DE MEDICINA TROPICAL, 2015, Fortaleza.
Anais Medtrop 2015. , 2015.
Palavras-chave: Hepatite B, Biossesores, Nanomateriais

9. SILVA, C. E.; SILVA, B. V. M.; RODRIGUES, B. A. G.; **Trindade, Erika K.G.**; CABRAL, D. G. A.; DUTRA, R. A. F.
Synergic effect of the carbon nanotube and polypyrrole in an electrochemical immunosensor of cardiac myocardial infarction In: XIV Brazil MRS Meeting SBPMAT, 2015, Rio de Janeiro - RJ.
Anais do XIV SBPMat. , 2015.

Trabalhos publicados em anais de eventos (resumo expandido)

1. **TRINDADE, E. K. G.**; Sá, P. H.; Prado, I. C.; DUTRA, R. A. F.
Desenvolvimento de imunossensor nanoestruturado utilizando nanopartículas de sílica para detecção de doenças renais In: I Simpósio em Avanços Tecnológicos de Diagnóstico em Saúde, 2018, Recife.
Anais do I Simpósio em Avanços Tecnológicos de Diagnóstico em Saúde. , 2018. v.1.
Palavras-chave: nanopartículas, Sílica, Cistatina C, Imunossensor

2. **Trindade, Erika K.G.**; DUTRA, R. A. F.
DESENVOLVIMENTO DE PLATAFORMA NANOSENSORA PARA TESTE RÁPIDO DE HIDRONEFROSE In: 4º Encontro Brasileiro para Inovação Terapêutica, 2016, Jaboatão dos Guararapes - PE.
Anais do 4º EBIT. , 2016. p.100 -

Apresentação de trabalho e palestra

1. **TRINDADE, E. K. G.**; DUTRA, R. A. F.
Biossensor para detecção da cistatina C, 2018. (Conferência ou palestra, Apresentação de Trabalho)
Palavras-chave: Cistatina C, Imunossensor, Diagnóstico
Áreas do conhecimento: Nanotecnologia, Nanomateriais

2. **Trindade, Erika K.G.**; SILVA, B. V. M.; SANTANA, G. M.; DUTRA, R. A. F.
Graphene oxide and aminoferrocene nanoplatform for cystatin C detection in renal failure patients, 2018. (Congresso, Apresentação de Trabalho)

3. **Trindade, Erika K.G.**; DUTRA, R. A. F.

Desenvolvimento de Plataforma Nanoestruturada para Teste Rápido de Hidronefrose, 2017. (Congresso, Apresentação de Trabalho)

4. **TRINDADE, E. K. G.**; RODRIGUES, B. A. G.; CABRAL, D. G. A.; DUTRA, R. A. F. **DESENVOLVIMENTO DE MATRIZ ELETROQUÍMICA PARA DETECÇÃO DE ANTI-HBC**, 2015. (Congresso, Apresentação de Trabalho)
Palavras-chave: Biossesores, Hepatite B, Nanomateriais
Áreas do conhecimento : Biossensores,Nanotecnologia

5. Menezes, C. E. L.; **TRINDADE, E. K. G.**; DUTRA, R. A. F.
DESENVOLVIMENTO DE NANOIMUNOSSENSOR PARA DETECÇÃO DE ANTICORPOS CONTRA O NUCLEOCAPSEIDO DO VÍRUS DA HEPATITE B (ANTI-HBc), 2015. (Congresso, Apresentação de Trabalho)
Palavras-chave: Eletrodos Interdigitados, HBcAg, Nanoimunossensor, Nanotubos de Carbono
Áreas do conhecimento : Biotecnologia

6. **TRINDADE, E. K. G.**; SOARES, E. C. L.; CABRAL, D. G. A.; DUTRA, R. A. F.
DETEÇÃO ELETROQUÍMICA DE ANTICORPOS ANTI-HBc PARA HEPATITE B, 2015. (Congresso, Apresentação de Trabalho)
Palavras-chave: HBcAg, Nanoimunossensor, Nanotubos de Carbono
Áreas do conhecimento : Biotecnologia,Medicina Tropical

Eventos

Participação em eventos

1. Apresentação Oral no(a) **XVII Brazil MRS Meeting**, 2018. (Congresso)
Graphene oxide and aminoferrocene nanoplatform for cystatin C detection in renal failure patients.

2. **US-Brazil Workshop on Biosensors and 5th Bioanalytical School**, 2017. (Oficina).

3. **XXI Simpósio Brasileiro de Eletroquímica e Eletroanalítica**, 2017. (Simpósio)
Desenvolvimento de Plataforma Nanoestruturada para Teste Rápido de Hidronefrose.

4. Apresentação Oral no(a) **10º Congresso de HIV/AIDS e 3º Congresso de Hepatites Virais**, 2015. (Congresso)
DESENVOLVIMENTO DE MATRIZ ELETROQUÍMICA PARA DETECÇÃO DE ANTI-HBC.

5. Apresentação de Poster / Painel no(a) **51º CONGRESSO DA SOCIEDADE BRASILEIRA DE MEDICINA TROPICAL**, 2015. (Congresso)
Desenvolvimento De Nanoimunossensor Para Detecção De Anticorpos Contra O Nucleocapsídeo Do Vírus Da Hepatite B (Anti-HBc).

6. Apresentação de Poster / Painel no(a) **51º CONGRESSO DA SOCIEDADE**

BRASILEIRA DE MEDICINA TROPICAL, 2015. (Congresso)
Deteção Eletroquímica De Anticorpos Anti-HBc Para Hepatite B.

Organização de evento

1. DUTRA, R. A. F.; **TRINDADE, E. K. G.**; MENDONCA, P. D.; SANTANA, G. M.
I Simpósio em Avanços Tecnológicos de Diagnóstico em Saúde, 2018. (Congresso, Organização de evento)
Palavras-chave: Diagnóstico, Tecnologia, Biossesores, Nanomateriais, Computação biomédica, Biologia molecular

---

Totais de produção

Produção bibliográfica

Artigos completos publicados em periódico.....	2
Capítulos de livros publicados.....	2
Trabalhos publicados em anais de eventos.....	14
Apresentações de trabalhos (Conferência ou palestra)	1
Apresentações de trabalhos (Congresso).....	8

Eventos

Participações em eventos (congresso).....	7
Participações em eventos (simpósio).....	1
Participações em eventos (oficina).....	1
Organização de evento (congresso).....	1